GEOSPHERE

GEOSPHERE; v. 12, no. 4

doi:10.1130/GES01285.1

27 figures; 3 tables

CORRESPONDENCE: eric_christiansen@byu.edu

CITATION: Best, M.G., Christiansen, E.H., de Silva, S., and Lipman, P.W., 2016, Slab-rollback ignimbrite flareups in the southern Great Basin and other Cenozoic American arcs: A distinct style of arc volcanism: Geosphere, v. 12, no. 4, p. 1097–1135, doi:10.1130/GES01285.1.

Received 26 October 2015
Revision received 12 February 2016
Accepted 17 March 2016
Published online 27 May 2016

GOLD OPEN ACCESS

THE GEOLOGICAL SOCIETY OF AMERICA®

Slab-rollback ignimbrite flareups in the southern Great Basin and other Cenozoic American arcs: A distinct style of arc volcanism

Myron G. Best[1], Eric H. Christiansen[1], Shanaka de Silva[2], and Peter W. Lipman[3]

[1]Department of Geological Sciences, Brigham Young University, Provo, Utah 84602-4606, USA
[2]College of Earth, Ocean, and Atmospheric Sciences, Oregon State University, Corvallis, Oregon 97331-5503, USA
[3]U.S. Geological Survey, Menlo Park, California 94025, USA

ABSTRACT

In continental-margin subduction zones, basalt magmas spawned in the mantle interact with the crust to produce a broad spectrum of volcanic arc associations. A distinct style of very voluminous arc volcanism develops far inland on thick crust over periods of 10–20 m.y. and involves relatively infrequent caldera-forming explosive eruptions of dominantly calc-alkaline rhyolite, dacite, and trachydacite with repose times of 10^4–10^6 yr. Volumes of individual eruptions are large (10^2–10^3 km^3), and nested super-eruptions of thousands of cubic kilometers are common. Calderas are as much as 60–75 km in diameter, and surrounding individual ignimbrite outflow sheets extend outward as much as 150 km, blanketing upwards of 10^5 km^2. Little or no basalt is extruded, whereas andesitic differentiates coeval with silicic ignimbrites range from minor to dominant in relative volume. A common feature in these flareups is essentially nonextending, thick, inland crust overlying a subducting oceanic plate with transverse tears that rolled back to a steeper dip from a previously flat configuration. Lithospheric delamination is locally possible. Large volumes of basalt that provide heat and mass for silicic magma generation in the crust form by fluid fluxing of the growing mantle wedge overlying the steepening dehydrating slab and from asthenospheric decompression. Variations in the mantle input, together with variations in crustal thickness, temperature, and composition, modulate the expression of the flareups. As a consequence of the high flux of mantle-derived magma into the thick crust, geotherms become elevated, and the brittle-ductile transition can rise to depths as shallow as 7 km. At this transition, diapirically rising magmas from a melting, assimilation, storage, and homogenization (MASH) zone are blocked and spread laterally into discoid chambers that grow until a thermomechanical threshold is attained, triggering climactic eruption and caldera collapse.

This ignimbrite flareup style of continental arc volcanism is exemplified by the mid-Cenozoic southern Great Basin ignimbrite province; other examples include the contemporaneous Southern Rocky Mountain, Mogollon-Datil, vast Sierra Madre Occidental volcanic fields, and the late Cenozoic Altiplano-Puna volcanic complex in the Central Andes. Rhyolitic and trachydacitic ignimbrites typically have erupted, but where the crust was predominantly felsic, prewarmed, and orogenically thickened, well-developed MASH zones have spawned multiple super-eruptions of phenocryst-rich dacite, or monotonous intermediates, and smaller volumes of calc-alkaline rhyolite ignimbrite. In the Great Basin, eruptions of dry, hot trachydacite magma followed the monotonous intermediates. Partial melting in thinner crust with a major mafic component yielded more alkalic rhyolite and related trachydacite.

INTRODUCTION

Large-scale, subduction-related, explosive silicic volcanism has developed in many places around the globe, such as in the late Cenozoic Central high Andes of western South America (e.g., Salisbury et al., 2011). The moniker "ignimbrite flareup" was coined by Coney (1978) for the great burst of mid-Cenozoic silicic volcanism in southwestern North America. This flareup—recognized earlier by Lipman et al. (1971) and Noble (1972)—is manifested in the vast Sierra Madre Occidental province in western Mexico and the voluminous Mogollon-Datil, Southern Rocky Mountain, Great Basin, and Challis volcanic fields northward in the United States (Fig. 1). It ranks as one of the premier expressions of explosive silicic volcanism in a continental arc in the global geologic record and was a major episode of crustal growth and hybridization (Johnson, 1991). Significant ignimbrites were deposited from 50 Ma until recently, but the most voluminous explosive silicic volcanism, the peak of the ignimbrite flareup, occurred at ca. 36–18 Ma, near the close of arc volcanism, which began along the southwestern margin of North America in the early Mesozoic. During the flareup, on the order of 500,000 km^3 of silicic magma explosively erupted.

Continental arc volcanism is controlled by many geodynamic factors. One of the most important is the dip of the subducting slab of oceanic lithosphere (e.g., Lipman et al., 1971; Keith, 1978; Ward, 1995; DeCelles et al., 2009). Typically, slabs dip at moderate angles of 30° to 70°, and near-trench volcanic eruptions are small (<1 km^3) and frequent (decades to centuries). Basaltic to intermediate-composition lavas and minor silicic ignimbrites create stratovolcanoes at central vents over <10^5 yr. This more familiar normal, or steady-state, activity (de Silva, 2008) of an arc may persist for tens of millions of years. In another type of subduction, the slab dips at a low angle, arc magmatism is suppressed, and the continental crust commonly thickens by deformation. The mantle lithosphere may be cooled, hydrated, and/or eroded by the flat oceanic slab (e.g., Humphreys, 2009; English et al., 2003). Later, the slab may steepen,

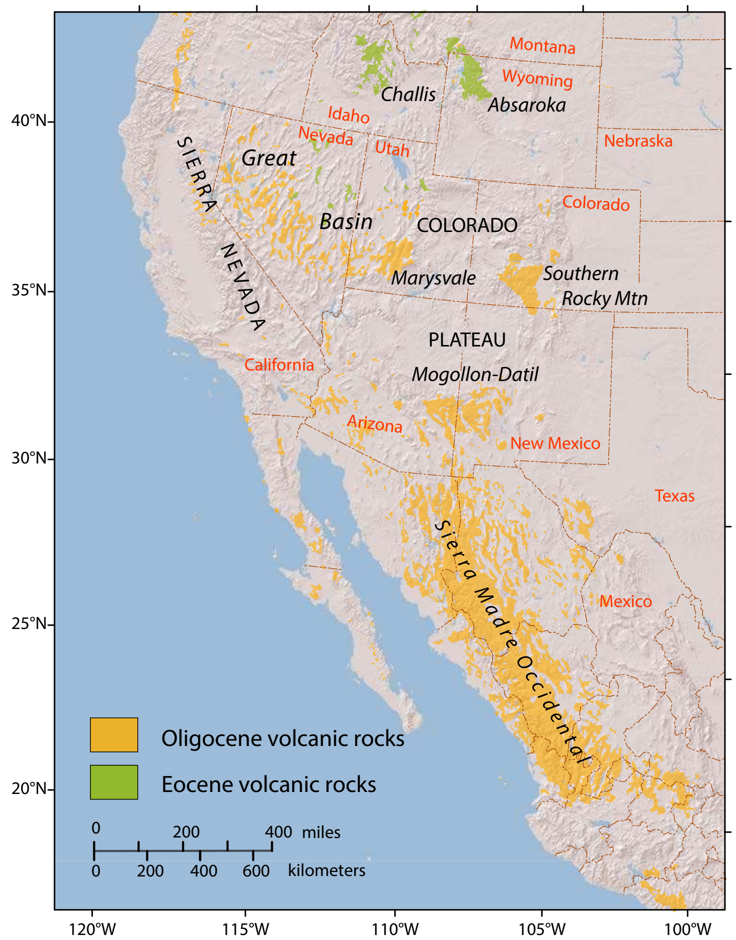

Figure 1. Mid-Cenozoic volcanic rocks in southwestern North America. Volcanic fields mentioned in the text are labeled. Oligocene volcanic rocks include some early Miocene rocks. The southern Great Basin–Marysvale–Southern Rocky Mountain segment of the mid-Cenozoic arc volcanism developed at a divergent angle from the continental margin and extends farthest inland at its eastern end. Small laccoliths east of the Marysvale volcanic field, mentioned in the text, are too small to show. Figure is modified from Garrity and Soller (2009).

or rollback, locally accompanied by segmentation, tears, and lithospheric delamination (Kay and Coira, 2009; DeCelles et al., 2009). As used here, "rollback" refers to slab steepening, as opposed to hinge migration. After approximately 10–20 m.y. of rollback, the slab reestablishes a steep dip, but during the transition, large volumes of silicic magma are produced and explosively erupted with recurrence times of 10^4 to 10^6 m.y. far inland from the trench over broad areas of thick crust. The largest eruptions have volumes[1] of at least 1000 km^3 of tephra (volcanic explosivity index [VEI] 8), or 450 km^3 of magma, qualifying as super-eruptions (Rampino and Self, 1992; Sparks et al., 2005; Self, 2006; Miller and Wark, 2008; de Silva, 2008; Wilson, 2008).

In this article, we document slab-rollback ignimbrite flareups as a distinct and significant genre in continental arc volcanism, present a comprehensive survey of their character, and evaluate the relevant geodynamic factors in their origin. To achieve this goal, we first describe one part of the mid-Cenozoic southwestern North American flareup—the southern Great Basin ignimbrite province (Fig. 2). It is ideally suited as an example of this flareup style of arc volcanism: First, it harbors on the order of 75,000 km^3 of silicic ignimbrite and more than 50 calderas as much as 60 km in diameter. Of the >230 explosive eruptions, at least 25 had volumes of 1000 to 5900 km^3, thus qualifying as super-eruptions. Second, many hundreds of modal, chemical, Sr isotope, $^{40}Ar/^{39}Ar$, and paleomagnetic analyses characterize the province, and dimensional data are also available for most ignimbrite sheets. Third, geologic maps at scales as large as 1:24,000 cover most of the province, and its structural architecture is well documented, including inferences on its character during the mid-Cenozoic flareup. A detailed and comprehensive anatomy of the southern Great Basin ignimbrite province is available for the first time in this themed issue of *Geosphere* (Best et al., 2013a, 2013b, 2013c; Henry and John, 2013).

Following this review of the southern Great Basin ignimbrite province, we then compare attributes of other volcanic fields that have experienced a flareup, focusing on the mid-Cenozoic Southern Rocky Mountain, Mogollon-Datil, and Sierra Madre volcanic fields (Fig. 1), and the late Cenozoic Altiplano-Puna volcanic complex of the Central Andes. Similarities and contrasts among these areas provide opportunities to resolve uncertainties in the genesis of voluminous ignimbrite flareups related to slab rollback. Fundamentally, with the tectonic setting of flareups as a backdrop, how were the vast volumes of mantle magmas produced that powered the generation of the silicic magmas in the crust? What aspects of the crust and processes in it allowed the flareups to develop?

GEOLOGIC SETTING OF THE SOUTHERN GREAT BASIN AND VICINITY

Tectonic and Magmatic History

The crust beneath the Great Basin area consists of two terranes of contrasting composition and thickness, thus offering an opportunity to evaluate the role of these factors in ignimbrite flareups. To the west, the basement consists of an

[1]All volume estimates used herein can be considered, for all intents and purposes, as minimum magma equivalents. Recalculation of typically densely welded tuff in ignimbrite flareups to a magma equivalent would only decrease the volume by 5% to 10%. Such conversions are small compared to the other uncertainties involved in the volume estimates, which include the amount of posteruption tectonic extension, paleotopography, intervening erosion, contouring, intracaldera fill thickness, etc. Moreover, distal fallout ash is not included. We estimate the volumes given herein might have errors of –20% to +50% (for discussion of error estimates, see Folkes et al., 2011; Best et al., 2013b, 2013c).

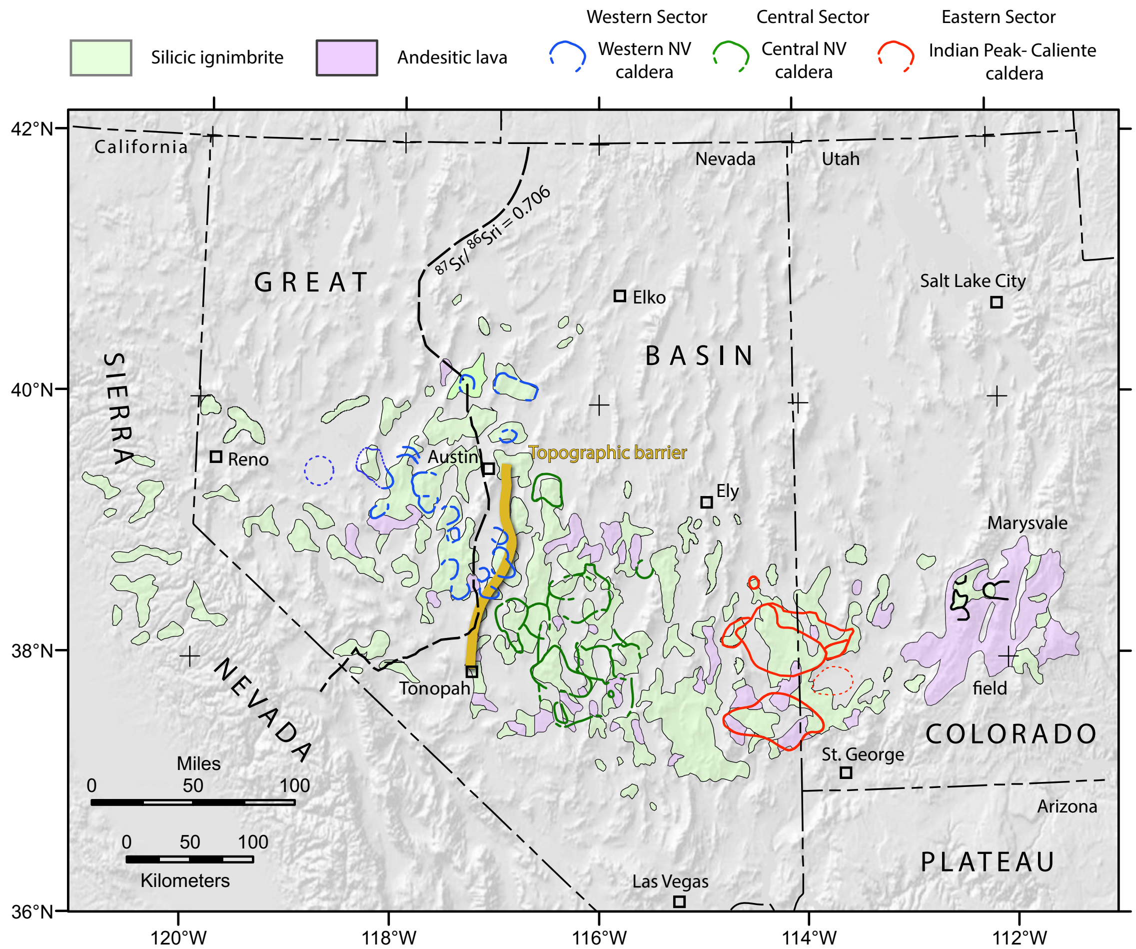

Figure 2. The southern Great Basin ignimbrite province in Nevada (NV) and Utah resulted from a 36–18 Ma flareup. Calderas (blue) in the western sector developed west of the edge of the Precambrian continental basement (indicated by the dashed initial $^{87}Sr/^{86}Sr$ = 0.706 line; modified from Wooden et al., 1999). Just to the east, the yellow band denotes an apparent topographic barrier on the western lip of the mid-Cenozoic Great Basin altiplano (Best et al., 2009). Calderas in the central (green) and eastern (red) sectors developed on the Great Basin altiplano. The Marysvale volcanic field (small calderas in black), which lies on the margin of the Colorado Plateau, although not part of the southern Great Basin ignimbrite province, is shown to indicate the contrasting dominance of andesitic lavas over silicic ignimbrites. Volcanic rock distribution is modified from Stewart and Carlson (1976).

assemblage of accreted Phanerozoic oceanic terranes including relict island arcs intruded by Mesozoic granitic plutons. In contrast, to the east (Figs. 2 and 3), the basement is Precambrian crystalline rocks, mainly Proterozoic igneous and metamorphic rocks with arc affinities (Whitmeyer and Karlstrom, 2007). Following the rifting of Rodinia in the Neoproterozoic, a thick prism of marine sediment accumulated on the rifted and thinned margin (Dickinson, 2006; Yonkee et al., 2014). This prism lies between the north-trending Wasatch hinge line in central Utah and the edge of the Precambrian basement in central Nevada (Fig. 4). Paleozoic strata are only ~1.5 km thick east of the hinge line, whereas to the west, the mostly carbonate rocks are ~12 km thick, and underlying predominantly siliciclastic late Proterozoic sedimentary rocks are 4–10 km thick (Stewart, 1980).

Farmer and DePaolo (1983) concluded that the lower crust in the eastern Great Basin consists of mostly felsic rocks that were thinned during the Neoproterozoic rifting, whereas the nonrifted crust under the Colorado Plateau of eastern Utah and western Colorado consists of stronger, more mafic rocks (Wannamaker et al., 2008; Lipman et al., 1978).

Initial Sr isotopic compositions of igneous rocks across the region reflect this inferred crustal composition (Fig. 5), with low values (<0.706) in western Nevada rising to as high as 0.718 eastward where the orogenically thickened wedge of sediment is the thickest, and then falling back to lower values across the Colorado Plateau and the San Juan sector of the Southern Rocky Mountain volcanic field in Colorado.

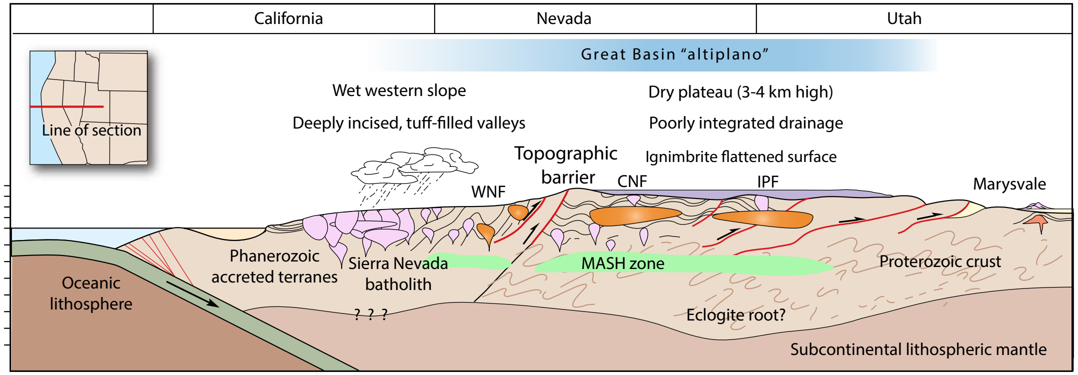

Figure 3. Conceptual east-west cross section at approximately 38.5°N through the mid-Cenozoic Great Basin altiplano showing unusually thick crust, especially beneath the eastern sector of the ignimbrite province (Indian Peak–Caliente volcanic field, IPF). The crust thins beneath the central sector (Central Nevada field, CNF), and still more on the western slope of the altiplano beneath the western sector (Western Nevada field, WNF). Note change in vertical scale at sea level. No horizontal scale is shown because of variable amounts of east-west crustal extension postdating mid-Cenozoic volcanism. Mesozoic plutons are shown in pink; caldera-forming mid-Cenozoic magma bodies are shown in orange. The distributions of the ignimbrite outflow sheets (Best et al., 2013c), coupled with stable isotope proxy data (Cassel et al., 2014), indicate the presence of a topographic divide near the western margin of the Precambrian crust in central Nevada. Thus, the Great Basin altiplano in eastern Nevada and western Utah was an internally drained plateau, whereas the west slope drained to the ancestral Pacific Ocean. Figure is modified from Best et al. (2009, their fig. 17). MASH zone—zone of melting, assimilation, storage, and homogenization.

The late Paleozoic–Mesozoic history of the region is dominated by the development of the Cordilleran orogenic belt during plate convergence (e.g., Burchfiel et al., 1992; DeCelles, 2004; Dickinson, 2006; Hintze and Kowallis, 2009). In central Nevada, Devonian–Jurassic thrust systems transported deep-water marine rocks eastward as much as 200 km onto shallower-water rocks (Fig. 4). In the eastern Great Basin area, during the Cretaceous Sevier orogeny, as many as eight extensive slices of Precambrian basement and overlying Phanerozoic sedimentary strata were transported eastward. Total east-west shortening across the Cordilleran orogenic belt in the Great Basin area at the latitude of central Utah is estimated to have been at least 350 km (DeCelles, 2004), creating thickened crust beneath a high-elevation plateau—the Great Basin altiplano (Fig. 3; Best et al., 2009). We believe it resembled in many respects the late Cenozoic Central Andean plateau, where the crust is 70–80 km thick (e.g., Yuan et al., 2002; McGlashan et al., 2008). In the Great Basin, the crust was as much as ~70 km thick in a roughly north-south belt in easternmost Nevada but thinned to perhaps 50–60 km to the west (Best et al., 2009; Coney and Harms, 1984; DeCelles, 2004; Chapman et al., 2015). Peak metamorphic conditions in the thicker eastern belt in the Late Cretaceous were ~800 °C at 35 km depth (DeCelles, 2004). For comparison, the temperature of typical continental crust at this depth would be 400 °C to 500 °C (Blackwell, 1971). Metamorphic grades were lower to the east and west, where the crustal thickness was less.

As large-scale contractile deformation waned during the Sevier orogeny, eastward-propagating crustal shortening began at ca. 75–66 Ma in the Rocky Mountain foreland in eastern Utah and western Colorado (Fig. 1), creating basement-cored uplifts. The magnitude of this Laramide deformation was much less than to the west. For example, in the Laramide foreland, including the Southern Rocky Mountain volcanic field, typical shortening was 10%–15%, whereas in the Sevier fold-and-thrust belt, shortening was 50% (Erslev, 1993). Laramide contraction continued until the beginning of the magmatic flareup, about 35 Ma in central Utah (Dickinson et al., 1988; Willis, 1999).

Subduction-related Jurassic magmatism extended far inland, reaching central Utah (Christiansen et al., 2015). Then, during the latest Cretaceous–Paleocene, arc magmatism ceased over much of the western United States (e.g., Lipman, 1992), manifesting shallow, or "flat," subduction of the oceanic Farallon plate (Coney and Reynolds, 1977; Severinghaus and Atwater, 1990; Humphreys, 2009; for a critique of the flat slab model, see Jones et al., 2011). Magmatism in the Great Basin area during the Late Cretaceous consisted of a few, strongly peraluminous two-mica granite plutons (initial Sr isotope ratios as high as 0.7246) in eastern Nevada just north of the Indian Peak caldera complex (Fig. 6). These peraluminous magmas originated by partial melting of metasedimentary rocks in the miogeoclinal wedge without input of mantle-derived basaltic magma (Best et al., 1974; Lee and Christiansen, 1983; Farmer and DePaolo, 1983).

Beginning in the Eocene, arc magmatism resumed north of the Great Basin at ca. 54–38 Ma in the Challis and Absaroka volcanic fields (Fig. 1). At about 45 Ma, magmatism began in the northern Great Basin and swept southward into southern Nevada, where it stalled in the mid-Miocene at about 15 Ma (Lipman et al., 1972; Christiansen and Lipman, 1972; Best and Christiansen, 1991, their fig. 2; Christiansen et al., 2007b). This time-transgressive arc magmatism was more or less parallel to the trench and corresponded with progressive steepening, or rollback, of the subducting Farallon slab that began first in the north and moved southward. Steepening of slab dip probably resulted from the combined effects of Siletzia accretion (Humphreys, 2009), the passage of a subducted oceanic plateau (Saleeby, 2003), and a slowing rate of convergence (Severinghaus and Atwater, 1990).

No basalt (International Union of Geological Sciences [IUGS] classification of Le Maitre, 1989) was extruded in the Great Basin until after ca. 20 Ma as the arc signature in the volcanic rocks disappeared, and intraplate, extension-related

Figure 4 is interactive. You can view different items in the legend by moving the cursor over them or you can toggle the symbols on and off with the Layers panel in Adobe Acrobat or Adobe Reader.

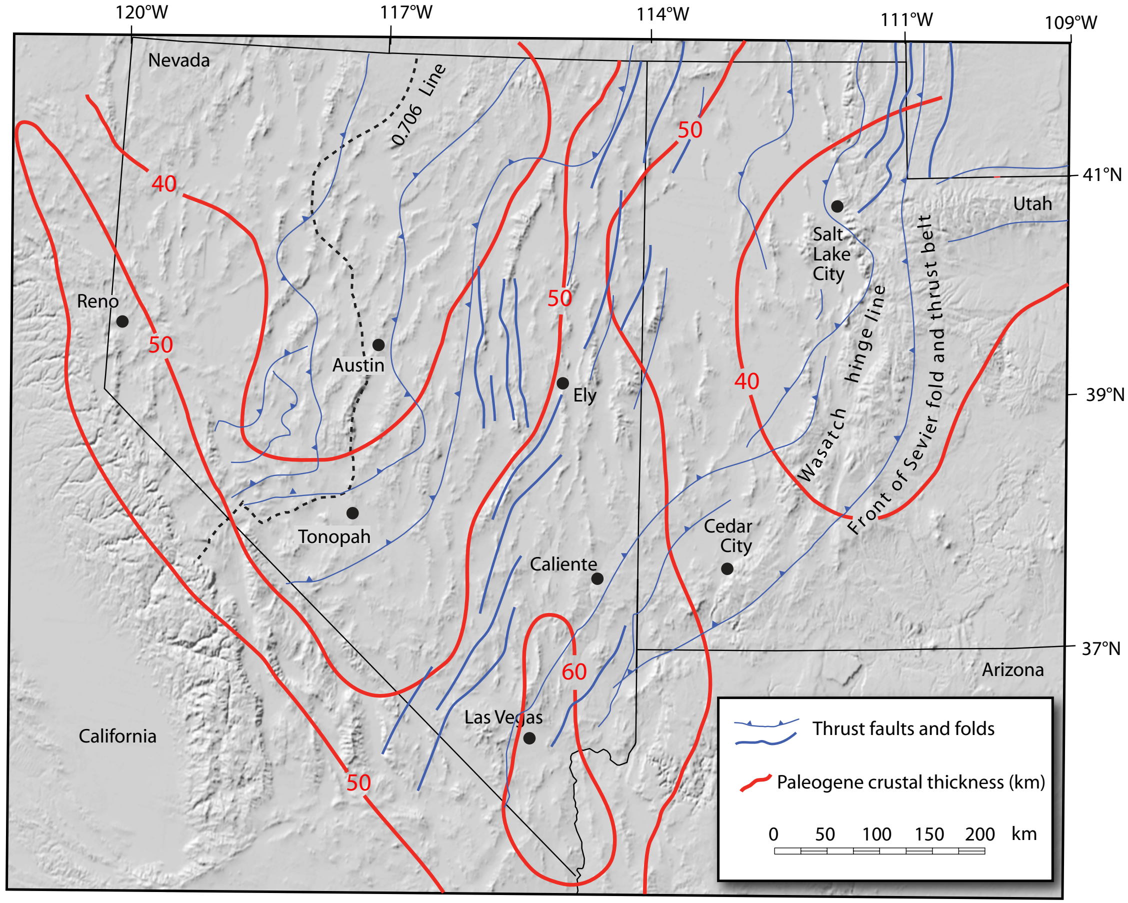

Figure 4. Major fold-and-thrust belts in the Great Basin of Nevada and western Utah (Oldow et al., 1989; McQuarrie and Chase, 2000; DeCelles, 2004; Long et al., 2014) and hypothetical contours (in km) of early Cenozoic (Paleogene) crustal thickness (Coney and Harms, 1984). The western edge of the Precambrian continental basement near 117°W is indicated by the black dashed $^{87}Sr/^{86}Sr_0$ = 0.706 line (modified from Wooden et al., 1999). The Wasatch hinge line passes approximately through Salt Lake City and Cedar City, Utah. Figure is modified from Best et al. (2009, their fig. 1).

compositions took their place (Christiansen et al., 2007a, their fig. 11). The extension-related bimodal suite included both aluminous and peralkaline rhyolites (e.g., Farmer et al., 1991). During the ignimbrite flareup, extrusion of intermediate-composition, chiefly andesitic, lavas was an order of magnitude smaller in volume than silicic explosive eruptions (Fig. 2; Best et al., 2013b, 2013c).

In western Utah and eastern Nevada, southward-sweeping magmatism (ca. 45–18 Ma) is expressed by more or less separate, subparallel, roughly east-west belts of volcanic rocks and minor granitic intrusions (e.g., Stewart and Carlson, 1976). The greatest volume of mid-Cenozoic volcanic rocks occurs in a swath of mostly mountain-range exposures of silicic ignimbrite and lesser andesitic lava extending from the southwestern corner of Utah westward across the southern Great Basin and beyond into the Sierra Nevada (Fig. 2). This is the 36–18 Ma southern Great Basin ignimbrite province.

Absence of Significant Regional Tectonic Extension during the Ignimbrite Flareup

Controversy surrounds the time when the orogenically thickened crust in the Great Basin altiplano was subjected to significant extensional faulting and thinning to its current thickness of ~30 km (Allmendinger et al., 1987). The timing of extensional thinning of the crust—before, during, or after the ignimbrite flareup—has a critical bearing on the role of crustal thickness in the ignimbrite flareup.

Prevolcanic extension has been advocated by, for example, DeCelles (2004, p. 149), who concluded that, in view of the excess gravitational potential energy residing in a thick orogenic plateau, “Within limits of available temporal resolution, hinterland extension and frontal thrusting were coeval in the

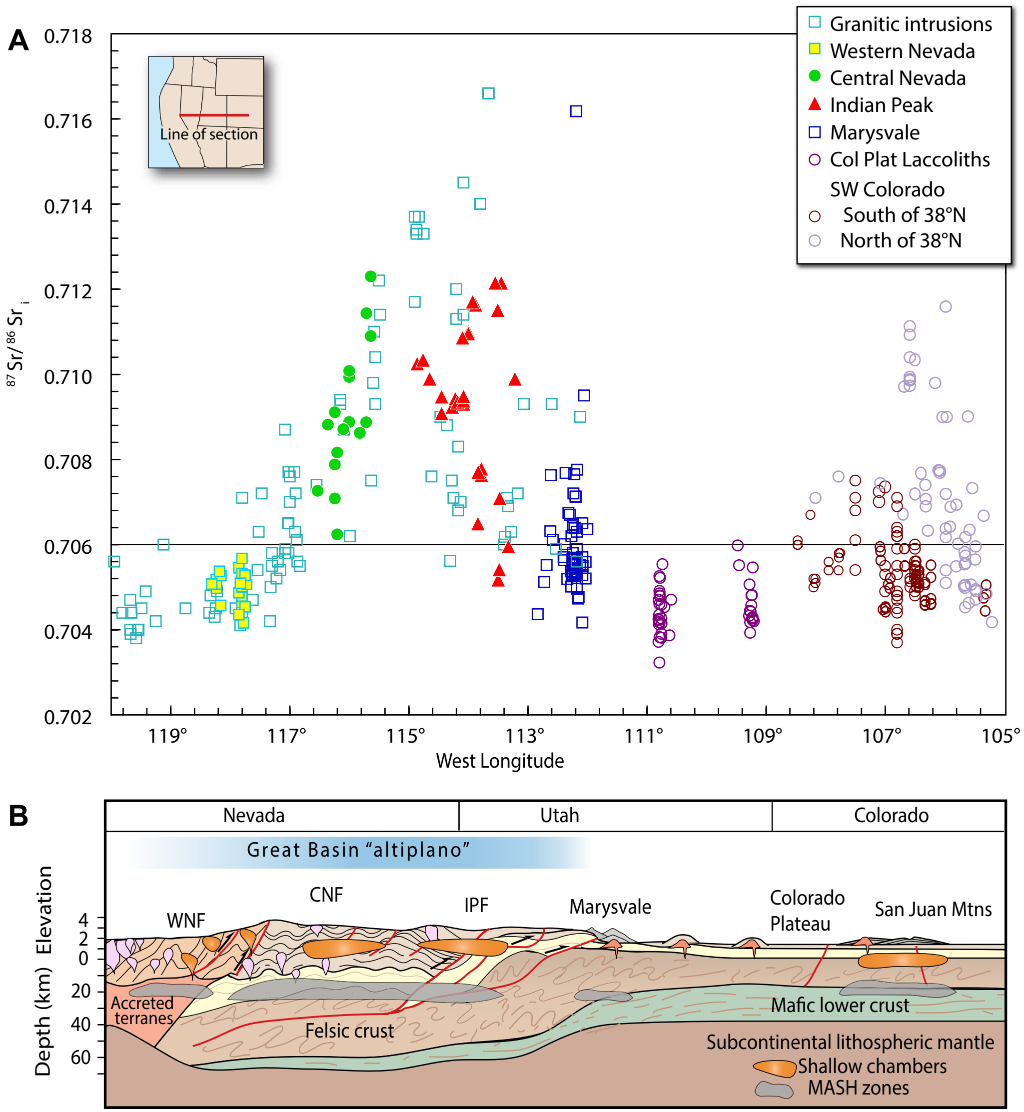

Figure 5. Sr isotopic compositions of igneous rocks in relation to composition and structure of the basement in the western United States. (A) Isotopic compositions of igneous rocks (ignimbrites, lavas, and intrusions) in Nevada, Utah, and Colorado between 37°N and 40°N. Some Mesozoic rocks are included in western Nevada as a proxy for Cenozoic volcanic rocks for which few data are available. Data are from: Southern Rocky Mountain volcanic field—Lipman et al. (1978), Johnson and Fridrich (1990), Stein and Crock (1990), Colucci et al. (1991), Campbell (1994), Riciputi et al. (1995), Parat et al. (2005), Memetti and Lipman (2014), and Lake and Farmer (2015); Colorado Plateau—Nelson and Davidson (1993, 1998); Marysvale—Cunningham et al. (1997); Great Basin—John (1992, 1995), Wooden et al. (1999), and Best et al. (2013a, 2013b). (B) Simplified cross section of the lithosphere underneath western North America during the Oligocene, constrained by the structures exposed at the surface and the Sr isotopic compositions in A. From west to east: young mafic accreted terranes, a thick sequence of continental margin sediments thickened further by Mesozoic thrusting, and mafic lower crust that is thin under the eastern Great Basin but thickens below the Colorado Plateau. MASH zones—zones of melting, assimilation, storage, and homogenization; IPF—Indian Peak–Caliente volcanic field; CNF—Central Nevada field; WNF—Western Nevada field.

Cordilleran thrust belt during Late Cretaceous time." However, he added that, "Paradoxically, no surface-breaking large-scale normal faults have been documented that might have facilitated this crustal extension." Long (2012) concurred that large-magnitude, regionally distributed, prevolcanic extensional faults do not exist in the Cordilleran hinterland.

Broad synchroneity of mid-Cenozoic volcanism and extension in the Great Basin was advocated by, for example, Gans et al. (1989), Constenius (1996), Humphreys (2009), and DeCelles et al. (2009); volcanism and coincident extension in some metamorphic core complexes were extrapolated over the entire Great Basin. However, in at least one of these metamorphic

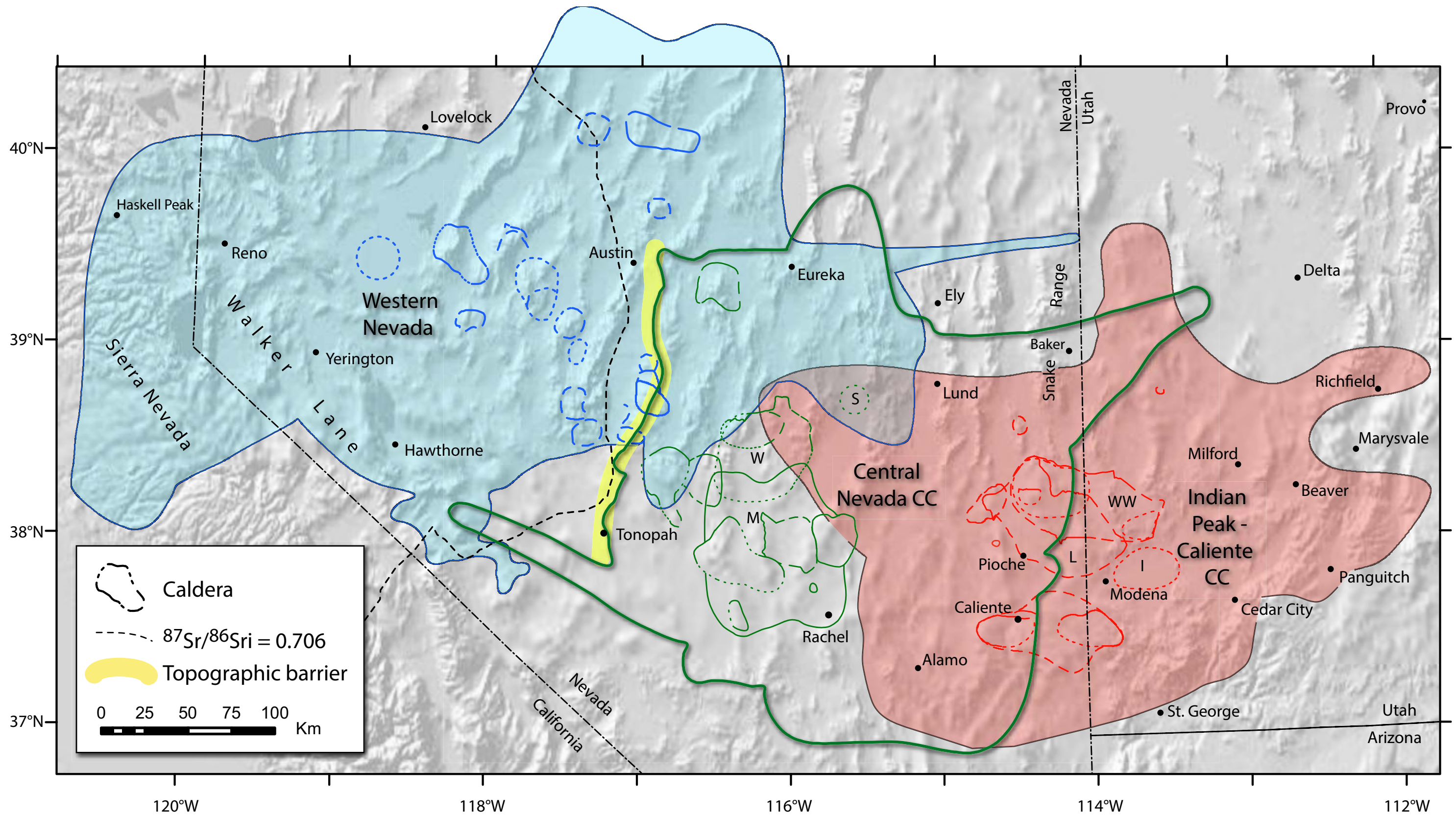

Figure 6. Map distinguishing three sectors of the 36–18 Ma southern Great Basin ignimbrite province (Fig. 2). Each is delineated by the outer limit of exposed outflow sheets that surround their source calderas (dashed lines indicate approximate locations where concealed beneath younger deposits). In the eastern sector, the Indian Peak–Caliente caldera complex (CC) and field (red): WW—source caldera of the Wah Wah Springs, L—Lund, and I—Isom ignimbrites. In the central sector, the Central Nevada caldera complex (CC) and field (green); source calderas are eccentrically positioned on the west side of the field, including those for the Windous Butte (W) and Monotony (M) ignimbrites. The partially overlapping Indian Peak-Caliente and Central Nevada fields formed on the mid-Cenozoic Great Basin altiplano east of a topographic barrier (yellow band) on its western lip that blocked the westward dispersal of all but the Monotony ash flow from Central Nevada calderas. Three ash flows from western Nevada calderas (blue—Henry and John, 2013) were dispersed to the east.

complexes, in the Snake Range in easternmost central Nevada, fission-track dating has revealed that large-magnitude extension in the early Miocene at 17 Ma had been "seriously underestimated" relative to the originally conceived "synvolcanic" late Eocene–early Oligocene extension (Miller et al., 1999, p. 902). Ward (1995) concluded that subduction-related ignimbrite flareups were related to changes to trench-normal extension. Bryan and Ferrari (2013) considered the Sierra Madre Orientale, the southern continuation of the U.S. flareup, to be an intraplate silicic large igneous province related to extension.

Because of the persisting viewpoint of synvolcanic extension during the ignimbrite flareup, we offer nine independent lines of evidence that, in our opinion, argue against significant regional extension during the ignimbrite flareup in the southern Great Basin province.

(1) There is a lack of substantial and widespread angular discordances and deposits of erosional debris within outflow ignimbrite sequences (Best and Christiansen, 1991; Best et al., 2013a, their fig. 7; Best et al., 2013b, their fig. 60; Best et al., 2013c, their figs. 28, 47, and 49).

(2) The ignimbrites cover a great areal extent. Had there been significant fault-induced synvolcanic topography, younger ash flows would not have been dispersed so widely from their sources (Best et al., 2013b, 2013c).

(3) Paleomagnetic directions are consistent throughout single widespread ignimbrites, coupled with significant differences between mean directions in

stratigraphically adjacent ignimbrites (Grommé et al., 1972; see also, for example, Best et al., 2013c, their fig. 48). Had the ignimbrites been draped over a highly faulted terrane, the distinctions between paleomagnetic directions of different ignimbrites would have been considerably blurred.

(4) In the eastern sector of the province, ratios of east-west to north-south dimensions of outflow sheets imply that east-west crustal extension took place after deposition of ignimbrites (Best et al., 2013b, their table 8).

(5) Structural and stratigraphic analyses of basin sediments in nearby areas of the Great Basin have shown that large-magnitude extension began in the Miocene, after ca. 23 Ma (e.g., Colgan and Henry, 2009; Henry et al., 2011; Smith et al., 1991; McQuarrie and Wernicke, 2005, their table 1; Anderson et al., 2013).

(6) Thermochronology of several ranges in the Great Basin shows that large-magnitude extension began after ca. 23 Ma (e.g., Miller et al., 1999; Stockli et al., 2001, 2002; Armstrong et al., 2003).

(7) Ren et al. (1989) and Kowallis et al. (1995) showed that Basin and Range extensional stresses were not recorded in microcracks in granites until after about 20 Ma.

(8) Stable isotope data (e.g., Mix et al., 2011; Folkes et al., 2013; Cassel et al., 2014) indicate that the high (~3.5 km) elevations of the Great Basin altiplano persisted to the late Oligocene, ca. 24 Ma.

(9) The elemental and isotopic compositions of the mid-Cenozoic volcanic rocks indicate the Great Basin crust was likely as thick as about 70 km in its eastern part, somewhat thinner westward, and had not yet been thinned by extension (Best et al., 2009).

We conclude that major regional tectonic extension and collapse of the Great Basin altiplano mostly followed the 36–18 Ma ignimbrite flareup in the southern Great Basin province. This evidence does not preclude local faulting and extension related to magma intrusion, caldera collapse, or resurgence.

CHARACTER OF THE SOUTHERN GREAT BASIN IGNIMBRITE PROVINCE

This mid-Cenozoic province is an exceptional example of the ignimbrite flareup style of continental arc volcanism because of its >230 explosive eruptions of silicic magma, at least 25 of which had volumes of 1000 to 5900 km^3, a provincewide volume on the order of 75,000 km^3, and ~50 calderas to as much as about 60 km in diameter (Table 1).

TABLE 1. DATA FOR SECTORS OF THE SOUTHERN GREAT BASIN IGNIMBRITE PROVINCE

Sector:	Western	Central	Eastern
Volcanic field:	Western Nevada	Central Nevada	Indian Peak–Caliente
Mid-Cenozoic crust thickness (km)	~50	~60	~70
Ignimbrite age (Ma)	34–23, 19	36–18	36–18
Present area of field (km^2)*	100,000	65,000	60,000
Calderas, number	23 (possibly 37)	11 (1 concealed)	9 (8? concealed)
Calderas, maximum diameter (km)	~35 (N-S)	~50 (N-S)	60 (N-S)
Volume contemp. andesitic lavas (km^3)	~200	~2000	~3900
Volume ignimbrite (km^3)†	15,000–20,000?	25,000	33,000
Volume ratio andesitic lavas:ignimbrites	0.01?	0.08	0.12
Ignimbrite cooling units			
Recognized total	>100	~76	>51
Regional (>100 km^3)	20?	20?	22
Super-eruptive (>1000 km^3)	13?	Possibly 8	At least 7
Monotonous intermediates§	0	1	3 (4?)
Smaller phenocryst-rich dacite	1?	0	1
Calc-alkaline rhyolite	28	16	10
Alkalic rhyolite	15	4	4
Zoned rhyolite-dacite		2	2
Rhyolite-trachydacite	At least 4	0	0
Isom-type trachydacite	2; very small	9; ~600 km^3	8; 4200 km^3
Peraluminous	0	0	0

*Uncorrected for east-west postvolcanic extension.
†All volume estimates used are considered to be minimum magma equivalent volumes.
§Super-eruption.

Rock Compositions

Rhyolite ignimbrites of all ages (36–18 Ma) occur throughout the province and are accompanied by temporally more restricted dacite and trachydacite ignimbrites, especially in the eastern sector (Fig. 7). Most ignimbrites contain variable proportions of plagioclase, sanidine, quartz, biotite, hornblende, Fe-Ti oxides, pyroxene, and trace amounts of zircon, apatite, and, rarely, titanite, that equilibrated in relatively wet magmas at shallow crustal depths of 7–9 km. Dacites show phenocryst-rich compositions, upward of 50% of the tuff on dense rock equivalent basis (Best et al., 2013b); nearly all formed by super-eruptions, and their relatively unzoned, uniform nature qualifies them as monotonous intermediates in the sense of Hildreth (1981). These dacite magmas are interpreted to have originated by mixing of andesitic and rhyolitic magmas in the deeper crust (Best et al., 2013b). Unusual trachydacites (Best et al., 2013b) have sparse (<15%) phenocrysts of plagioclase, two pyroxenes, and Fe-Ti oxides that were derived from drier, hotter magmas equilibrated at greater crustal depth. These Isom-type tuffs (Figs. 7–9) have >300 ppm Zr and high TiO_2/CaO ratios.

Ignimbrites are alkalic to calcic (Fig. 8); their high-K to shoshonitic nature (Fig. 9) is consistent with the thick crust in which the magmas originated.

Intermediate-composition lavas in the southern Great Basin province are mostly high-K andesite (Best et al., 2009). Notably, their volume is an order of magnitude less than that of silicic ignimbrite (Table 1; Stewart and Carlson, 1976; Best et al., 2013b, 2013c). As previously indicated, basalt is absent until after ca. 20 Ma.

Lavas and ignimbrites have an arc geochemical signature—wet, oxidized, with low Fe/Mg ratios, enrichments of fluid-soluble elements, and depletions of high field strength elements, producing high Ba/Nb ratios (Best et al., 2013b, 2013c; Henry and John, 2013). Sr and O isotopic ratios are high and consistent with the assimilation of large proportions of felsic crust in the eastern sector of the Great Basin province; Sr isotope ratios are much lower in the western sector, where the crust is younger and more mafic (Figs. 5 and 10).

Three Sectors

The southern Great Basin province is conveniently divided into three contrasting sectors, each corresponding to discrete clusters of calderas surrounded by more or less separate ignimbrite outflow fields (Fig. 6; Table 1). In the eastern sector, the Indian Peak–Caliente field (Best et al., 2013b) surrounds the nested calderas of the Indian Peak–Caliente caldera complex astride the Utah-Nevada state line. In the central sector of the southern Great Basin province, the Central Nevada caldera complex of nested sources is surrounded by the Central Nevada field, the defining ignimbrite outflow sheets of which partly overlap those of the Indian Peak–Caliente field. All but one ash flow from Central Nevada caldera sources lie entirely to the east of a north-south topographic barrier, or drainage divide, near the western edge of the Precambrian basement (Figs. 2, 3, and 6; Best et al., 2009, 2013c). In the western sector of the Great Basin province, the Western Nevada ignimbrite field surrounds 23

Figure 7 is interactive. You can view different items in the legend by moving the cursor over them or you can toggle the symbols on and off with the Layers panel in Adobe Acrobat or Adobe Reader.

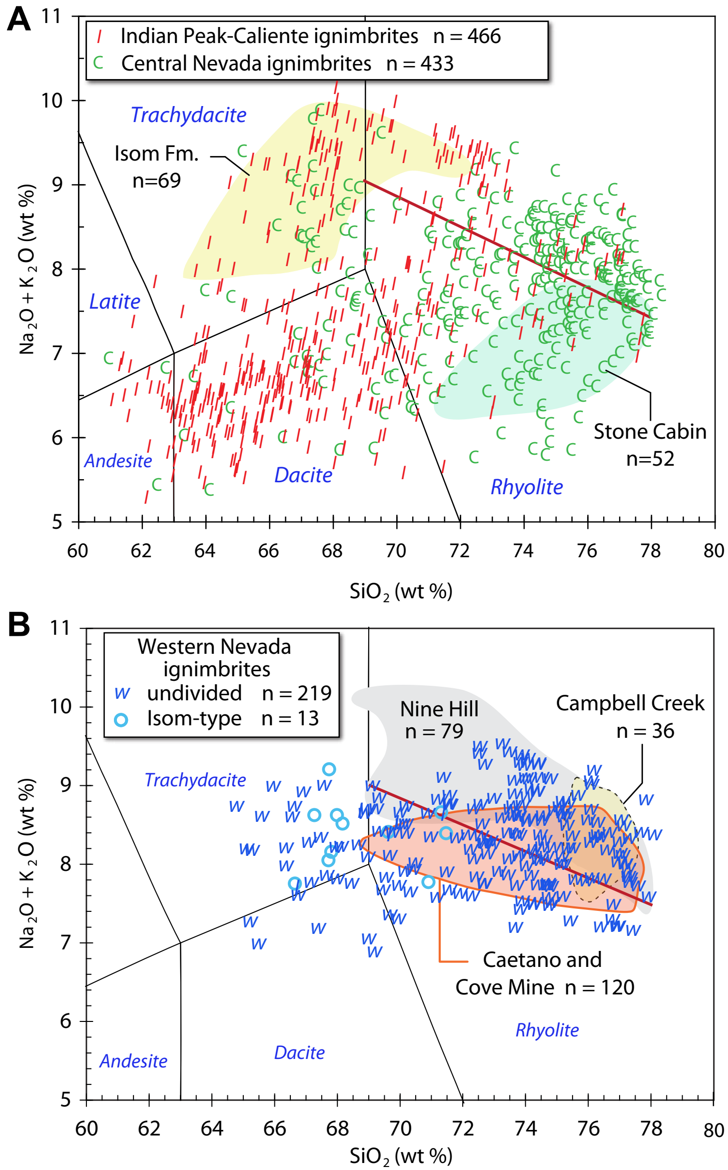

Figure 7. International Union of Geological Sciences (IUGS) classification (Le Maitre, 1989) for southern Great Basin ignimbrites. Red line separates alkalic (above) from calc-alkaline (below) rhyolites. (A) Central Nevada and Indian Peak–Caliente fields (central and eastern sectors). Nearly all the trachydacite ignimbrites are Isom type (yellow shade). (B) Western Nevada field (western sector). For clarity, fields for four much-analyzed ignimbrites are shaded. Many trachydacites in this sector are not Isom type, and dacites and calc-alkaline rhyolites are less common than in A.

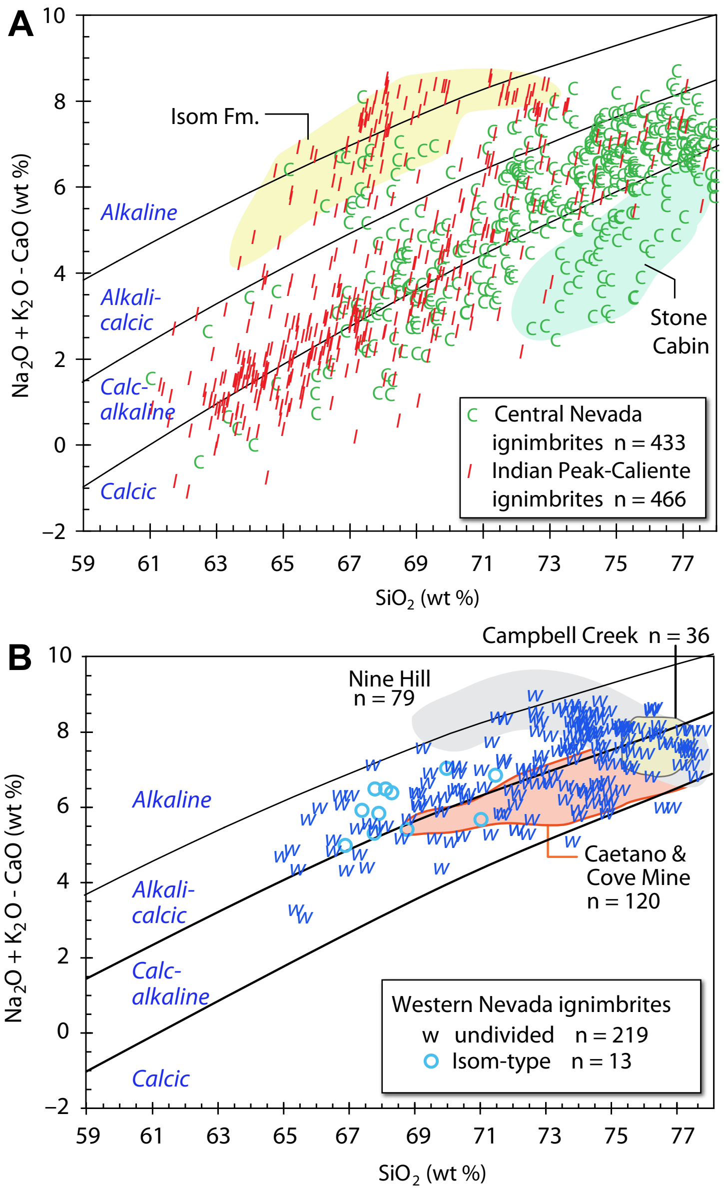

Figure 8. Modified alkali-lime index (Frost et al., 2001) for southern Great Basin ignimbrites. (A) Central Nevada and Indian Peak–Caliente fields. Nearly all alkaline and alkali-calcic samples are trachydacitic Isom-type ignimbrites (yellow shade). (B) Western Nevada field. Four ignimbrite units are shaded, as in Figure 7. Calcic ignimbrites are absent; compare with A.

Figure 8 is interactive. You can view different items in the legend by moving the cursor over them or you can toggle the symbols on and off with the Layers panel in Adobe Acrobat or Adobe Reader.

known source calderas that are more widely scattered and apparently smaller than those to the east.

In the western sector, dacites are rare, and rhyolites dominate (Figs. 7, 11, and 12); subordinate trachydacites have mineral assemblages that equilibrated—like rhyolites—in relatively wet magmas. Notably, ignimbrites are relatively more alkalic overall (Figs. 8 and 9) because of greater concentrations of Na_2O. In contrast, all trachydacites to the east are Isom type. These tuffs are especially voluminous in the eastern sector, where immediately older phenocryst-rich dacites, or monotonous intermediates, are the dominant ignimbrite. In the central sector, both Isom-type tuffs and monotonous intermediate ignimbrites are less voluminous than to the east.

Figure 13A reveals further details of the ignimbrites in the eastern sector. After a few million years of small, precursory rhyolite eruptions, three super-eruptions totaling 12,300 km^3 of monotonous intermediate magmas occurred from 31.1 to 29.2 Ma (all $^{40}Ar/^{39}Ar$ ages are based on an age of 28.20 Ma for the Fish Canyon Tuff). The source calderas of these three eruptions overlap (Fig. 14), indicating a sustained and narrowly focused supply of a large volume of crystal-rich dacite magma to the shallow crust in just a few million years. Following this burst of activity, at least four Isom-type trachydacite ignimbrites totaling 3600 km^3 were erupted from a concealed source just to the southeast at 27.9 to 27.3 Ma (Fig. 6). After a hiatus in explosive activity of ~4 m.y., voluminous eruptions from nested calderas in the Caliente complex (Fig. 6) occurred episodically until ca. 18 Ma; rhyolite dominated, but a super-eruption of 2200 km^3 at 22.6 Ma created an unusual phenocryst-rich, andesite-latite ignimbrite that may be a monotonous intermediate unit.

The central sector of the province (Fig. 13B) shares aspects with the adjacent sectors to the west and east. To the west, most eruptions were of rhyolite, but, in the central sector, three super-eruptions totaling 4500 km^3 of monotonous intermediate dacite occurred in rapid succession at 27.6 Ma. Only about 600 km^3 of slightly younger Isom-type trachydacite is recognized. In lieu of an earlier monotonous intermediate ignimbrite paralleling the brief burst of this activity in the eastern sector, 4800 km^3 of zoned rhyolite-dacite erupted at 31.7 Ma.

As previously noted, during the mid-Cenozoic ignimbrite flareup, the crust in the western sector of the southern Great Basin province was thinner (~50 km), younger, and more mafic (accreted Phanerozoic oceanic terranes) than the two eastern sectors, which were founded on thicker Precambrian metamorphic-granitoid basement covered by a thick wedge of sedimentary rock (Fig. 3). How these east-west contrasts in the crust influenced the contrasting nature of the ignimbrites in the province will be considered after a review of other Cenozoic volcanic fields.

COMPARISONS WITH OTHER CENOZOIC VOLCANIC FIELDS

Mid-Cenozoic fields in southwestern North America (Fig. 1; Table 2) developed on continental crust above subducting oceanic lithosphere (e.g., Severinghaus and Atwater, 1990; DeCelles, 2004; Dickinson, 2006; Humphreys, 2009).

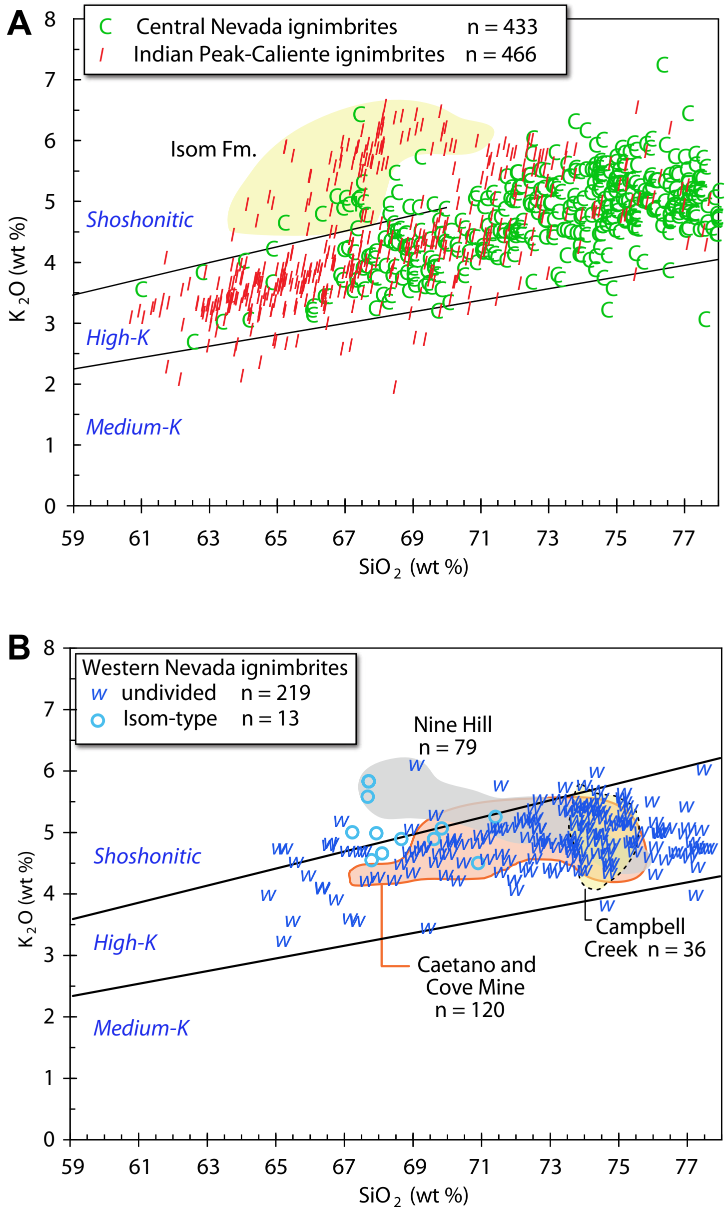

Figure 9. K_2O-SiO_2 classification of Ewart (1982) and Le Maitre (1989). (A) Central Nevada and Indian Peak–Caliente fields. Nearly all of the shoshonitic samples with <73 wt% SiO_2 are trachydacitic Isom-type ignimbrites. (B) Western Nevada field. Four ignimbrite units are shaded.

Figure 9 is interactive. You can view different items in the legend by moving the cursor over them or you can toggle the symbols on and off with the Layers panel in Adobe Acrobat or Adobe Reader.

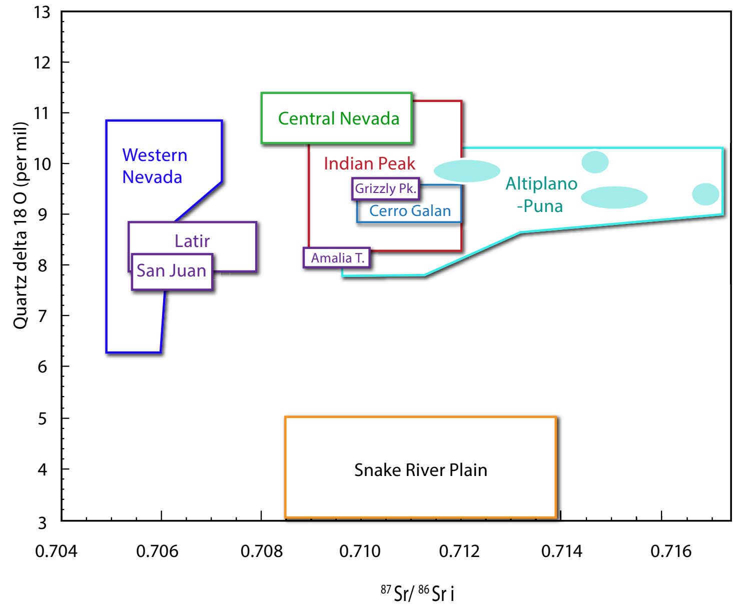

Figure 10. Sr-O isotope relations for quartz-bearing rhyolites and dacites from flareup volcanic fields. Peraluminous tuffs from the Altiplano-Puna are shown as light blue ellipses. Most of the rocks from the Southern Rocky Mountain volcanic field fall in the boxes for the San Juan and Latir centers, but the Grizzly Peak Tuff from the northern part of the field and the peralkaline Amelia Tuff from southern have distinctly higher initial Sr isotope ratio. Data are from: Indian Peak and central Nevada—Best et al. (2013a, 2013b), Hart (1997), and Larson and Taylor (1986); for western Nevada—Henry et al. (2013) and Colgan et al. (2013); San Juan focus—Larson and Taylor (1986) and Lipman et al. (1978); Grizzly Peak—Johnson and Fridrich (1990); Latir—Johnson et al. (1990); and the Altiplano-Puna—Kay et al. (2010, 2011) and Folkes et al. (2013). Low ^{18}O rhyolites from the Central Snake River Plain are shown for comparison (Boroughs et al., 2005; Ellis et al., 2013).

The mid-Cenozoic volcanic rocks in these fields possess arc chemical signatures consistent with a subduction heritage: Marysvale (Cunningham et al., 1997); Southern Rocky Mountain (Lipman et al., 1978; Askren et al., 1997; Bachmann et al., 2002; Parat et al., 2005); Mogollon-Datil (Bornhorst, 1980; Davis et al., 1993); Sierra Madre Occidental (Ferrari et al., 2007). The flareups, which totaled perhaps 400,000 km^3 of ignimbrite in these volcanic fields, were nearly synchronous from ca. 36 to 18 Ma, with the greatest eruptive volumes ca. 32 to 23 Ma.

Marysvale Volcanic Field and Colorado Plateau Laccoliths: No Ignimbrite Flareup

This modest-sized field, which contains a cluster of small calderas, lies just east of the southern Great Basin ignimbrite province on the northwestern margin of the Colorado Plateau; it was active ca. 28–19 Ma (Table 2; Figs. 1

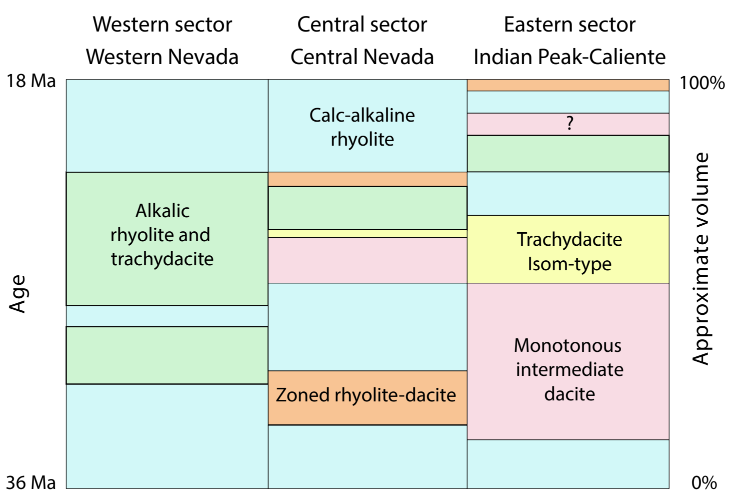

Figure 11. Schematic comparison of approximate volumes and eruptive times of ignimbrite types in the three sectors of the southern Great Basin province.

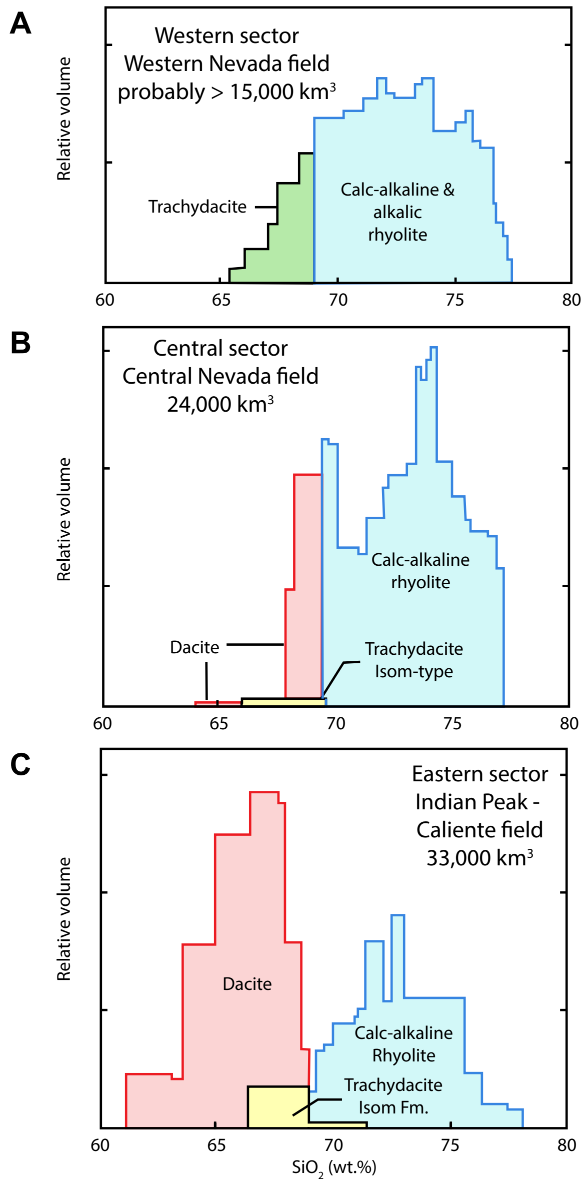

Figure 12. Volume-silica relations of ignimbrites in the southern Great Basin ignimbrite province. (A) Western Nevada field (Henry and John, 2013). Volumes are probably minimum estimates because many units have few chemical analyses. A small volume of dacite is not shown. (B) Central Nevada field. (C) Indian Peak–Caliente field. In B and C, virtually all of the dacite consists of four (1 and 3, respectively) super-eruptive monotonous intermediate ignimbrites.

and 2; Steven et al., 1984; Cunningham et al., 2007; Rowley et al., 2002). The time-composition pattern from early phenocryst-rich dacite ignimbrite to trachydacite and then rhyolite mimics the trend in the adjacent eastern sector of the Great Basin province (Fig. 15). However, the Marysvale field differs from the Great Basin province. The number (7) and the total volume (~1000 km^3) of ignimbrite eruptions are an order of magnitude smaller. The dominant volume (11,000 km^3) of the Marysvale field consists of coalesced andesitic-dacitic stratovolcanoes that were built primarily about 26–23 Ma. The initial Sr isotopic composition of the tuffs and lavas is significantly lower than for the adjacent Great Basin (Fig. 5; Cunningham et al., 1997).

These contrasts with the contemporaneous Great Basin ignimbrite flareup are likely related, at least in part, to thinner crust (currently ~30 km) beneath the Marysvale field. This crust might have been thicker during volcanism, because late Cenozoic extensional tectonism has thinned the crust below the western part of the field (Wannamaker et al., 2008). Crust to the east, under the essentially unextended Colorado Plateau (<3%; according to Davis, 1999), is ~45 km thick. The low Sr isotope ratios and some of the compositional differences are probably due to the more mafic lower crust beneath this region, as noted previously.

Farther east on the Colorado Plateau (Fig. 1), mid-Cenozoic magmatism generated local, highly alkaline dikes (e.g., Tingey et al., 1991), explosive breccia pipes (Usui et al., 2003), and shallow, composite laccolithic complexes mostly intruded at 29–23 Ma (Nelson et al., 1992). The laccoliths have a relatively modest cumulative volume (estimated ~140 km^3) and are composed almost entirely of a sodic diorite porphyry that is depleted in Nb and Ti, manifesting an arc signature (Nelson and Davidson, 1993, 1998). Low initial Sr iso-

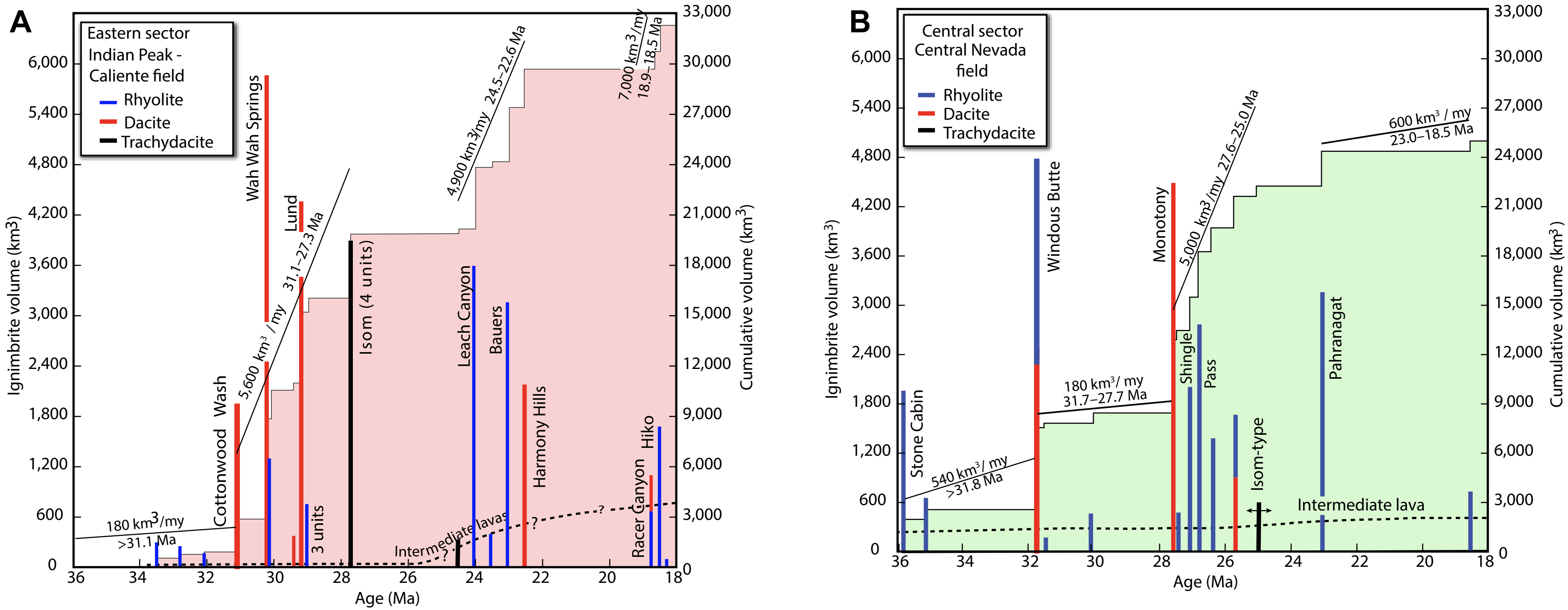

Figure 13. Volume-time relations of silicic ignimbrites and intermediate-composition lavas in the two eastern sectors of the Great Basin province. Larger-volume ignimbrites are named. Monotonous intermediates (phenocryst-rich dacite) are shown with blue vertical lines, rhyolite is shown in red, and Isom-type ignimbrites are shown in black. Shaded area indicates cumulative ignimbrite volume. Sloping lines show rates of erupted ignimbrite volume for the indicated time periods. Lulls in explosive activity are as long as ~4 m.y. Roughly estimated cumulative volume of intermediate-composition (mainly andesite) lavas is shown with a dashed line; their volume is an order of magnitude less than that of ignimbrite. (A) Indian Peak–Caliente field (Best et al., 2013b). For the trachydacitic Isom Formation, at least four cooling units erupted at 27.90–27.25 Ma are indicated by a single line at 27.7 Ma. (B) Central Nevada field (Best et al., 2013c). Several cooling units of Isom-type tuff deposited ca. 27–23 Ma are shown as a single line at 25.0 Ma. Bicolor Windous Butte is a zoned rhyolite-dacite.

tope ratios <0.706 and common xenoliths of amphibolite indicate derivation from a mafic crustal source. This magmatism is strikingly different from that in contemporaneous volcanic fields to the west and east.

Southern Rocky Mountain Volcanic Field

In this major well-documented field on the northeastern margin of the Colorado Plateau (Fig. 1; Table 2; Lipman, 2007; Lipman and Bachmann, 2015), 28 regional ignimbrites (>100 km^3) were emplaced from 21 exposed calderas at 37 to 23 Ma. At about 26 Ma, magmatism switched to a more bimodal assemblage related to opening of the Rio Grande rift immediately east of most of the source calderas (Lipman et al., 1978). Thus, the Southern Rocky Mountain field lacks the youngest 5 m.y. of explosive activity evident in the southern Great Basin province. The south-southwest sweep of volcanism in the field resembles that in the Great Basin: Ignimbrites erupted at 37–33 Ma in the north, at 25 Ma in the south, and as young as 23 Ma in the west; peak activity was from 32 to 27 Ma, without a clear space-time pattern in the central, or San Juan Mountains, sector. Significantly, caldera fills are dominated by intermediate-composition lavas, with only modest proportions of sediment, whereas southern Great Basin calderas are mostly filled by ignimbrite.

As in the southern Great Basin, regional faulting that could generate major topographic barriers was absent during the main ignimbrite flareup; ash flows from western sources were able to traverse the future Rio Grande rift and spread widely to the east. Most ignimbrites (37–27 Ma) erupted prior to the surface expression of extensional faulting, through crust characterized by a neutral stress field, as indicated by development of radial dike swarms around central volcanoes. The two youngest major ignimbrites, the peralkaline Amalia Tuff (25 Ma) and Sunshine Peak Tuff (23 Ma), bridge the transition to inception

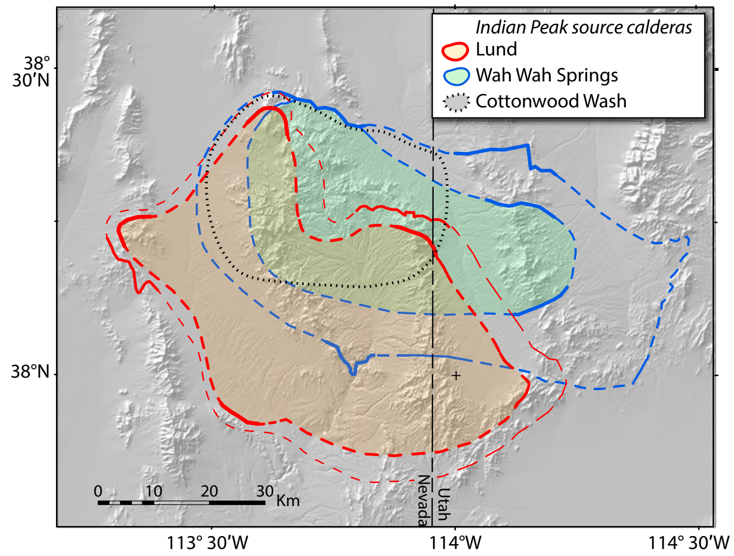

Figure 14. Overlapping source calderas for three super-eruptive monotonous intermediate ignimbrites in the Indian Peak complex. Structural calderas within ring faults for the 30.06 Ma Wah Wah Springs and 29.20 Ma Lund tuffs are shaded; margins are solid where definite and dashed where approximate or inferred. Compensating for postcaldera east-west crustal extension reduces the distance between the topographic and structural margins of the Wah Wah Springs caldera. Thickness and distribution of the outflow sheet of the 31.13 Ma Cottonwood Wash ignimbrite indicate its source caldera lies within the area enclosed by dotted black line, but because it was engulfed in the younger calderas, its true perimeter is unknown.

of regional extension along the Rio Grande rift zone. Another similarity to the Great Basin is the near absence of basalt during the flareup.

Ignimbrites in the Southern Rocky Mountain field have a comparable range in silica to those in the southern Great Basin province, but they tend to be more alkalic (Figs. 16A and 7A) because of relative enrichment in Na; in this respect, the field is like the Western Nevada field (Fig. 7B). Southern Rocky Mountain tuffs tend to have less hornblende and quartz than Great Basin tuffs, but clinopyroxene is more common. This implies that the magmas were drier, hotter, or crystallized at a lower pressure than their equivalents in the Great Basin. Sr and Nd isotopic compositions suggest less of a metasedimentary upper-crustal component, especially for the San Juan sector; no thick miogeoclinal section underlies this region (Fig. 5; Lipman et al., 1978; Riciputi et al., 1995). The $\delta^{18}O$ values of quartz are also lower, about 7.5‰ to 8‰, in the Fish Canyon Tuff, and as high as 8.2‰ in a few rhyolites (Larson and Taylor, 1986), compared to 8.3‰ to 11.1‰ for quartz from dacites and rhyolites in the central and eastern sectors of the Great Basin province (Fig. 10; Hart, 1997; Larson and Taylor, 1986). Just as in the southern Great Basin, compositions of ignimbrites from the Southern Rocky Mountain field display distinct temporal and geographic diversity. In comparison to the peak flareup in the central San Juan region, early northern ignimbrites (Sawatch trend) tend to be more alkalic (higher Zr and incompatible elements, more sodic sanidine) and have higher Sr isotope and $\delta^{18}O$ values (Fig. 10). Ignimbrites erupted from southeastern and western San Juan sources also differ from the central locus, mainly crystal-rich dacites in the southeast, crystal-poor rhyolites from western calderas, all lacking large compositional zonations, and also characterized by subtle regional isotopic differences (Lipman et al., 1978; Lake and Farmer, 2015).

The largest eruption in the field was the 28.2 Ma Fish Canyon Tuff with a magma volume of 5000 km^3 (Fig. 17A). The 34.2 Ma Badger Creek Tuff is a compositional clone, but only sparse remnants are preserved, making accurate volume estimates uncertain (>500? km^3). Most samples of the Fish Canyon Tuff (Fig. 16A) are dacite, but some with about 68% silica and upwards of 8% total alkalis are trachydacite. Mineralogically, the Fish Canyon Tuff is nearly identical to the 29.20 Ma Lund Tuff and similar to other Great Basin phenocryst-rich dacites, or monotonous intermediates (Figs. 13; Bachman et al., 2002). Apparently all shared similar crystallization conditions—about 2.5 kbar and 750–800 °C under water-undersaturated and oxidized conditions (Johnson and Rutherford, 1989).

Tuffs compositionally similar to the Isom-type trachydacites are not obvious in the Southern Rocky Mountain field (Fig. 16). In comparison to the phenocryst-poor (<15%) plagioclase-pyroxene Isom-type tuffs, phenocrysts are more abundant in the Southern Rocky Mountain trachydacitic tuffs (typically 20%–25%). The mineral assemblage (plagioclase, sanidine, biotite, and sparse hornblende) appears to record wetter and cooler magmatic environments than for the Isom-type tuffs in the Great Basin. In the more alkalic Latir volcanic locus, the youngest and southernmost part of the Southern Rocky Mountain field, Isom-type tuffs are also absent, although some precaldera trachydacite lavas are chemically similar to western Nevada Isom types. In addition, comendite lavas and the Amalia Tuff could be evolved Isom-type magma in terms of Ca-Ti-Zr, and alkali contents. However, these high-Zr rocks are peralkaline rhyolites, not trachydacites like those from the Great Basin.

With the exception of the 5000 km^3 Fish Canyon Tuff, volumes of individual ignimbrite eruptions are 1000 km^3 or less (Lipman and Bachmann, 2015); however, extreme synvolcanic erosion of the early ignimbrites makes their volume estimates especially uncertain. Unlike the southern Great Basin province, where eruptive activity was spread more or less uniformly throughout the flareup (Fig. 13; see also Henry and John, 2013), the Southern Rocky Mountain field has a well-defined peak in explosive eruptions of silicic magma from 30.3 to 27.1 Ma, during which 16 ignimbrites, each 100 to 1000 km^3, were erupted from the San Juan locus, before and following the 5000 km^3 Fish Canyon culmination at 28.2 Ma (Fig. 17A). This peak activity involved two thirds of the ignimbrite eruptions in less than one fifth the time of all the activity, and it constituted four fifths of the total ignimbrite volume in the field.

A prominent feature of the Southern Rocky Mountain field is the subordinate total volume of silicic ignimbrite (>17,000 km^3) relative to intermediate-composition lavas (~40,000 km^3) that built coalescing stratovolcanoes during

TABLE 2. OTHER FLAREUP FIELDS IN THE WESTERN AMERICAS (COMPARE TABLE 1)

Volcanic field	Marysvale*	Southern Rocky Mountain	Mogollon-Datil	Sierra Madre Occidental	Altiplano-Puna volcanic complex
Location	NW margin CP†	NE margin CP†	S margin CP†	Mexico	Central Andes
Mid-Cenozoic crust thickness (km)	>30	40–45	>40	~40 (55?)	Presently 58–76
Ignimbrite age (Ma)	28–19	37–23	36–24	34–28, 24–18	10–1
Present area of field (km^2)	15,000	>100,000	60,000	400,000	70,000
Calderas (number)	5	21	10	Possibly 350	6 known
Caldera maximum dimension (km)	25	75	40	35	60
Volume contemp. andesitic lavas (km^3)	11,000	40,000	Several 1000	Several 1000	<1000
Volume ignimbrite (km^3)§	1000	~17,000	>9000	400,000	>15,000
Volume ratio andesitic lavas:ignimbrites	11	2.4	>1?	?	<0.08
Ignimbrite cooling units					
Recognized total	7	28	44	100s	>30
Regional (>100 km^3)	4	25	19	?	>14
Super-eruptive (>1000 km^3)	0	6 (5 at 1000 km^3)	6 (<1250 km^3)	?	10
Monotonous intermediates#	0	1 (possibly 2)	0	None reported	10
Smaller phenocryst-rich dacite	2		0	?	>10
Phenocryst-rich trachydacite		12			
Calc-alkaline rhyolite	1	0	>3	Some	4
Alkalic rhyolite	2	>5	>17	Dominant	Some
Zoned rhyolite-dacite	0	0	2**	?	1
Alkalic rhyolite-trachydacite	0	>7	>1		
Isom-type trachydacite	3 very small	0	None reported	None reported	0
Peraluminous	0	0	0	0	At least 4

*Not a bona fide flareup field because of small size and number of ignimbrites; shown here only for comparison.
†CP—Colorado Plateau.
§All volume estimates used are considered to be minimum magma equivalent volumes.
#Super-eruption.
**Range to alkali rhyolite.

early activity and makes up most of the postcollapse caldera fills (e.g., Lipman, 2007). In this respect, the field is like the Marysvale field, on the opposite side of the Colorado Plateau, in having more lava than ignimbrite (Table 2).

The crust beneath the Southern Rocky Mountain volcanic field is currently 40 to 45 km thick; high regional elevations are supported by low crustal densities, rather than greater crustal thickness such as that under the High Plains to the east of the mountain front (Prodehl and Lipman, 1989; Gilbert, 2012; Hansen et al., 2013; Lipman and Bachman, 2015). Modest late Cenozoic extension along the Rio Grande rift apparently has not significantly modified crustal thickness beneath the volcanic field.

Mogollon-Datil Volcanic Field

In this field on the southern side of the Colorado Plateau (Fig. 1), volume-time relations for ignimbrites are similar to those in the Southern Rocky Mountain field, with a less well-defined peak in eruptions but at about the same time (Fig. 17B). However, individual eruptive and total volumes are smaller; five eruptions were >900 to 2200 km^3, and the total volume is >9000 km^3 (McIntosh et al., 1992). Eruptive activity migrated west to northwest through time. The ignimbrites are mostly alkalic rhyolite and lesser trachydacite; dacite tuffs are rare (Fig. 18A), and Isom-type tuffs have not been reported. Thus, the field resembles the western sector of the southern Great Basin (Fig. 7B). Like the Marysvale and Southern Rocky Mountain volcanic fields elsewhere on the margin of the Colorado Plateau, but unlike the southern Great Basin province, intermediate-composition lavas constitute a major proportion of the volcanism (Table 3).

The field currently lies on crust that is ~40 km thick (Prodehl and Lipman, 1989; Schneider and Keller, 1994), but variable postvolcanic extension, particularly in the south, makes this value a minimum during the ignimbrite flareup.

Sierra Madre Occidental Province

Products of the ignimbrite flareup in this remote province in Mexico (Fig. 1) cover an area of about 400,000 km^2 to depths of as much as 1 km. Only about 10% has been mapped geologically, chiefly along its margins, and less than

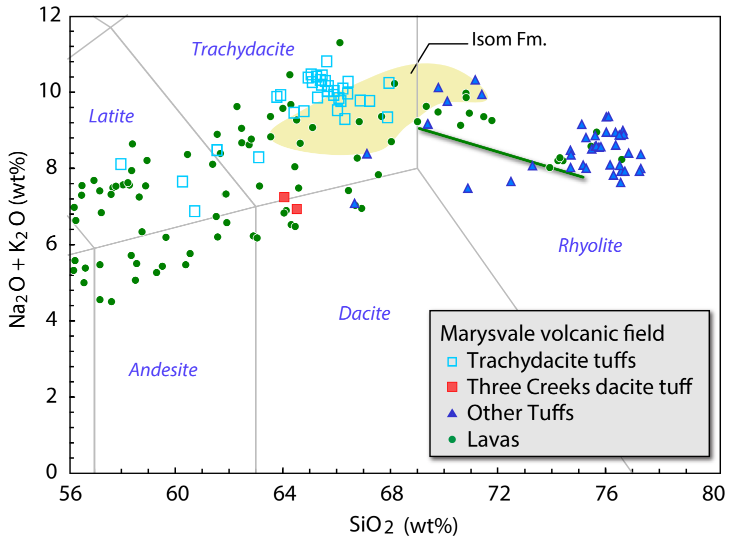

Figure 15. Total alkali-silica diagram for the Marysvale volcanic field. This field is dominated by intermediate-composition lavas but also erupted calc-alkaline rhyolite ignimbrite and two Isom-type (trachydacitic) ignimbrites; field for the Isom Formation tuffs from the eastern sector of the Great Basin is shown for comparison. Few analyses are available for small-volume, crystal-rich Three Creeks and other dacitic ignimbrites.

10% of the estimated 350 major calderas are known (Swanson et al., 2006). The subduction setting was similar to that in the adjacent United States; a Laramide episode of flat slab subduction was followed by Oligocene rollback to eventually form a narrow arc above a steeply dipping subducting slab by the Miocene (Severinghaus and Atwater, 1990; Ferrari et al., 2007; McDowell and McIntosh, 2012). Almost three fourths (~300,000 km^3) of the explosive activity in the field occurred between ca. 34 and 28 Ma; a second pulse of magmatism occurred between 24 and 18 Ma, when another 100,000 km^3 of silicic magma erupted (McDowell and McIntosh, 2012; Bryan and Ferrari, 2013).

Analyzed ignimbrites are dominantly rhyolite (Fig. 18B) with a tendency for alkalic compositions, but the full range in composition may not yet be documented. Dacite is rare, and no large-volume monotonous intermediate ignimbrites or Isom-type trachydacites have been reported (Ferrari et al., 2007; Bryan and Ferrari, 2013). Intermediate-composition lavas are subordinate to explosive silicic deposits; true basalt is rare to absent (Ferrari et al., 2007). Initial $^{87}Sr/^{86}Sr$ ratios range between 0.7041 and 0.7070 for the Eocene and Oligocene volcanic rocks (Ferrari et al., 2007). Thus, compositions of the tuffs in the Sierra Madre Occidental are similar to those in the western sector of the southern Great Basin province (Figs. 5 and 7B) and the Mogollon-Datil field (Fig. 18A). Basaltic andesite and andesite lavas became more common at the end of the Oligocene pulse (Cameron et al., 1989). They were accompanied by east-west extension on the margins of the province (Murray et al., 2013) and the eruption of high-silica rhyolites, including many F-rich topaz rhyolites (Christiansen et al., 1986). This Miocene pulse is similar to the transition to extensional magmatism seen in the United States. Murray et al. (2013) suggested that the ignimbrite flareup was synextensional but also recognized an unextended core in the province. Regional plate reconstructions show active subduction beneath central Mexico until about 12 Ma (e.g., Oskin et al., 2001; Dickinson, 2002). The geochemistry of the ignimbrites published so far is consistent with this tectonic setting.

Early determinations of crustal thickness in the Sierra Madre Occidental indicated values of 40–42 km, with thinning on the extended east and west flanks (Rivera and Ponce, 1986; Gomberg et al., 1988; Couch et al., 1991). However, a determination of 55 km (Bonner and Herrin, 1999) was used by Ferrari et al. (2007) to represent the unextended and magmatically thickened core of the province.

Central Andean Plateau

Geologic Setting

The late Cenozoic Central Andes has been recognized as a younger analog for the magmatism and tectonics of western North America, going back at least as far as Hamilton (1969). More recent detailed analyses include Coira et al. (1982, 1993), Allmendinger et al. (1997), and Kay and Coira (2009). These works establish the Central Andes as a useful model for the mid-Cenozoic Great Basin area. Thus, we review salient attributes of this region and show similarities in tectonic regime, volcanism, and geochemistry (de Silva et al., 2006; de Silva and Gosnold, 2007; Salisbury et al., 2011; Folkes et al., 2013) between these two regions.

The Altiplano-Puna plateau (Fig. 19A) is the widest and highest major element of the Central Andes. It is built on a platform of deformed Precambrian and Phanerozoic rocks. Since the Mesozoic, an oceanic plate has subducted beneath South America. To the north of ~13°S and south of ~27°S, where volcanism is currently inactive, the plate subducts at <30° to nearly flat. The sharp transitions in dip of the subducting slab and the variable age-dependent subduction dip along the continental margin (Capitanio et al., 2011) indicate the possibility of tears rather than abrupt warps in the slab. Plateau formation was a direct response to crustal shortening and thickening of the Central Andes, to as much as 70–80 km under the central plateau starting in the middle Cenozoic but continuing until as recently as the late Miocene. Crustal thickening is thought to be primarily the result of compressional failure of the thermally weakened (probably hydrated) continental lithosphere during flat slab subduction analogous to the North American Laramide orogeny (Isacks, 1988; Allmendinger et al., 1997). During this time, volcanism swept eastward to define a broad volcanic footprint. At approximately 30 Ma, a major change in subduction geometry is indicated by westward migration and focusing of volcanism, signaling the rollback and steepening of the slab essentially concurrent with an ignimbrite flareup.

Figure 16 is interactive. You can view different items in the legend by moving the cursor over them or you can toggle the symbols on and off with the Layers panel in Adobe Acrobat or Adobe Reader.

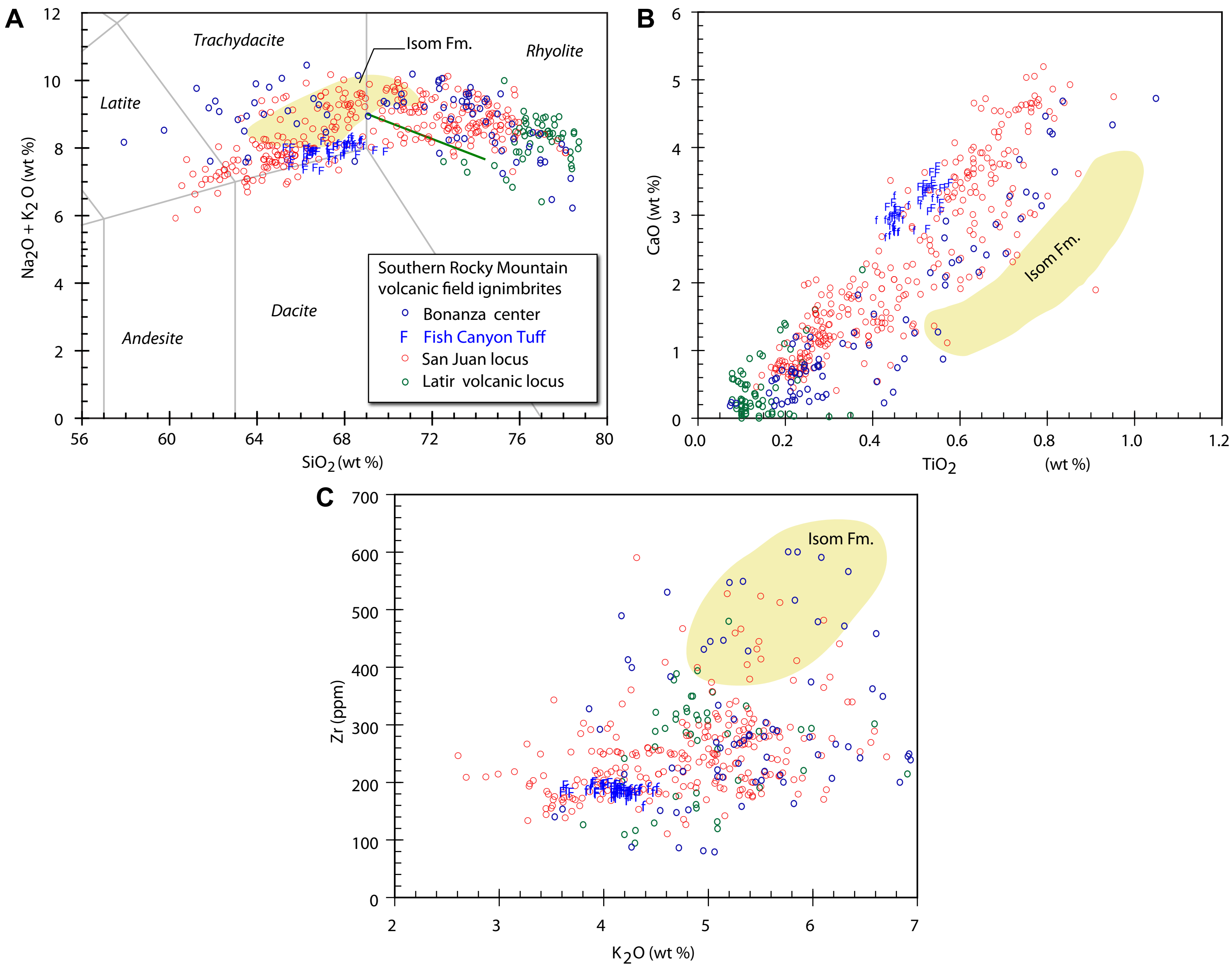

Figure 16. Chemical compositions of ignimbrites in the Southern Rocky Mountain volcanic field. Because of alkali (mainly Na_2O) enrichment, some tuffs designated as dacite on the basis of silica content by Lipman (2007) plot in the trachydacite field. Isom Fm. (yellow shade) refers to Isom-type trachydacite in the eastern sector of the Great Basin province (Fig. 7A). (A) International Union of Geological Sciences (IUGS) classification. Green line divides alkalic rhyolite (above) from calc-alkaline (below). (B) CaO-TiO_2. (C) Zr-K_2O.

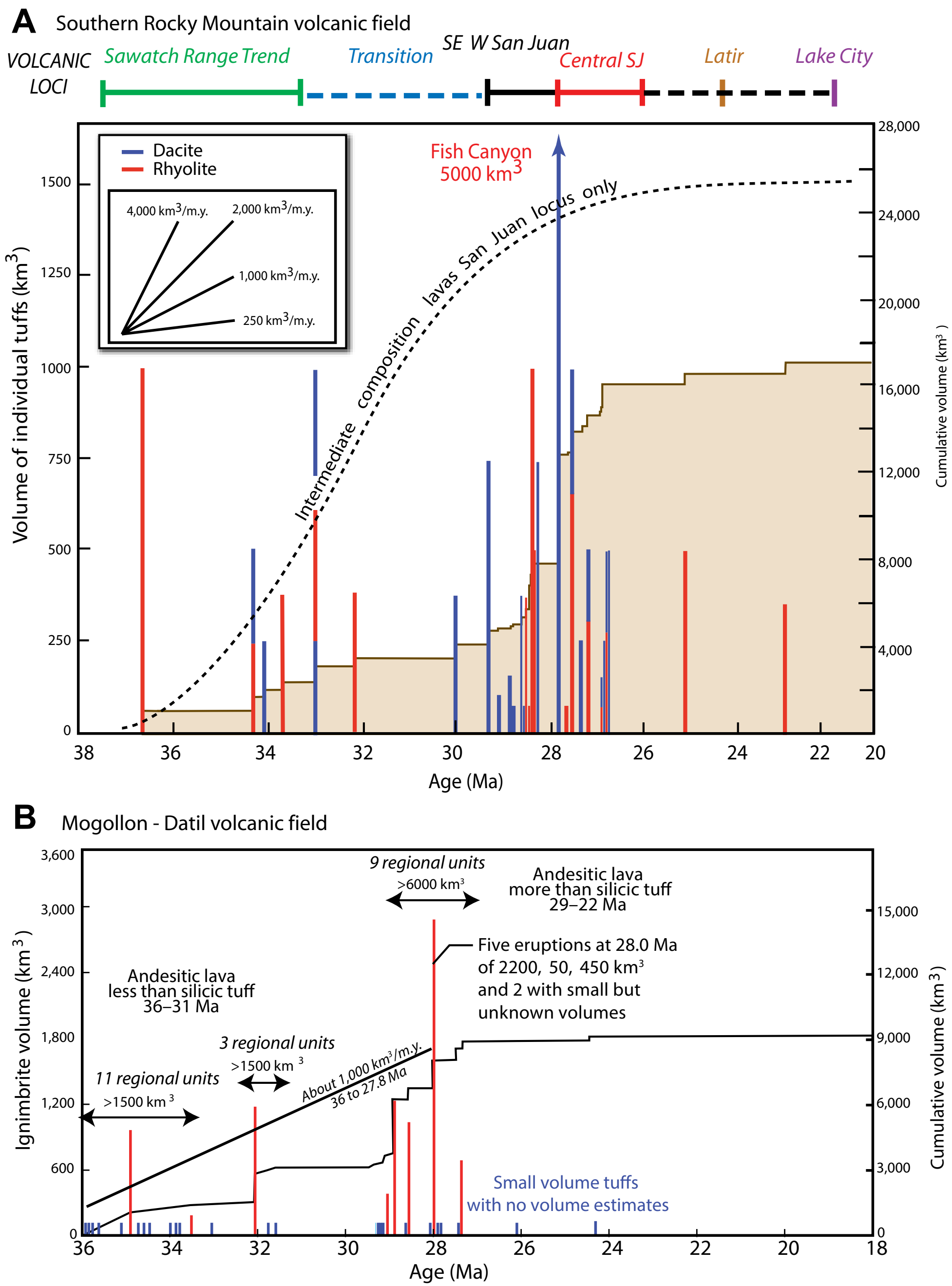

Figure 17. Volume-time relations of silicic ignimbrites and intermediate-composition lavas in volcanic fields involved in the ignimbrite flareup on the eastern and southern margin of the Colorado Plateau (Fig. 1). Vertical lines represent volumes of individual ignimbrites; the volume of the Fish Canyon Tuff is off the scale. Shaded area shows cumulative ignimbrite volume. Sloping lines show volume rates of erupted ignimbrites. (A) Southern Rocky Mountain field (updated from Lipman, 2007). Dashed line indicates cumulative volume of intermediate-composition lavas in the San Juan (SJ) locus; the total for the entire Southern Rocky Mountain volcanic field is probably about 40,000 km³. Most of the lavas were extruded prior to and during eruption of the ignimbrites, most of which were erupted in a restricted time period ca. 30–27 Ma. The longest lulls in explosive activity are ~2 m.y., i.e., distinctly less than for ignimbrites in the southern Great Basin (Fig. 13). (B) Mogollon-Datil volcanic field (McIntosh et al., 1992). Volume scale on left is different from A. Total volumes of ignimbrite are 1500 km³ for each of two periods from 36.2 to 33.5 Ma and from 32.0 to 31.4 Ma, consisting of 12 and 3 major cooling units, respectively. For nine major units from 29.1 to 27.4 Ma, the total volume is >6000 km³. Cumulative volume for the ignimbrite flareup is >9000 km³. Because thicknesses of andesitic lavas were not available to calculate their volumes, we measured areas of outcrop for silicic tuff and andesitic lava in the volcanic field (Table 3) as a basis for the qualitative statements on relative amounts in the figure.

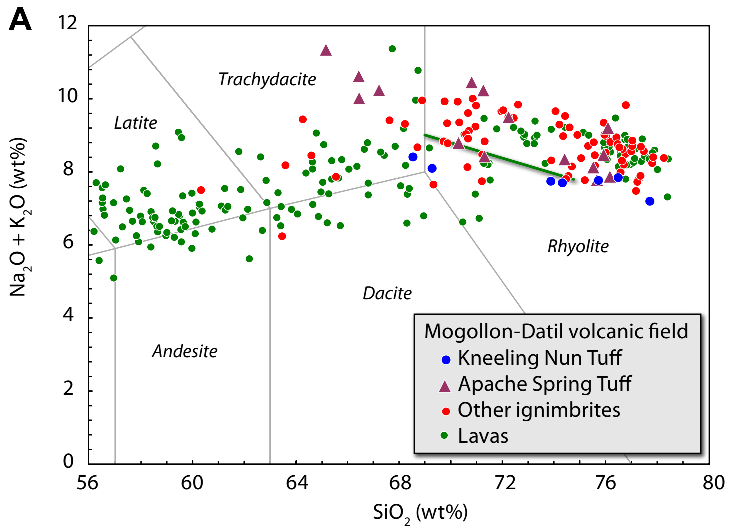

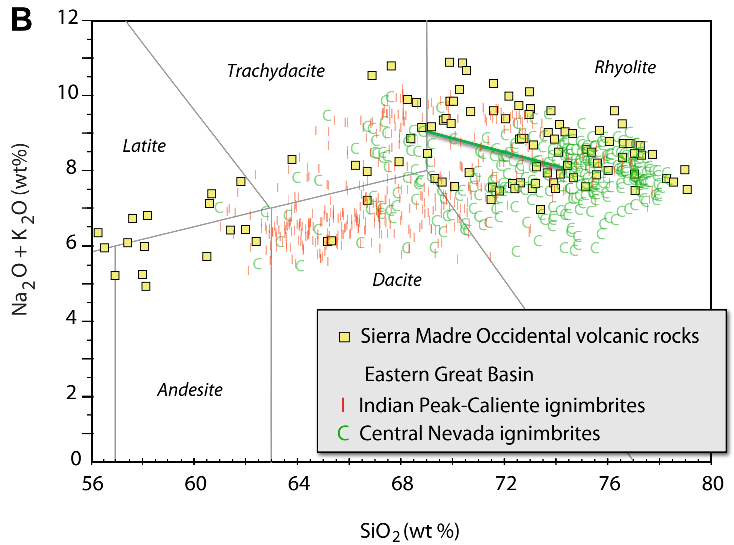

Figure 18. Tuffs and lavas of the (A) Mogollon-Datil volcanic field (Bornhorst, 1980; Davis et al. 1993; Davis and Hawkesworth, 1994) and the (B) Sierra Madre Occidental province (Ferrari et al., 2007; Cameron and Hanson, 1982) on the International Union of Geological Sciences (IUGS) classification diagram (Le Maitre, 1989). Green line separates calc-alkaline rhyolite (below) from alkalic (above).

Figure 18B is interactive. You can view different items in the legend by moving the cursor over them or you can toggle the symbols on and off with the Layers panel in Adobe Acrobat or Adobe Reader.

TABLE 3. OUTCROP AREAS FOR VOLCANIC ROCKS IN THE MOGOLLON-DATIL FIELD

	Silicic tuff (km^2)	Andesitic lava (km^2)	Silicic tuff and andesitic lava (km^2)
29–22 Ma	3300	5100	4700
36–31 Ma	2200	1300	2600
Total	5500	6400	7300

Note: Measured from the geologic map of New Mexico (New Mexico Bureau of Geology and Mineral Resources, 2003, scale 1:500,000).

The Central Andean Neogene ignimbrite province produced by the flareup covers the length and breadth of the Central Andes (de Silva and Francis, 1991; de Silva et al., 2006; Freymuth et al., 2015) over an area of ~250,000 km^2, comparable to that of the flareup in the United States (Fig. 19). Like the mid-Cenozoic North American flareup, several distinct fields and associated calderas developed (Fig. 19). What little is known about the entire province suggests that it was time transgressive, with the age of volcanism decreasing from north to south (de Silva, 1989; Freymuth et al., 2015). Available isotopic data indicate that the older ca. 20 Ma ignimbrites in the north are less "crustal" than the younger <10 Ma ignimbrites south of 22°S (Freymuth et al., 2015). Seismic and petrologic evidence in the Central Andes indicates the presence of delaminated slabs of lower continental crust, which are believed to include dense garnetiferous residua from melting, as well as of mantle lithosphere sinking into the underlying hotter mantle (Kay, 2014); some of the uplift might have been the result of delamination of dense crustal material.

Ignimbrite Flareup in the Altiplano-Puna Volcanic Complex

A distinct flareup within the Neogene Central Andean ignimbrite province produced the most voluminous ignimbrite plateau in the southern half of the province from 22°S to 24°S, the Altiplano-Puna volcanic complex (Fig. 19A; de Silva, 1989). Here, the crust is now 58–76 km thick (Yuan et al., 2002; McGlashan et al., 2008). Ignimbrite eruptions began at ca. 10 Ma and continued until ca. 1 Ma, with a distinct pattern of waxing, climax, and waning in three main pulses: >2400 km^3 at 8.41–8.33 Ma, >3000 km^3 at 5.65–5.45 Ma, and >5400 km^3 at 4.09–2.89 Ma (Fig. 20; Salisbury et al., 2011). This ignimbrite flareup created at least six major calderas as much as 60 km in diameter and several smaller ignimbrite shields (de Silva and Gosnold, 2007; Salisbury et al., 2011). The volume-time pattern of explosive activity is like that of the central and eastern sectors of the southern Great Basin (Fig. 13).

Ignimbrites in the Altiplano-Puna volcanic complex include dacite and rhyolite with minor trachydacite, andesite, and latite (Fig. 21). The compositional pattern of these ignimbrites resembles those of the eastern sector of the southern Great Basin ignimbrite province more closely than the dominantly rhyolitic and more alkalic fields previously discussed (Fig. 7A).

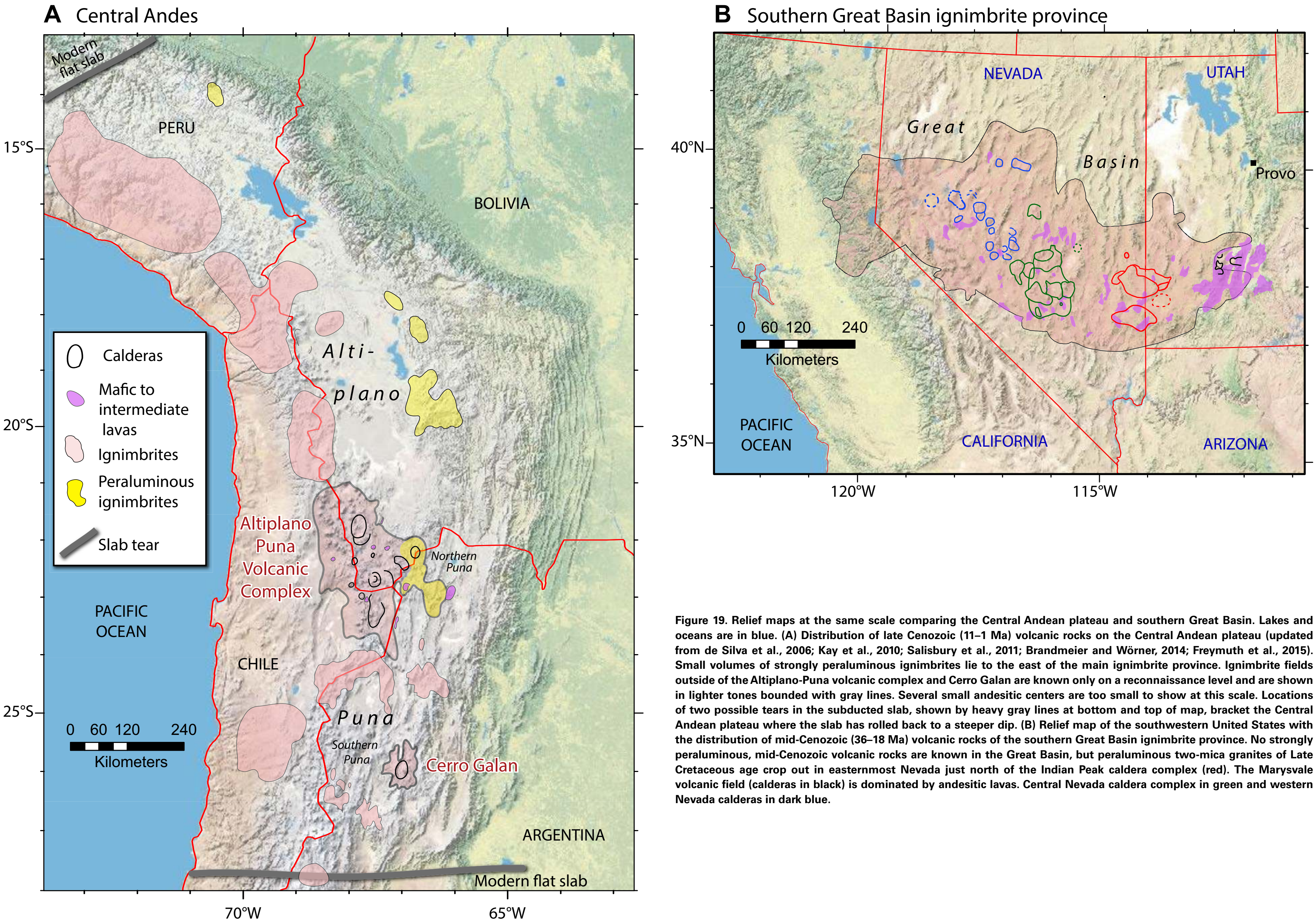

Figure 19. Relief maps at the same scale comparing the Central Andean plateau and southern Great Basin. Lakes and oceans are in blue. (A) Distribution of late Cenozoic (11–1 Ma) volcanic rocks on the Central Andean plateau (updated from de Silva et al., 2006; Kay et al., 2010; Salisbury et al., 2011; Brandmeier and Wörner, 2014; Freymuth et al., 2015). Small volumes of strongly peraluminous ignimbrites lie to the east of the main ignimbrite province. Ignimbrite fields outside of the Altiplano-Puna volcanic complex and Cerro Galan are known only on a reconnaissance level and are shown in lighter tones bounded with gray lines. Several small andesitic centers are too small to show at this scale. Locations of two possible tears in the subducted slab, shown by heavy gray lines at bottom and top of map, bracket the Central Andean plateau where the slab has rolled back to a steeper dip. (B) Relief map of the southwestern United States with the distribution of mid-Cenozoic (36–18 Ma) volcanic rocks of the southern Great Basin ignimbrite province. No strongly peraluminous, mid-Cenozoic volcanic rocks are known in the Great Basin, but peraluminous two-mica granites of Late Cretaceous age crop out in easternmost Nevada just north of the Indian Peak caldera complex (red). The Marysvale volcanic field (calderas in black) is dominated by andesitic lavas. Central Nevada caldera complex in green and western Nevada calderas in dark blue.

Figure 20 is interactive. You can view volcanic fields in the legend by moving the cursor over them or you can toggle the symbols on and off with the Layers panel in Adobe Acrobat or Adobe Reader.

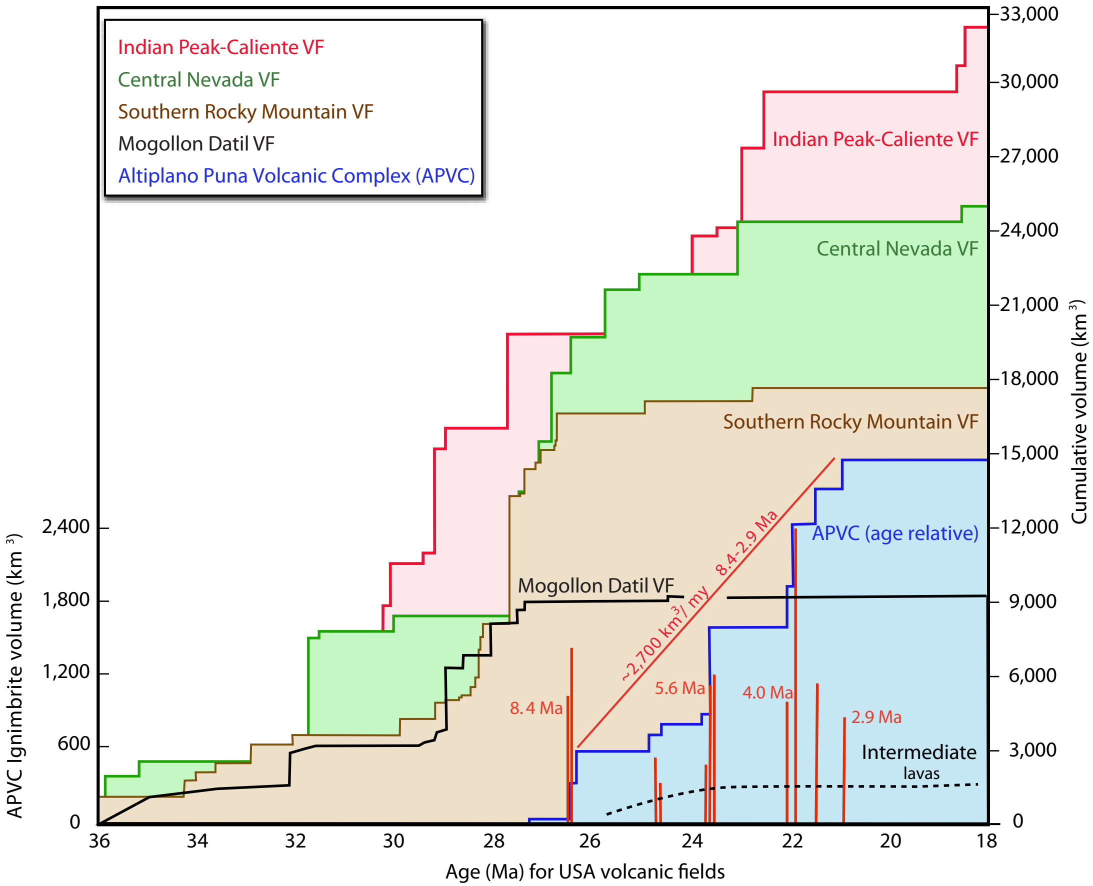

Figure 20. Volume-time relations of silicic ignimbrites in the Altiplano-Puna volcanic complex in the Central Andean plateau (Kay et al., 2010; Salisbury et al., 2011; de Silva and Gosnold, 2007). Vertical red lines indicate volumes of individual ignimbrite eruptions. Punctuated activity of several thousand cubic kilometers occurred at 8.4, 5.6, and 4.0 Ma. Blue area shows cumulative ignimbrite volume. Labeled sloping line shows average rate of erupted ignimbrite volume for the indicated time period. Volume of intermediate-composition lavas of the same age is small. Cumulative volumes for other volcanic fields (VF) from the United States that experienced ignimbrite flareups are compared at the same scale.

Summaries in de Silva et al. (2006), de Silva and Gosnold (2007), Lipman and McIntosh (2008, their table 4), and Kay et al. (2010) underscore the similarities between the dacite ignimbrites in the Altiplano-Puna volcanic complex and eastern sectors of the Great Basin and the Southern Rocky Mountain volcanic field. These are phenocryst-rich, calc-alkaline, high-K dacitic to rhyodacitic ignimbrites of the "monotonous intermediate" type of Hildreth (1981). The 40% to 50% phenocrysts are a low-pressure assemblage of quartz, plagioclase, biotite, and Fe-Ti oxides with accessory apatite and titanite. Amphibole is common in some northern Puna ignimbrites near the arc, minor amounts of clinopyroxene and orthopyroxene can occur in ignimbrites with <67% SiO_2, and sanidine is found in some dacite and rhyolite units. Pre-eruptive temperatures are generally near 700 °C to 850 °C, with pressures before eruption corresponding to depths of 5 to 10 km, while magmatic oxygen fugacities (~2 log units above Quartz-Fayalite-Magnetite [QFM]) are similar to many silicic tuffs of the Great Basin. Detailed information on specific monotonous intermediate ignimbrites in the Central Andes is available from Lindsay et al. (2001) for the 3.9 Ma, 2500 km³ Atana ignimbrite, and Schmitt et al. (2001) for the 1 Ma, 100 km³ Purico ignimbrite and 3.69 Ma, >800 km³ Tara ignimbrite. Rhyolites are less common, the largest being the ~300 km³ Toconao ignimbrite, which is interpreted to be from the upper zone of the Atana-Toconao magma reservoir (Lindsay et al., 2001).

A suite of peraluminous ignimbrites in the eastern Altiplano-Puna volcanic complex (Figs. 10 and 19) has the most "crustal" Sr and Nd isotopic compositions, attesting to the influence of a metapelitic basement in the east (Caffe et al., 2012). These are also monotonous intermediates and testify to hypersolidus temperatures in the orogenically thickened crust, in a similar manner as the Late Cretaceous peraluminous granites just north of the caldera complex in the eastern sector of the Great Basin province.

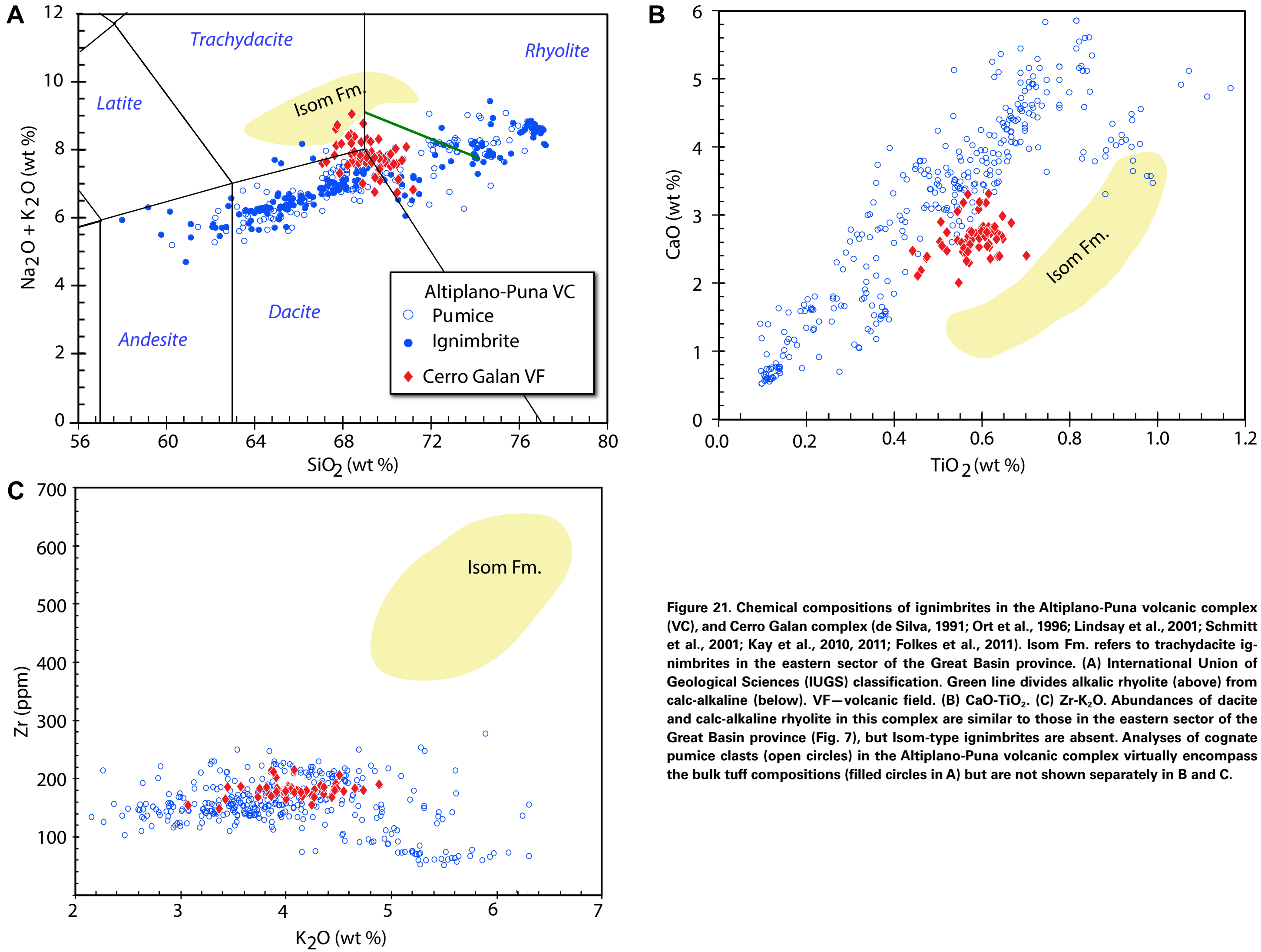

Figure 21. Chemical compositions of ignimbrites in the Altiplano-Puna volcanic complex (VC), and Cerro Galan complex (de Silva, 1991; Ort et al., 1996; Lindsay et al., 2001; Schmitt et al., 2001; Kay et al., 2010, 2011; Folkes et al., 2011). Isom Fm. refers to trachydacite ignimbrites in the eastern sector of the Great Basin province. (A) International Union of Geological Sciences (IUGS) classification. Green line divides alkalic rhyolite (above) from calc-alkaline (below). VF—volcanic field. (B) CaO-TiO_2. (C) Zr-K_2O. Abundances of dacite and calc-alkaline rhyolite in this complex are similar to those in the eastern sector of the Great Basin province (Fig. 7), but Isom-type ignimbrites are absent. Analyses of cognate pumice clasts (open circles) in the Altiplano-Puna volcanic complex virtually encompass the bulk tuff compositions (filled circles in A) but are not shown separately in B and C.

No Isom-type trachydacitic tuffs have been recognized in the Altiplano-Puna volcanic complex.

Andesitic components are found as rare individual pumices in some ignimbrites or more commonly as bands and inclusions in pumices in most ignimbrites (de Silva, 1991; Lindsay et al., 2001; Schmitt et al., 2001; Burns et al., 2015). While these are volumetrically insignificant, they provide evidence for the role of intermediate magmas in the evolution of the dacitic magmas, representing the thermal and material input from the deep roots into the upper-crustal system (Burns et al., 2015). The most mafic lavas in the Altiplano-Puna volcanic complex are small andesitic lava flows with 54%–58% silica in many of the calderas. These lavas have compositions similar to the andesitic pumices and mafic enclaves (e.g., Burns et al., 2015), and they reveal the ubiquity of relatively mafic compositions at depth. Much of the underlying zone of partial melt is considered to be of similar composition to these mafic lavas. Ages are rare and of low precision for scattered, rare, large andesitic-dacitic composite volcanoes; some are clearly older than the flareup based on superposition, while a few are intercalated with the ignimbrites, or have ignimbrites draped around them. In the several locations where pre-ignimbrite basement is seen beneath the ignimbrites, no evidence of mafic lavas preceding the flareup has been found. Current volume estimates emphasize the dominance of silicic ignimbrite over contemporaneous andesitic lavas; a ratio of 10:1 is considered a minimum, because erosion rates may artificially bias the estimate toward the andesites.

Oxygen isotope ratios in the volcanic rocks of the Altiplano-Puna volcanic complex and Cerro Galan are high ($\delta^{18}O_{Qtz}$ from +7.8‰ to +10.2‰), and initial $^{87}Sr/^{86}Sr$ ratios (0.709–0.718) are the highest of the flareup provinces (Fig. 10; Kay et al., 2010, 2011; Folkes et al., 2013). They are interpreted to be caused by extensive assimilation of high Rb/Sr, high $\delta^{18}O$ metasedimentary rock during magma generation. Folkes et al. (2013) posited that the absence of low $\delta^{18}O$ magmas may result from the plateau's high elevation and related arid climate. Low $\delta^{18}O$ magmas generally originate by assimilation of hydrothermally altered crust in wetter environments. However, the Southern Rocky Mountain tuffs lack low $\delta^{18}O$ values (+6.5‰ to +9.9‰), despite a wet environment—implied by the presence of caldera-filling lake sediments containing conifer pollen and leaf debris (e.g., Axelrod, 1987). Among large-volume ignimbrites of North America (e.g., Southern Rocky Mountain, Snake River Plain, Yellowstone), the closest analogs to the Central Andes are the ignimbrites of the mid-Cenozoic of the eastern Great Basin, where $\delta^{18}O_{Qtz}$ ranges from 8‰ to 11‰ (Fig. 10; Larson and Taylor, 1986; Hart, 1997). These findings constitute indirect support for the existence of a similarly high, dry, and unextended Great Basin altiplano during the mid-Cenozoic flareup (Fig. 3).

Viramonte et al. (1984) and Riller et al (2001) noted that many of the eruptive sources of the ignimbrites in the Altiplano-Puna volcanic complex lie along plateau-wide northwest-southeast–trending zones of right-lateral transtension. Riller et al. (2000) argued that the ignimbrite flareup coincides with a local change from compressional tectonics to plateau collapse. Indeed, the outlines of the calderas have some northwest-southeast control; however, a cause and effect relationship between tectonism and eruption remains to be demonstrated. We note that Kay and Coira (2009) made no mention of contemporary crustal extension during the latest Cenozoic ignimbrite volcanism; instead, contemporaneous deformation was contractional. Overall, none of the Central Andean, southern Great Basin, or Southern Rocky Mountain ignimbrite flareups was accompanied by obvious crustal extension.

Geophysical Underpinnings of the Altiplano-Puna Region

What is believed to be the largest active midcrustal zone of partial melt in Earth's continental crust underlies the Altiplano-Puna volcanic complex—the so-called Altiplano-Puna magma body (e.g., Zandt et al., 2003; Prezzi et al., 2009; del Potro et al., 2013; Ward et al., 2014; Comeau et al., 2015). A negative 335 mGal Bouguer gravity anomaly (with "depth" of about 50 mGal) coincides with a low-seismic-velocity zone (Fig. 22A) that defines a 200-km-wide body between 9 and 30 km below the surface, which is interpreted to be 500,000 km^3 of partially molten rock (Ward et al., 2014). Magnetotelluric studies (Fig. 22B) show a deep highly conductive zone (top at 25–30 km below the surface); fingers of conductive material (magma or magma plus saline fluid) extend above this nearly to the surface (Comeau et al., 2015). Gravity models also show what are interpreted to be diapirs of low-density material rising from the Altiplano-Puna magma body (del Potro et al., 2013). These geophysical studies suggest that the melt fraction below the Altiplano-Puna volcanic complex ranges from ~4% to 25%. The Altiplano-Puna magma body is interpreted to have produced the magmas that erupted during the flareup (e.g., de Silva et al., 2006; Muir et al., 2014; Burns et al., 2015) and could be an extensive zone where melting, assimilation, storage, and homogenization (MASH) modify mantle-derived magma (e.g., Hildreth and Moorbath, 1988) below upper-crustal magma reservoirs (Fig. 22). Annen (2009) called this a hot zone.

Summary Comments on Comparisons of Ignimbrite Flareups

In the continental arc ignimbrite flareups described herein (Tables 1 and 2), numerous caldera-forming eruptions of explosive silicic magma occurred over 10–18 m.y., with repose times ranging from a few hundred thousand to as much as a few million years. Super-eruptions were common. Aggregate volumes of ignimbrite in an individual field are at least several thousands of cubic kilometers, blanketing upwards of 10^5 km^2 surrounding source calderas tens of kilometers in diameter. Contemporaneous basalt is rare to absent, although significant andesitic precursors or evidence for mafic input through the silicic magmatic history is present. Flareups occurred far inland on thickened, nonextending crust, beneath which a previously flat subducting lithospheric slab rolled back to steeper dip. This distinct style of continental arc volcanism contrasts sharply with the near-trench, steady-state volcanism overlying steeply dipping slabs. Of all the ignimbrite flareups examined, the one most similar to the eastern sector of the southern Great Basin province is the Altiplano-Puna volcanic complex. Similarities include: calc-alkaline rhyolite and dacite ignimbrites (Figs. 7A and 21A), multiple super-eruptive monotonous intermediate ignimbrites (Figs. 13A and 20), similar Sr and O isotope ratios (Fig. 10), only minor coeval andesitic lavas (Figs. 2 and 19), and spatially associated production of peraluminous silicic magmas originating from crustal anatexis. Notably, both flareups occurred on the thickest (~70 km) orogenic crust. Nonetheless, the Andean volcanic complex differs in its shorter flareup time span, smaller total volume of ignimbrite, and absence of Isom-type trachydacite.

The Southern Rocky Mountain and Mogollon-Datil volcanic fields on the margin of the Colorado Plateau (Fig. 1; Tables 1 and 2) resemble the Altiplano-Puna volcanic complex with respect to flareup duration, ignimbrite volume, and absence of Isom-type tuffs. However, these two fields differ from the Altiplano-Puna complex and the eastern sector of the southern Great Basin province in having smaller volumes of ignimbrite than intermediate-composition

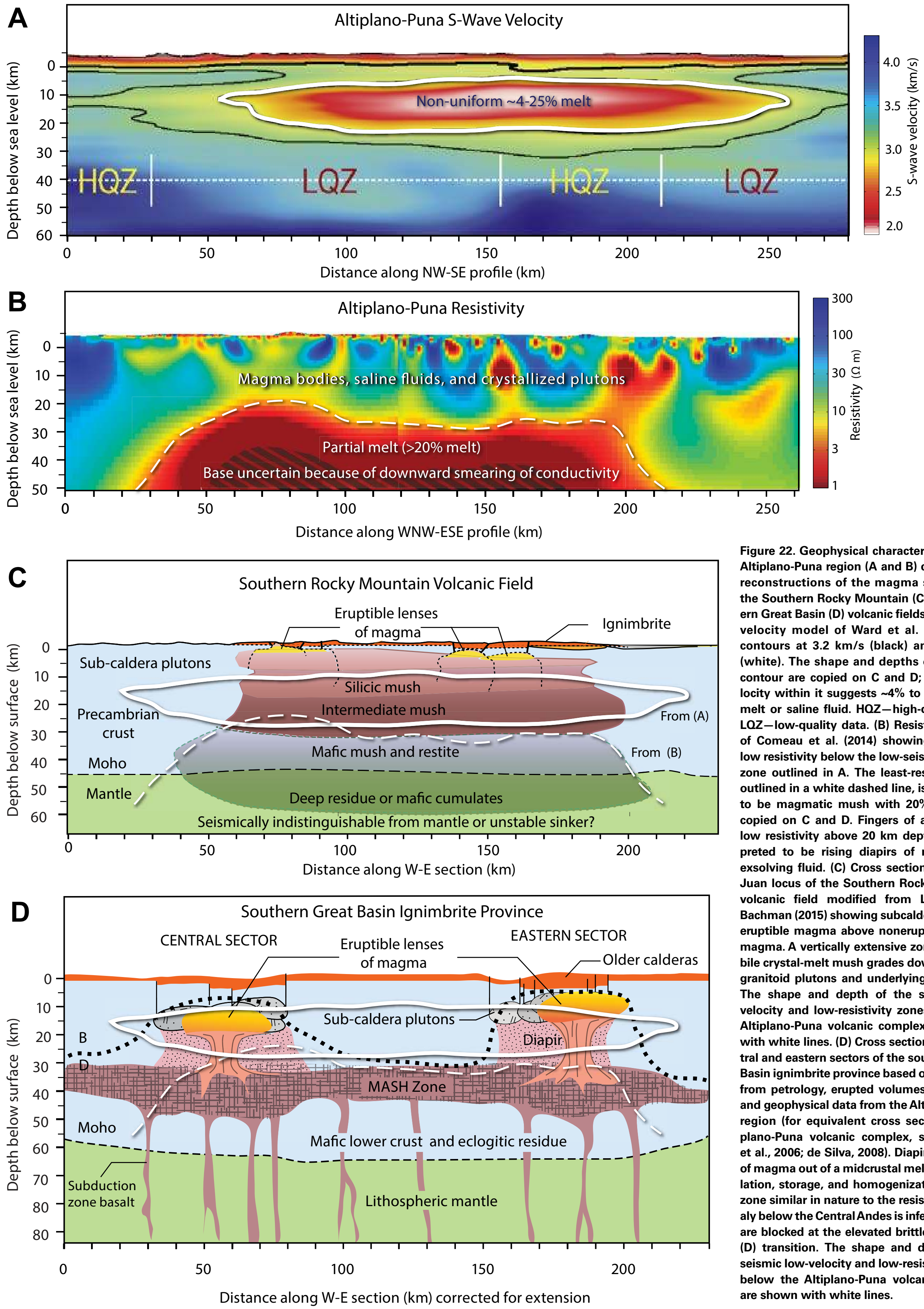

Figure 22. Geophysical characteristics of the Altiplano-Puna region (A and B) compared to reconstructions of the magma systems for the Southern Rocky Mountain (C) and southern Great Basin (D) volcanic fields. (A) S-wave velocity model of Ward et al. (2014) with contours at 3.2 km/s (black) and 2.9 km/s (white). The shape and depths of the inner contour are copied on C and D; the low velocity within it suggests ~4% to 25% silicate melt or saline fluid. HQZ—high-quality data; LQZ—low-quality data. (B) Resistivity model of Comeau et al. (2014) showing a zone of low resistivity below the low-seismic-velocity zone outlined in A. The least-resistive zone, outlined in a white dashed line, is interpreted to be magmatic mush with 20% melt. It is copied on C and D. Fingers of anomalously low resistivity above 20 km depth are interpreted to be rising diapirs of magma and exsolving fluid. (C) Cross section of the San Juan locus of the Southern Rocky Mountain volcanic field modified from Lipman and Bachman (2015) showing subcaldera lenses of eruptible magma above noneruptible mushy magma. A vertically extensive zone of immobile crystal-melt mush grades downward into granitoid plutons and underlying cumulates. The shape and depth of the seismic low-velocity and low-resistivity zones below the Altiplano-Puna volcanic complex are shown with white lines. (D) Cross section of the central and eastern sectors of the southern Great Basin ignimbrite province based on inferences from petrology, erupted volumes of magma, and geophysical data from the Altiplano-Puna region (for equivalent cross section of Altiplano-Puna volcanic complex, see de Silva et al., 2006; de Silva, 2008). Diapiric transport of magma out of a midcrustal melting, assimilation, storage, and homogenization (MASH) zone similar in nature to the resistivity anomaly below the Central Andes is inferred. Diapirs are blocked at the elevated brittle (B)–ductile (D) transition. The shape and depth of the seismic low-velocity and low-resistivity zones below the Altiplano-Puna volcanic complex are shown with white lines.

lava (Tables 1 and 2; Fig. 20) and the Mogollon-Datil volcanic field has no monotonous intermediate ignimbrite. Also, the Colorado Plateau crust had experienced less orogenic thickening than that in the Central Andes and the southern Great Basin, where we postulate a longer-lived mid- to upper-crustal MASH zone (Fig. 23) efficiently blocked ascending mafic magmas. The Colorado Plateau crust was not only thinner, but also more mafic; and partial melting resulted in more alkalic ignimbrites with lower initial $^{87}Sr/^{86}Sr$ ratios compared to the calc-alkaline ones of the eastern Great Basin and Central Andes (Figs. 5, 7A, 10, 16A, and 18). Exceptions to this generalization are the Grizzly Peak Tuff, which was underlain by crust that was isotopically distinct from that below the San Juan locus, and New Mexico's Amalia Tuff, which was extensively contaminated by upper-crustal materials (Fig. 10; Johnson and Fridrich, 1990; Johnson et al., 1990).

ORIGIN OF SLAB-ROLLBACK IGNIMBRITE FLAREUPS

Voluminous ignimbrite flareups related to rollback of a formerly flat subducting plate are a distinct style of continental arc volcanism that are powered by an elevated influx of mantle basalt magma into thickened crust. How-

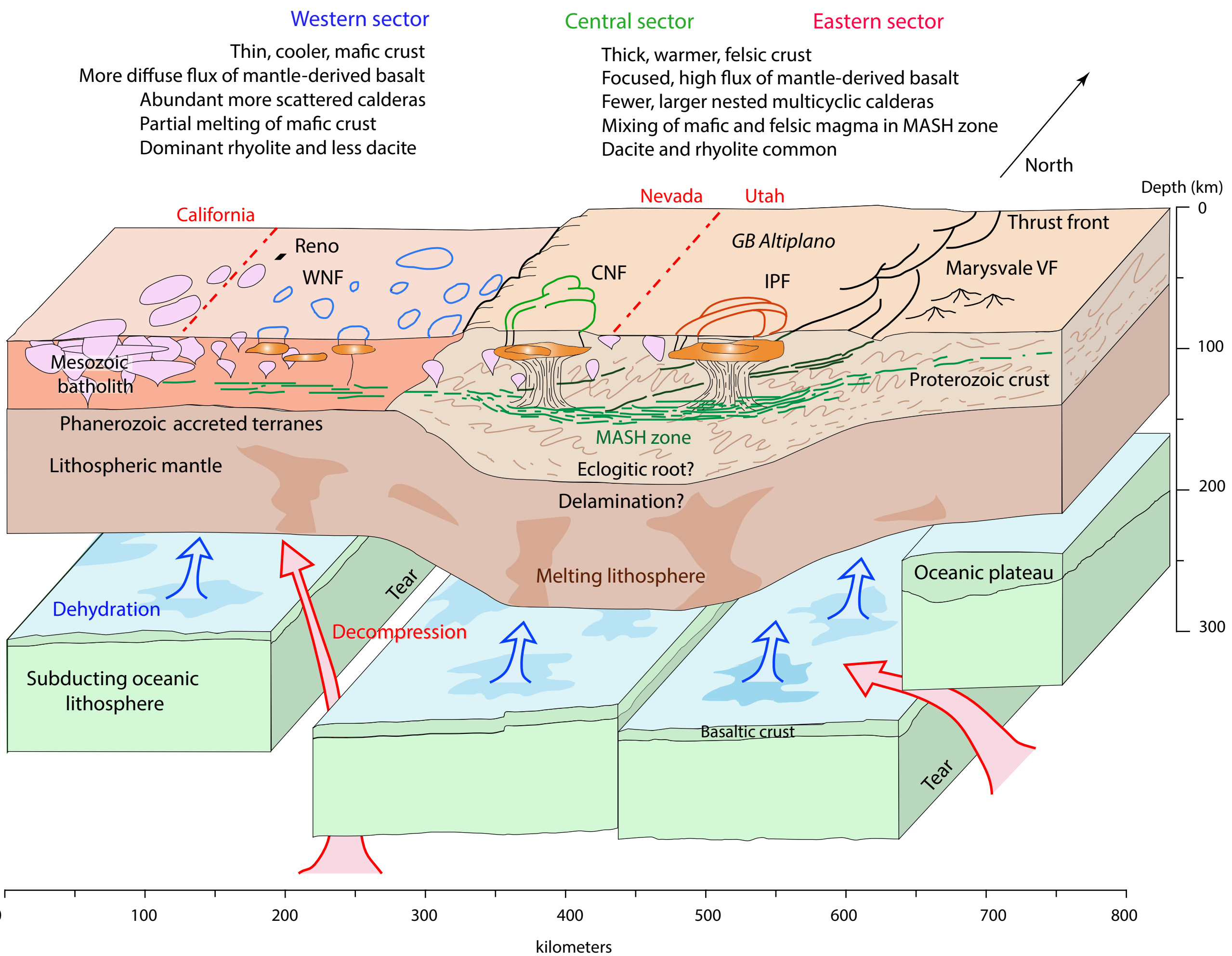

Figure 23. Schematic west-east block diagram summarizing the differences among the three sectors of the southern Great Basin (GB) ignimbrite province. WNF—Western Nevada field scattered calderas in dark blue; CNF—Central Nevada field caldera complex in green; IPF—Indian Peak field caldera complex in red; MASH—zone of melting, assimilation, storage, and homogenization; VF—volcanic field. See text for further description.

ever, little of this basalt magma is extruded at the surface. Before considering how these basalt magmas were created in the mantle, we examine how the thickness and composition of the crust modulated the influence of this flux of mantle-derived magma during ignimbrite flareups. The southern Great Basin province provides a focal point for our discussion.

Crustal Factors

All of the flareups developed on crust at least 40 km thick that was not subject to significant contemporaneous tectonic extension. Concurrent extrusions of andesitic lavas were subordinate to silicic ignimbrites where the crust was thicker in the southern Great Basin and Altiplano-Puna, whereas apparently thinner crust, as in the Southern Rocky Mountain and Mogollon-Datil volcanic fields, allowed more andesitic magmas to rise to the surface. As discussed in detail in the following, thicker crust played two significant roles in flareups:

(1) Adjustment of the thermal gradient after orogenic thickening led to elevated temperatures in the lower to middle crust.

(2) Ample fertile source rock was available to create voluminous silicic magmas, and the compositional profile of the crust governed the details of ignimbrite composition.

Elevated Temperatures in Thick Crust

In the eastern Great Basin, where the mid-Cenozoic crust was an estimated 70 km thick (Fig. 3), Late Cretaceous two-mica granites with initial Sr isotope ratios as high as 0.7246 (Best et al., 1974; Lee and Christiansen, 1983; Farmer and DePaolo, 1983) are exposed 50–150 km north of the Indian Peak caldera complex (Fig. 2). These strongly peraluminous granites originated without a mantle contribution by partial melting of metasedimentary rocks where orogenic thickening was greatest. After thickening and thermal re-equilibration, temperatures in the lower to middle crust can reach near-solidus values (e.g., England and Thompson, 1984; Patiño-Douce et al., 1990; Vanderhaeghe et al., 2003). As previously indicated, peak metamorphic conditions as great as 800 °C at about 35 km depth prevailed in eastern Nevada in the Late Cretaceous (DeCelles, 2004). From thermal models, England and Thompson (1984) concluded that temperatures in the middle and lower crust increased for 40 to 60 m.y. after the crust doubled in thickness and then slowly decreased. Thus, following the Late Cretaceous contraction, the Great Basin crust would have been anomalously warm in the Eocene and Oligocene. Then, as huge volumes of basaltic magma intruded the crust during the mid-Cenozoic slab rollback, the added heat and feedbacks among crustal temperature, thermal diffusivity, and melt production (e.g., Whittington et al., 2009; Nabelek et al., 2012) resulted in copious production of silicic magmas of the Great Basin ignimbrite flareup. Orogenically thickened and prewarmed crust invaded by mantle magmas resulted in elevation of the geothermal gradient as well as the brittle-ductile transition, creating a largely ductile crust (de Silva and Gregg, 2014). In the Southern Rocky Mountain volcanic field, where little orogenic thickening had occurred, precursory large-scale andesitic magmatism resulted in a similar modification of the thermomechanical regime of the crust. This modified regime had at least three significant consequences for flareups:

(1) Instead of ascent through extensional fissures, as in some arc volcanism (e.g., Hughes and Mahood, 2008; Cashman and Sparks, 2013), silicic magma transport through the ductile crust during ignimbrite flareups likely involved rising diapirs. This transport process probably prevailed in the southern Great Basin, the Altiplano-Puna, and most of the Southern Rocky Mountain volcanic field. Diapiric magma transport was the natural result of a neutral stress field in a ductile crust (e.g., Vigneresse and Clemens, 2000; Weinberg and Podladchikov, 1994). Maughan et al. (2002) argued that a quasi-isotropic horizontal stress field prevailed during the flareup in the Great Basin, as it did in the Southern Rocky Mountain volcanic field, with the exception of the late Questa-Latir, New Mexico, locus (Lipman, 1982, 1988), and also during much of the post-thickening history of the Central Andes, particularly in the deeper, more ductile parts of the crust. The diapirs were probably spawned in crustal MASH zones (Figs. 22 and 23). In the southern Great Basin and Altiplano-Puna, where the crust was thickest, the MASH zone appears to have been in the mid- to upper crust, based on geophysical data in the latter, whereas in the Southern Rocky Mountain field, it was probably in the lower crust, based on the isotopic compositions of the rocks (Lipman et al., 1978; Lake and Farmer, 2015).

In the Central Andes, seismic, gravity, geodetic, and magnetotelluric data gathered by Fialko and Pearse (2012), del Potro et al. (2013), Ward et al. (2014), and Comeau et al. (2015) indicate a 10- to 15-km-diameter diapir is actively rising from the top of the mushy Altiplano-Puna magma body 20 km below the surface (Fig. 22). Buoyant ascent probably results from Rayleigh-Taylor instability in the partially molten zone and is fed by inward migration and collapse; this radial mass transfer has created a broad zone of surface subsidence about 120 km in diameter.

(2) Barring other factors such as crystallization or crustal structures that might stall rising magma at even deeper levels, the ultimate height to which diapirs of silicic magma can ascend within the crust is not governed by the level of neutral buoyancy because their densities (2.3–2.5 g/cm^3) are consistently less than that of most crustal wall rocks (2.5–2.9 g/cm^3); even solid granite is less dense than most enclosing wall rocks. Instead, ascending diapirs of silicic magma are probably trapped at the brittle-ductile transition, where the stress required to fracture the brittle lid is two orders of magnitude greater than that provided by the driving force for diapirism resulting from the contrast in density between magma and host rock (Vigneresse, 1995). However, the transition level is not static, but it is further elevated as a result of upward transfer of heat from the top of the entrapped and spreading magma. For crystal-poor rhyolite ignimbrites of the Southern Rocky Mountain volcanic field, the pressure of crystallization has been estimated at only 1 to 2 kbar (4 to 8 km) on the basis of experimental phase equilibria, particularly, absence of quartz in quartz-normative magma (Lipman et al., 1978; Bachmann et al., 2014). The depth of the brittle-ductile transition beneath the eastern sector of the Great Basin province, as indicated by the equilibration pressure of phenocrysts in the

three pre-eruption monotonous intermediate magmas (Best et al., 2013b), was as shallow as 7–9 km. Mineral barometers in the dacites and rhyolites in the central sector where the crust may have been slightly thinner (Fig. 3) indicate greater depths of ~14 km (Phillips, 1989; Radke, 1992; Blaylock, 1998).

Whereas the Southern Rocky Mountain volcanic field experienced significant precursory andesitic volcanism before the ignimbrite flareup, which probably played some role in elevating the brittle-ductile transition, the Great Basin had no such significant precursory volcanism. Instead, its greater crustal thickening, sufficient to yield late Mesozoic S-type granite magmas, influenced the elevation of the transition.

(3) The characteristic accumulation during flareups of colossal volumes of silicic magma (several hundreds to thousands of cubic kilometers) in the shallow crust before eruption at intervals of 10^4 to 10^6 yr was made possible by a ductile crust. Recent theoretical considerations highlight the importance of the rheology of the wall rock in the growth of a magma reservoir (Jellinek and DePaolo, 2003; Gregg et al., 2012, 2013, 2015). Largely a function of the thermal energy associated with the reservoir and its history, small chambers (<100 km^3) are likely to be surrounded by cool (<400 °C), brittle wall rocks, while larger chambers that yield super-eruptions are built under prograde conditions that result in ductile wall rocks (Fig. 24). Absent tectonic or other external influence, smaller eruptions are typically triggered by dike propagation when the elastic limit (~2× tensile strength) of the wall rocks is exceeded by an overpressure (e.g., through recharge or fluid saturation) in the chamber. For larger chambers of eruptible magma surrounded by warmer ductile wall rocks, theoretical models indicate such diking is inhibited. Eruption is suppressed, and a reservoir grows until the roof breaks (Fig. 24). This mechanical threshold is a function of the aspect ratio of the roof; an uplifting and extending roof above the growing reservoir has a finite mechanical strength that is eventually exceeded, and faults may propagate from the surface to the chamber, triggering eruption and caldera collapse. In one scenario, when pressure on the magma is reduced, it becomes fluid-saturated and expands explosively through these fracture vents. The long repose times of large (>1,000 km^3) caldera-forming eruptions during ignimbrite flareups (e.g., Figs. 13, 17, and 20) are consistent with some studies of zircon age spectra (Brown and Fletcher, 1999; Schmitt et al., 2003; Costa, 2008; Bachmann et al., 2007; Wotzlaw et al., 2013) and thermal models (Spera, 1980; Annen et al., 2009; Gelman et al., 2013; de Silva and Gregg, 2014) that indicate extended melt-rich lifetimes of several hundred thousand years.

Wholesale expulsion of magma along outward-dipping (reverse) ring faults along caldera margins provides increasingly open channels as subsidence progresses (Fig. 24; Best et al., 2013b, see their figs. 43 and 52). Resulting catastrophically high eruption rates yield sustained and continuously collapsing columns of ejecta. Precursory plinian eruptions (e.g., Druitt and Sparks, 1984) are effectively bypassed, as appears typical of all the flareup fields discussed (e.g., de Silva et al., 2006; Lipman et al., 2015).

Diapiric feeding of a shallow magma chamber is likely pulsed, with long periods of time between pulses, because it takes time to regenerate the gravitational instability of buoyant magma. This concept might apply to the excep-

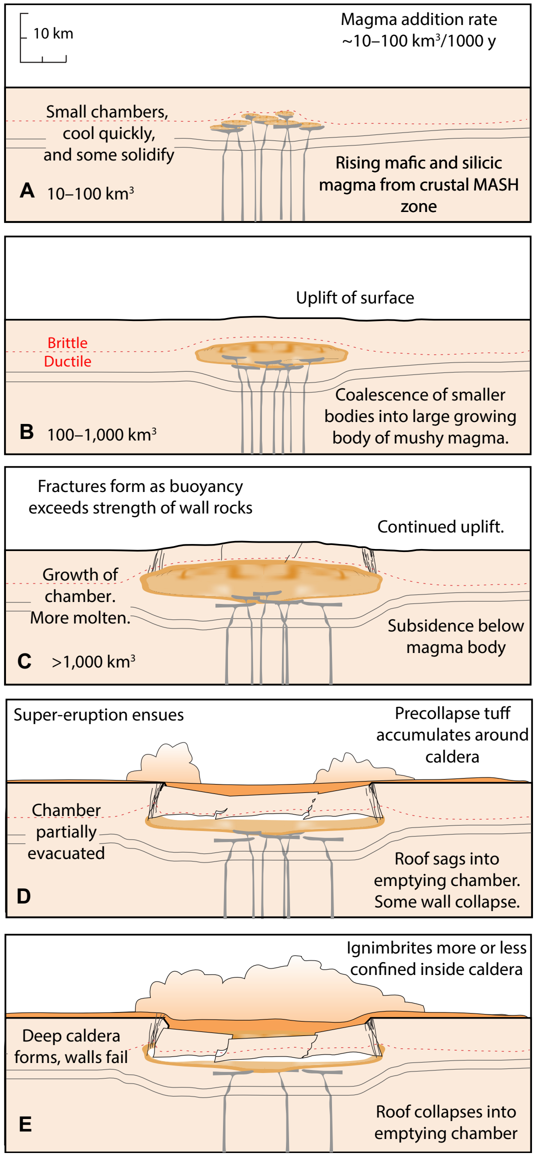

Figure 24. Schematic diagrams showing growth (from A at top to E at bottom) of large magma chamber, roof collapse, and eruption (modified from Christiansen, 2005). The gray lines are used to show the significance of floor subsidence. The thin lenticular magma body represents the eruptible uppermost portion of a vertically much more extensive plutonic system, several tens of kilometers thick (Fig. 22). MASH—zone of melting, assimilation, storage, and homogenization.

tional burst at ~1 m.y. intervals of three monotonous intermediate magmas erupted at the same focus from 31.1 to 29.2 Ma in the Indian Peak caldera complex in the eastern sector of the southern Great Basin province (Figs. 13A and 14). The three super-eruptions, totaling 12,300 km^3, were fed from similar depths of about 7–9 km; each batch of magma evolved somewhat independently, as indicated by their distinctive chemical variation trends (Best et al., 2013b). We envisage a scenario in which a hybridized mixture of andesite and rhyolite magma rose diapirically from a midcrustal MASH zone and stalled at the brittle-ductile transition in the upper crust (Fig. 23). The mixed crystal-rich dacite magma accumulated until the roof of the chamber failed, resulting in eruption of the Cottonwood Wash Tuff and caldera formation at 31.1 Ma. Subsequent pulses of similar crystal-rich dacitic magma ascended through the weakened conduit already established in the crust. These new drafts of magma were also trapped in much the same place as the older chamber until the growing Wah Wah Springs magma reservoir grew to the point of roof failure and erupted at 30.06 Ma. Finally, the third super-eruptive monotonous intermediate magma—the Lund—accumulated and vented at 29.2 Ma in much the same way and in the same place as the two preceding ones, forming a nested caldera complex. Similar processes have been suggested for the Altiplano-Puna volcanic complex (de Silva et al., 2006; de Silva and Gosnold, 2007; de Silva and Gregg, 2014), and they probably apply to the accumulation of large magma bodies in other ignimbrite flareups.

In regions where the crust was not as thick, and the pre-flareup geothermal gradient was lower, such as in the Southern Rocky Mountain field, a greater volume of mantle-derived magma may have been required to overcome this energy deficit and produce voluminous bodies of silicic magma. A higher flux might also explain the much greater volume of erupted andesite in the Southern Rocky Mountain province (estimated to exceed 40,000 km^3; Table 2) than in the coeval Great Basin province, where intermediate composition magmas were much less voluminous (6000 km^3; Table 1). Farmer et al. (2008) estimated the volume of basaltic magma that powered the San Juan segment of the Southern Rocky Mountain volcanic field to be 384,000 to 719,000 km^3. In contrast, Christiansen and Best (2014) estimated that 300,000 to 400,000 km^3 of basalt powered the Indian Peak–Caliente volcanic field.

Composition of the Crust

Hughes and Mahood (2008) argued that crustal composition, independent of its thickness, influences the style and composition of caldera-related magmatism in volcanic arcs. Arcs on oceanic crust have fewer rhyolite calderas per unit length than arcs built on Mesozoic or older continental crust. However, this is the opposite of the southern Great Basin ignimbrite province: Caldera-related, relatively alkalic rhyolite ignimbrites dominate the western sector, which is underlain by young, thinner, mafic crust, whereas dacites dominate the eastern sector, underlain by old, thicker, felsic crust (Figs. 3, 5, and 10).

Experiments show how magma generation in these two contrasting sectors of the Great Basin is related to different crustal sources and contaminants. Partial melting of arc basaltic rocks, like those that underlie the western sector, produces trachydacites and high-alkali rhyolites at low degrees of melting (e.g., Sisson et al., 2005; Whitaker et al., 2007). In contrast, melting of more felsic crustal rocks with quartz or with a large metasedimentary component creates calc-alkaline dacites and rhyolites (e.g., Patiño-Douce and Harris, 1998; Holtz and Johannes, 1991). These latter melts typically have lower Na/K ratios as well. These contrasting experimental melts are compared with magmatic trends in the southern Great Basin in Figure 25. Many of the more alkalic rhyolite and trachydacite ignimbrites in the western sector (Fig. 7B) are similar to the experimental melts of gabbro (i.e., arc basalt; 0.10 to 0.17 melt fractions in Sisson et al., 2005). The western rhyolites, therefore, could have been direct melts of this type of mafic crust; initial Sr isotope ratios are low and permissive of this interpretation (Fig. 5; Best et al., 2013c). Alternatively, they could have been produced when differentiating mafic magmas hybridized with such crustal melts. In any case, thinner, cooler mafic crust, like that below western Nevada, yielded small batches of alkali-rich rhyolite and lesser trachydacite where it was intruded and heated by mantle-derived basalt. On the other hand, thicker, hotter, felsic crust like that in the eastern sector yielded large batches of calc-alkaline rhyolite magma (melt fractions of 0.20 to 0.30). This rhyolite magma then interacted with the flux of mantle-derived magma to create the andesite-dacite-rhyolite spectrum, spawned in the midcrust. Sr isotope ratios show that the erupted ignimbrites are unlikely to have been pure crustal melts—a significant mantle component was required (Fig. 10).

Another way that crustal composition modulates ignimbrite compositions is revealed by the seemingly unique Isom-type trachydacite magmas in the southern Great Basin that are especially evident in the two eastern sectors. These hot, dry trachydacite magmas appear only to have formed when and where the crust was less fertile and incapable of yielding rhyolitic melts to mix with evolving mafic magmas. Infertility was caused by prior extraction of low-melting-point felsic material during the large-scale episode of monotonous intermediate magma production, or by hybridization of the crust by massive intrusion of mafic magma. Differentiation of mafic magmas without extensive crustal contamination is the hallmark of Isom-type magmas (Best et al., 2013b), but we cannot rule out the influence of other tectono-magmatic factors in their origin.

Mantle Contributions to the Southern Great Basin Ignimbrite Flareup

Input of mantle-derived basalt magmas into thick crust is fundamental to generation of ignimbrite flareups, but where and how were these empowering but unseen magmas generated?

Lithospheric Delamination or Dripping

One way to produce basaltic magma is by decompression of asthenospheric mantle as it rises and takes the place of dense delaminated mantle lithosphere and crust. Seismic data are consistent with such a mechanism for

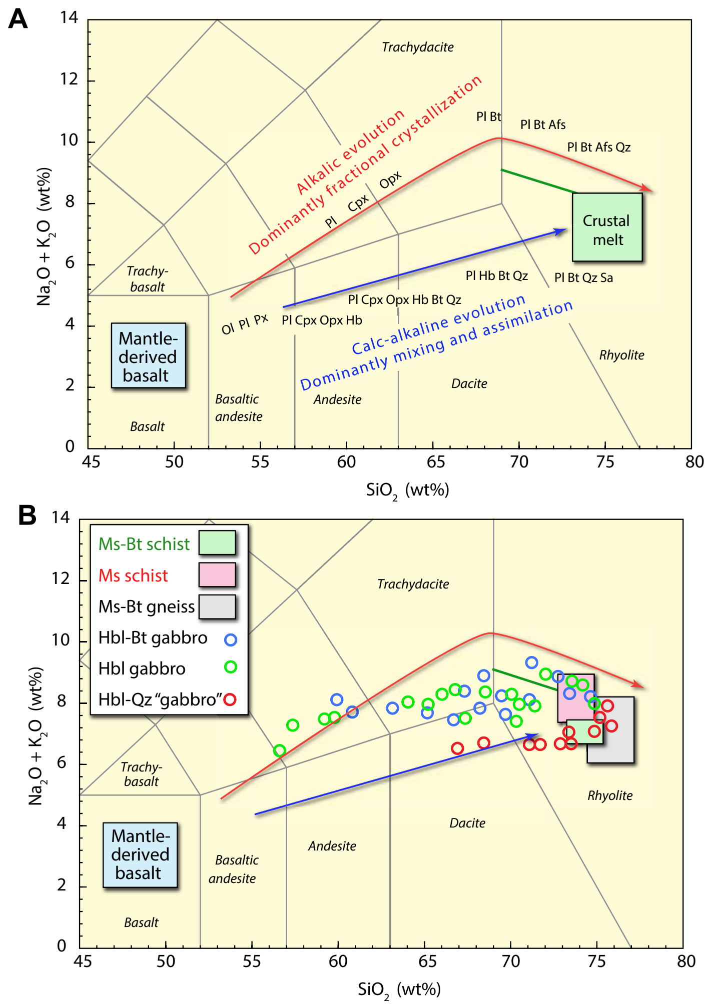

Figure 25. Two contrasting magmatic trends are apparent among ignimbrites of the southern Great Basin province. Green line separates calc-alkaline (below) from more alkalic (above) rhyolites (Fig. 7). (A) Relatively alkalic magmas can follow a fractional crystallization trend to trachydacite and alkali rhyolite. The calc-alkaline trend involves more crustal assimilation and mixing with crustally derived melts and includes dacite and calc-alkaline rhyolite. Representative mineral assemblages are listed on both trends: Pl—plagioclase; Cpx—clinopyroxene; Opx—orthopyroxene; Bt—biotite; Afs—alkali feldspar; Qz—quartz; Ol—olivine; Px—pyroxene; Hb—hornblende; Sa—sanidine. Alkali feldspar (sanidine and/or anorthoclase) appears early, and quartz later, in the alkalic-trend magmas. Compare with Figures 7, 15, 16A, 18, and 21A. (B) Compositions of partial melts of various crustal source rocks compared with the two magmatic trends in A. Partial melts of gabbro are more alkalic and lower in silica than are partial melts of quartz-bearing rocks (Sisson et al., 2005; Patiño-Douce and Harris, 1998; Holtz and Johannes, 1991). The hornblende-quartz "gabbro" in Sisson et al. (2005) is a basaltic andesite on the $Na_2O + K_2O$-SiO_2 diagram.

the ignimbrite flareup in the Central Andean plateau (e.g., Kay and Kay, 1993; Kay et al., 2014). These authors speculated that garnet was stabilized at the expense of plagioclase deep in the orogenically thickened crust below the plateau, causing subsequent delamination of the dense eclogitic lower crust. This triggered more magmatism by decompression melting of asthenosphere that flowed in to take its place; the extent of melting might have been limited by thick lithosphere, unless it had already sloughed away. DeCelles et al. (2009) have made lower-crustal delamination and decompression melting an integral element in their model of cyclicity in Cordilleran orogenic systems.

In view of the evidence for crust as thick as about 70 km beneath the southern Great Basin ignimbrite province during the flareup (Best et al., 2009), dense eclogite should have developed in the lower crust. If this was the case, then some of the lower crust of the Great Basin may have been removed by delamination, or dripping, in the closing stages of or after the ignimbrite flareup (Best et al., 2009). If the crust during the ignimbrite flareup was 70 km thick, after 50% postvolcanic extension (Best et al., 2013a), it should now be 45 km thick, compared to a current thickness of about 30–35 km (e.g., Allmendinger et al., 1987; Gilbert, 2012). Thus, the missing 10–15 km of crust might have been removed after the flareup. Another possibility to account for the missing 10–15 km of crust is that an eclogitic lower-crustal residue became seismically indistinguishable from the underlying mantle; in other words, the seismic Moho is imaged at a shallower depth than the petrologic Moho.

Steepening of the Subducting Plate

Rollback of a formerly flat slab is an essential feature of flareup models for southwestern North America (e.g., Coney, 1978; Lipman, 1980; Best and Christiansen, 1991) and for the Central Andes (e.g., de Silva and Gosnold, 2007; Kay and Coira, 2009). However, the exact nature of the flat slab subduction and especially the thermal regime of the slab and its dehydration, or lack thereof, are subjects of current debate (e.g., English et al., 2003; Usui et al., 2003; Humphreys, 2009; Jones et al., 2011, 2015); this lends a degree of uncertainty to inferences regarding the dynamic interaction of the crust and mantle during the flareup. For the southern Great Basin, Christiansen and Best (2014) concluded that it might have been difficult to derive enough mantle magma to drive silicic magma production from the lithospheric mantle alone (contrast this with the conclusions of Farmer et al. [2008] and Lake and Farmer [2015] for the Southern Rocky Mountain field). Thus, a major contribution from a sublithospheric source for the mafic magma may be required. Furthermore, English et al. (2003), Usui et al. (2003), and Liu et al. (2016) argued that the slab was only partly dewatered during the flat subduction stage (for more general models for slab dewatering, see also Rupke et al., 2004). We suggest that additional dehydration accompanied heating during slab rollback and immersion in the hotter asthenosphere, providing a major generating mechanism for basaltic partial melts in the overlying mantle wedge. We do not view this as a one-time event; ongoing subduction would continue to fuel dehydration and flux melting for several millions of years after rollback started.

Tears in the Subducting Plate

The manner of slab rollback was also significant for the flareup in western North America. Lipman (1980) identified the Jemez trend (a northeast-trending volcanic lineament) in New Mexico and interpreted it to be controlled by northeast -trending structures in the continental lithosphere and by an offset in the downgoing slab of oceanic lithosphere. McQuarrie and Oskin (2010) proposed that a major discontinuity in the pattern of migrating volcanism in southwestern North America (Fig. 26A) was the result of a tear in the subducting slab as it rolled back beneath the continental plate. This tear is roughly coincident with the Pioneer fracture zone and the hypothetical contact between the Hess oceanic plateau to the south and the Shatsky plateau to the north (Liu et al., 2010). The buoyant Shatsky Plateau apparently inhibited rollback and the development of a mantle wedge beneath the Colorado Plateau, thus accounting for the relatively small amount of unusual magmatism in its interior.

A nonuniform rollback of the Farallon slab is envisaged to have begun beneath the Pacific Northwest in the Eocene and migrated southward into Nevada-Utah-Colorado in the Oligocene (Lipman, 1980, 1982; Severinghaus and Atwater, 1990; Humphreys, 1995). Seismic tomography has confirmed the existence of remnants of the torn, segmented Farallon slab beneath the northern United States (e.g., Sigloch et al., 2008; Humphreys, 2009). Colgan et al. (2011) postulated that an Eocene–Miocene tear in the subducting Farallon plate resulted in the offset of the western Cascade volcanic arc in coastal Washington and Oregon from the Ancestral Cascade arc in northeastern California and Nevada.

In the southwestern United States (Fig. 26B), steepening of the slab, as indicated by the pattern of migrating magmatism, was relatively uniform from the eastern to western margins of the Colorado Plateau, that is, from the Southern Rocky Mountain volcanic field to the Marysvale field (Fig. 1). However, to the west in the Great Basin, the migration isochrons are less uniform, prompting us to speculate on the existence of additional tears in the slab. An apparent southward jog in the migration isochrons implies a pair of tears existed in the subducting plate before ca. 24 Ma. Between the tears, the slab rolled back to a much greater extent by 36 Ma, less so at 38 Ma and 30 Ma, relative to the rollback to the east and west of the paired tears (Fig. 26C). The region of the subducting slab between the two postulated northerly trending tears coincides with the central and eastern sectors of the Great Basin where a colossal volume (58,000 km^3) of mid-Cenozoic ignimbrite was erupted onto the thickest crust of the Great Basin altiplano east of the Precambrian continental margin and west of the stable Colorado Plateau (Table 1; Figs. 3 and 13). Between the two tears, the 36 to 24 Ma isochrons are closely spaced, implying a steeper slab. This might have resulted in a more focused release of fluids from the slab fragment and caused greater mantle melting and silicic magma production in the crust, thus accounting for the great eruptive volume in these sectors. As the slab dropped away from the overlying continental plate between the tears, hot asthenospheric mantle invaded the growing wedge region from around the edges of the slab (Fig. 26C). This decompressing asthenosphere could have experienced some partial melting, but the degree of melting might have been limited by the thickness of the overlying lithosphere, unless decompression was concurrent with lithospheric delamination or dripping. As the hot asthenosphere contacted the base of the partially hydrated lithosphere, additional melting could have taken place. In concert with fluids released from the heated underlying slab, these secondary melting processes are likely to have resulted in an unusually high flux of basaltic magma into the crust beneath the central and eastern sectors. The chemical and isotopic compositions of some ignimbrites, such as those of the Isom type (Best et al., 2013c, their p. 57), suggest they have components from flux melting and from decompression melting of the asthenosphere. Some of the basalt magma produced near the east tear in southwestern Utah otherwise destined for the Marysvale volcanic field could have moved west of the tear to feed the eastern sector (Fig. 26C), thus accounting for the striking contrast in the volume and nature of volcanism in these two fields.

The nested calderas in the central and eastern sectors of the Great Basin (Figs. 2 and 14) testify to pulsed ascent of diapirs along the same established path from the well-developed MASH zone fed by an unusually high flux of basaltic magma into the crust between the two tears.

The western of the paired tears (Fig. 26B) is close to the eastern boundary of the western sector of the Great Basin province (Figs. 2 and 6), where a more gradual slab rollback took place. In this sector, caldera-forming eruptions were distributed northward over a larger area, and apparently fewer were nested, compared to the east. Subsequently, the gently dipping segment of the plate seems to have taken on a "normal" subduction configuration with a northerly strike approximately along the present eastern Sierra Nevada front, creating the Ancestral Cascade arc (Christiansen and Lipman, 1972; Cousens et al., 2008; Colgan et al., 2011).

Volcanic activity related to tears and segmentation of subducting slabs appears to be common in other arcs. In the case of the late Cenozoic Andean ignimbrite flareup, a possible tear lies south of the Cerro Galan and Altiplano-Puna volcanic complexes (Fig. 19A). Elsewhere, tears have been discussed for the Sunda arc (Page et al., 1979, p. 575; Pesicek et al., 2008) and the Eolian arc (Faccenna et al., 2011). In the Central American arc, slab tears have been proposed by Dougherty and Clayton (2014), while Ferrari et al. (2007) argued for slab rupture beneath the Sierra Madre Occidental, and a tear associated with rollback has been identified beneath the Trans-Mexican volcanic belt (Ferrari et al., 2012).

IGNIMBRITE FLAREUPS AND SUBDUCTION

According to Bryan and Ferrari (2013) and Cather et al. (2009), the mid-Cenozoic ignimbrite flareup of southwestern North America was part of an intraplate silicic large igneous province. However, the criteria laid out by Bryan et al. (2008) and Bryan and Ferrari (2013) for such a province are not consis-

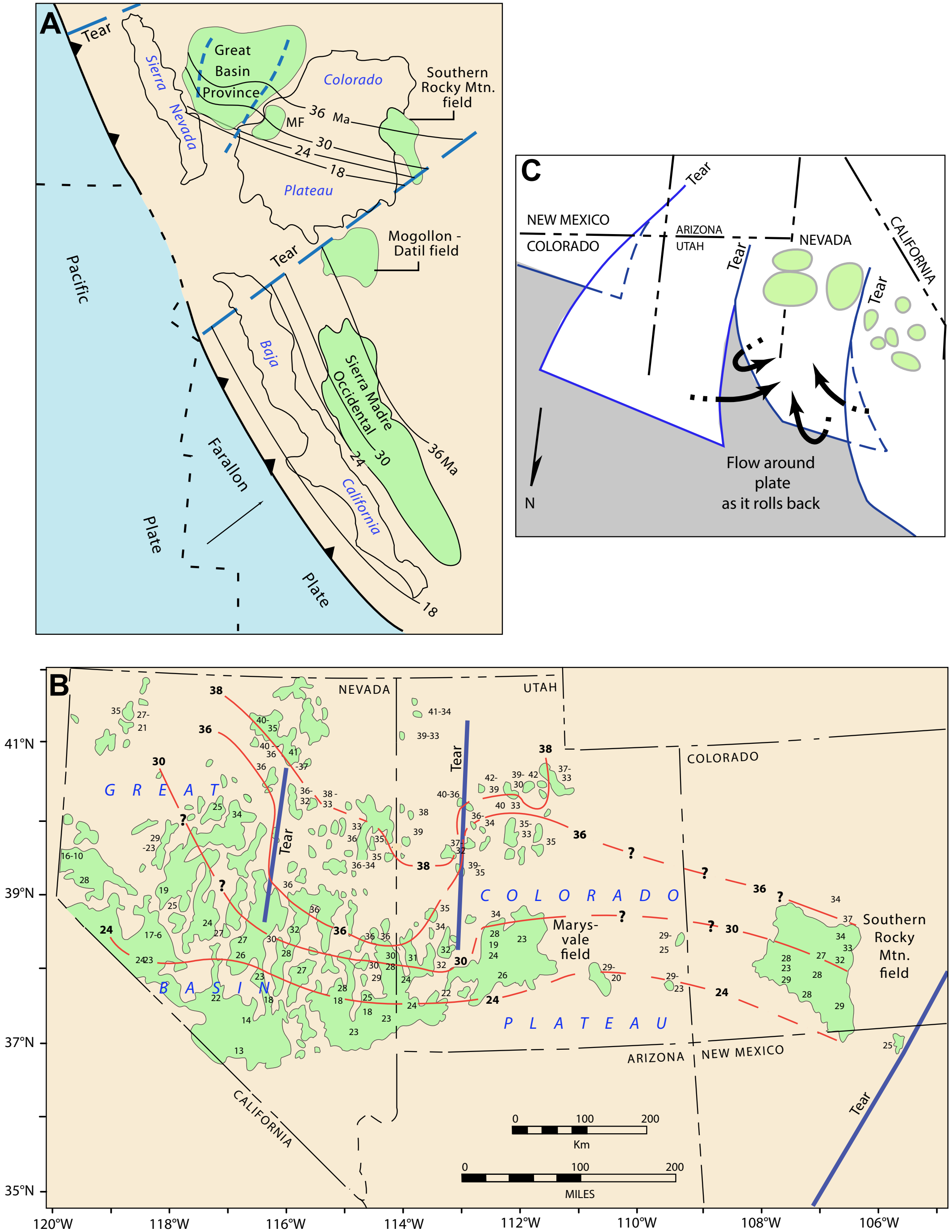

Figure 26. Patterns of migrating mid-Cenozoic volcanism in southwestern North America (cf. Fig. 1) and postulated tears in the underlying subducting slab during rollback from a previous flat configuration. (A) Map modified from Lipman (1980, his fig. 14.7) and McQuarrie and Oskin (2010, their fig. 5B) showing a proposed tear in the subducting Farallon plate offsetting the Southern Rocky Mountain and Mogollon-Datil volcanic fields. Isochron lines (36 Ma, 30, etc.) indicate southernmost advance of volcanism at indicated time; 36 Ma and 30 Ma lines in the Great Basin are from diagram in B. MF—Marysvale volcanic field. Miocene slab tear for Cascade arc of Colgan et al. (2011) is shown in northwest corner of map. Base map is a tectonic reconstruction at 24 Ma and shows relative positions of the unextended Sierra Nevada, Colorado Plateau, and Baja California. (B) Great Basin–Colorado Plateau magmatic belt showing outlines of subduction-related 43–6 Ma magmatic rocks (modified from Stewart and Carlson, 1976; Lipman, 2007). Some occurrences are too small to appear on this scale. Red isochron lines are generalized southernmost advance of magmatism at indicated time from data in Best et al. (2013a, 2013b), Nelson et al. (1992), Lipman (2007), Hintze and Kowallis (2009), Gans et al. (1989), du Bray, (2007), and our data. North-south jogs in isochrons in Nevada and Utah are interpreted to represent northerly trending tears (blue) in the subducting plate. The base map has not been corrected for east-west extension. (C) Simplified perspective view from the north looking south of the upper surface of the subducting plate at about 36 Ma interpreted from the isochrons in diagram B. Caldera complexes in the Great Basin are shown schematically in green. Note the three tears in the plate. Arrows indicate possible flow of mantle asthenosphere into the wedge region above the more steeply dipping slab between the paired tears in the Great Basin.

tent with the southwestern North America flareup, which was clearly related to subduction beneath the margin of the North America plate. The ignimbrite flareup followed a long period of prior contractional deformation, whereas regional tectonic extension mostly followed the flareup. No basalt, much less flood basalt, accompanied the flareup, and the compositions of the volcanic rocks have more geochemical similarities to those in arcs than in intraplate settings. For example, flareup magmas in the mid-Cenozoic southern Great Basin province contrast strongly with those in silicic large igneous provinces like the Yellowstone hotspot (Fig. 10; Christiansen, 2001, 2005; Christiansen and McCurry, 2008) or Africa-Arabia (Ukstins-Peate et al., 2005). Magmas in large silicic igneous provinces are typically rhyolitic, with low fO_2 and fH_2O, elevated concentrations of high field strength elements (with low solubilities) like Nb and Zr, and low ratios of large ion lithophile (soluble) elements to high field strength elements (e.g., La/Nb; Ba/Nb). Additionally, they have high eruption temperatures for a given silica content and, importantly, form bimodal suites with chemically distinctive basalts. The volcanic rocks of the southern Great Basin and other Cenozoic ignimbrite flareups summarized here range from basaltic andesite to rhyolite and formed from magmas that were mostly cool, wet, oxidized, and typically, but not universally, magnesian rather than ferroan, and calc-alkalic rather than alkalic. The dacites and rhyolites are depleted in high field strength elements and have high Ba/Nb (and other large ion lithophile element to high field strength element ratios). These attributes reflect their subduction heritage. The distinctive Isom Formation ignimbrites could mark a switch to intraplate magmatism, but they retain enrichments of large ion lithophile elements, high Ba/Nb ratios, and higher fO_2 like their predecessors and lack a bimodal association with erupted basalt. Moreover, subduction-related rhyolites in the southern Great Basin both preceded and followed after eruption of the Isom ignimbrites.

It is clear that Cenozoic voluminous ignimbrite flareups of the western American Cordillera were fundamentally subduction-related features and not formed by intraplate processes, although one can certainly transition to the other.

CONCLUSIONS

Continental margin arc volcanism above subducting oceanic plates is expressed by a broad spectrum of magma systems and corresponding surface manifestations (Fig. 27). The more familiar, near-trench, steady-state activity is represented by many arc systems around the globe. These volcanic arcs generally form on crust thinner than 40 km and have relatively frequent and small eruptions building stratovolcanoes of mafic to intermediate lavas and minor pyroclastic rocks. In contrast, slab-rollback ignimbrite flareups constitute a distinct, recognizable style of arc volcanism. Their attributes include: several tens of explosive, caldera-forming eruptions of dacitic, rhyolitic, and trachydacitic magma over 10–20 m.y periods; eruptions that are relatively infrequent (recurrence intervals of 10^4 to 10^6 yr) but individually of large magnitude (10^2 to 10^3 km^3); and common super-eruptions (>10^3 km^3). Individual outflow sheets extend to 150 km from the caldera source and cover as much as 30,000 km^2 to thicknesses of several hundred meters, even where no prior topographic low existed. An entire composite field surrounding a multicyclic caldera complex can blanket 100,000 km^2. Little or no basalt lava is extruded, but derivative andesite magmas play significant roles in production of silicic ignimbrite magma, even where their extruded volume is as little as one tenth the volume of contemporaneous silicic ignimbrite.

The mid-Cenozoic southern Great Basin ignimbrite province serves as a prime example of this ignimbrite flareup style of continental arc volcanism (Table 1). Other contemporaneous volcanic fields in southwestern North America that experienced voluminous ignimbrite flareups and share similar attributes (Table 2) include: the Southern Rocky Mountain and the Mogollon-Datil fields peripheral to the Colorado Plateau (Fig. 1) and the contiguous, vast Sierra Madre Occidental province in Mexico. The late Cenozoic flareup in the Central Andean Altiplano-Puna volcanic complex is an especially significant example that provides geophysical insights because of its recent activity.

An inventory of these Cenozoic flareup fields discloses that a dynamic interaction of key factors governs their development:

(1) After a period of "flat" subduction, slab rollback to a steeper dip beneath thick continental crust results in volcanism far inland from the trench.

(2) Copious basalt magma is generated by transient dehydration of the foundering slab and flux melting of the overlying mantle. Additional processes might include lithospheric delamination, decompression melting of ascending asthenosphere, and melting of the base of the overlying hydrated lithosphere as hot asthenosphere is contacted (Fig. 23).

(3) Tears in the slab produce variations in the rate of rollback and the amount of mantle magma that invades the crust (Fig. 26).

(4) Voluminous basalt magma intrudes nonextending crust, elevating the geothermal gradient, rendering much of the crust ductile, generating large MASH zones, and creating huge volumes of hybridized silicic magma.

(5) Hybridized silicic magmas ascend from the MASH zones as diapirs, rather than through dikes as in steady-state arc volcanism. Diapirs ascend to the elevated brittle-ductile transition in the shallow crust, where the magma spreads laterally. In this ductile storage regime, magma accumulates over 10^4 to 10^6 yr, forming large, broadly discoidal melt-rich zones prior to erupting, rather than erupting in small increments (Fig. 22).

(6) The variable thickness, temperature, and composition of the crust modulate the character of flareups. Where the crust is felsic, thickest, and most prewarmed by orogenic thickening, voluminous dacite (monotonous intermediate) is the dominant erupted product, accompanied by lesser calc-alkaline rhyolite. Voluminous, unusually hot and dry Isom-type trachydacites develop where crustal assimilation into evolving andesitic magmas is minimized by prior extraction of the low-melting-point materials. In places where the crust was thinner and more mafic, alkali-rich rhyolite and related trachydacite dominate the volcanic record.

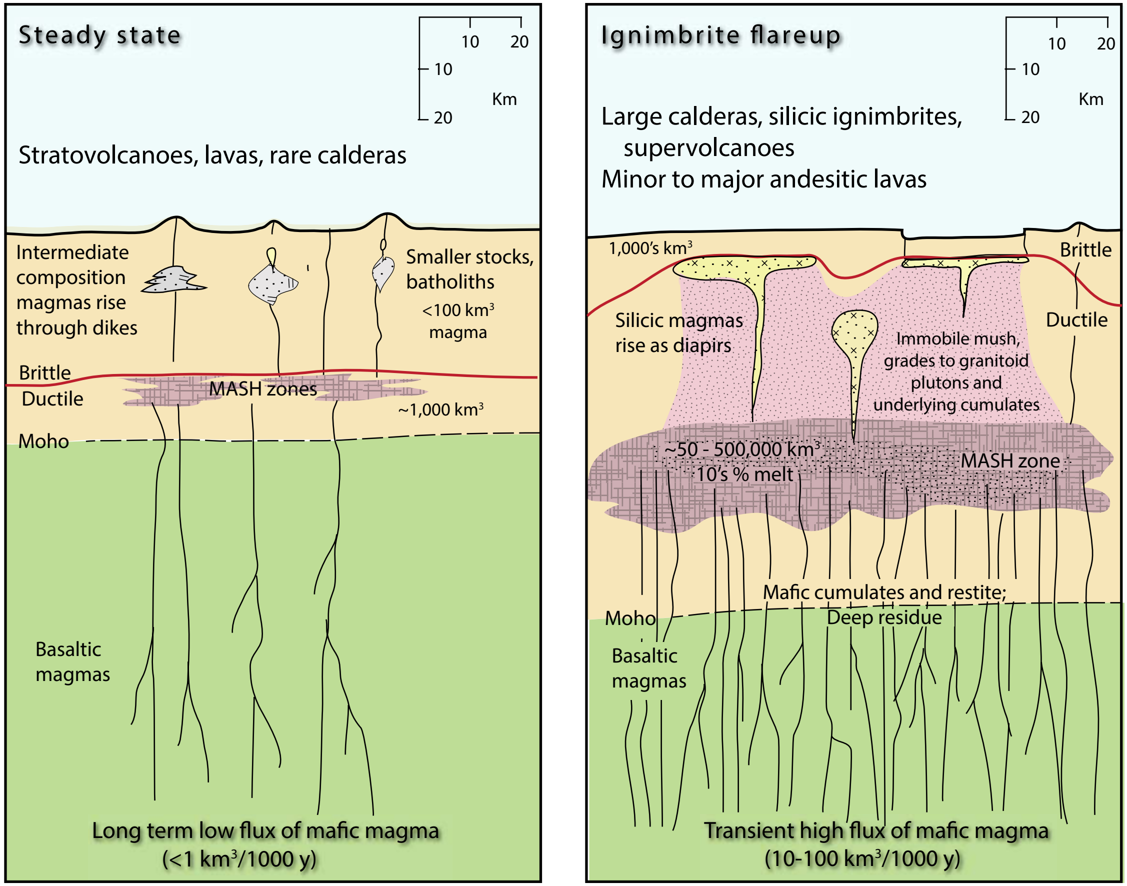

Figure 27. Contrasting styles of continental arc volcanism (compare de Silva, 2008; de Silva et al., 2015; Lipman and Bachmann, 2015, their fig. 13). Note especially contrasts in the flux of mantle-derived basalt, depth, and extent of melting (MASH) zones, location of brittle-ductile transition, mode of magma ascent in crust, size of pre-eruption magma chambers and related intrusions, volcanic constructs, and composition and volume of erupted magma. A vertically extensive subvolcanic batholith develops beneath the flareup volcanic field (compare Fig. 22C).

ACKNOWLEDGMENTS

Study of the southern Great Basin ignimbrite province by Best and Christiansen has benefited from the assistance of numerous individuals over the past decades; they are acknowledged in Best et al. (2013a, 2013b, 2013c). We especially recognize the collaboration of our colleagues Sherman Grommé and Alan Deino for their crucially important paleomagnetic and chronologic data and Chris Henry and Dave John for their work on the Western Nevada field that provided an important comparison for the volcanism in the central and eastern sectors of the province. Financial support was provided by the National Science Foundation through grants EAR-8604195, EAR-8618323, EAR-8904245, EAR-9104612, EAR-9706906, and EAR-0923495 to M.G. Best and E.H. Christiansen. The U.S. Geological Survey and Nevada Bureau of Mines and Geology supported quadrangle mapping. The continuing financial and material assistance of Brigham Young University is gratefully acknowledged. Also, de Silva acknowledges the many students and colleagues (too numerous to mention here but acknowledged in specific publications) who have been crucial to the work in the Central Andes. The late Peter Francis is singled out with deep gratitude for introduction to the area and early mentoring. Financial support from the Royal Society of the UK, National Aeronautics and Space Administration (grant NAGW-1167), and the National Science Foundation (EAR-0710545, EAR-0838536, and EAR-0908324) is gratefully acknowledged. Geologic mapping and other long-term research in the Southern Rocky Mountain volcanic field by Lipman have been supported by several parts of the U.S. Geological Survey, including the Volcanic Hazards, National Geologic Mapping, and Mineral Resources Programs. Especially critical in recent years have been geochronologic studies in collaboration with William McIntosh and Matthew Zimmerer at the New Mexico Bureau of Geology and Mineral Resources. We are grateful for the comments of Susanne McDowell and one anonymous reviewer and Lang Farmer for his editorial assistance.

REFERENCES CITED

Allmendinger, R.W., Hauge, T.A., Hauser, E.C., Potter, C.J., and Oliver, J., 1987, Tectonic heredity and the layered lower crust in the Basin and Range Province, western United States, *in* Coward, M.P., Dewey, J.F., and Hancock, P.L., eds., Continental Extension Tectonics: Geological Society of London Special Publication 28, p. 223–246, doi:10.1144/GSL.SP.1987.028.01.16.

Allmendinger, R.W., Jordan, T.E., Kay, S.M., and Isacks, B.L., 1997, The evolution of the Altiplano-Puna plateau of the Central Andes: Annual Review of Earth and Planetary Sciences, v. 25, p. 139–174, doi:10.1146/annurev.earth.25.1.139.

Anderson, R.E., Beard, L.S., Mankinen, E.A., and Hillhouse, J.W., 2013, Analysis of Neogene deformation between Beaver, Utah, and Barstow, California: Suggestions for altering the extensional paradigm, *in* Anderson, R.E., ed., Neogene Deformation between Central Utah and the Mojave Desert: Geological Society of America Special Paper 499, p. 1–67, doi:10.1130/2013.2499(01).

Annen, C., 2009, From plutons to magma chambers: Thermal constraints on the accumulation of eruptible silicic magma in the upper crust: Earth and Planetary Science Letters, v. 284, no. 3, p. 409–416, doi:10.1016/j.epsl.2009.05.006.

Armstrong, P.A., Ehlers, T.A., Chapman, D.S., Farley, K.A., and Kamp, P.J.J., 2003, Exhumation of the central Wasatch Mountains, Utah: 1. Patterns and timing of exhumation deduced from low-temperature thermochronology data: Journal of Geophysical Research, v. 108, p. 17, doi:10.1029/2001JB001708.

Askren, D.R., Roden, M.F., and Whitney, J.A., 1997, Petrogenesis of Tertiary andesite lava flows interlayered with large-volume felsic ash-flow tuffs of the western USA: Journal of Petrology, v. 38, p. 1021–1046, doi:10.1093/petroj/38.8.1021.

Axelrod, D.I., 1987, The Late Oligocene Creede Flora, Colorado: University of California Publications in Geological Sciences 130, 235 p.

Bachmann, O., Dungan, M.A., and Lipman, P.W., 2002, The Fish Canyon magma body, San Juan volcanic field, Colorado: Rejuvenation and eruption of an upper-crustal batholith: Journal of Petrology, v. 43, p. 1469–1503, doi:10.1093/petrology/43.8.1469.

Bachmann, O., Oberli, F., Dungan, M., Meier, M., Mundil, R., and Fischer, H., 2007, $^{40}Ar/^{39}Ar$ and U-Pb dating of the Fish Canyon magmatic system, San Juan volcanic field, Colorado: Evidence for an extended crystallization history: Chemical Geology, v. 236, no. 1–2, p. 134–166, doi:10.1016/j.chemgeo.2006.09.005.

Bachmann, O., Deering, C.D., Lipman, P.W., and Plummer, C., 2014, Building zoned ignimbrites and recycling silicic cumulates: Insight from the 1000 km^3 Carpenter Ridge Tuff, CO: Contributions to Mineralogy and Petrology, v. 167, p. 1025, doi:10.1007/s00410-014-1025-3.

Best, M.G., and Christiansen, E.H., 1991, Limited extension during peak Tertiary volcanism, Great Basin of Nevada and Utah: Journal of Geophysical Research, v. 96, p. 13,509–13,528, doi:10.1029/91JB00244.

Best, M.G., Armstrong, R.L., Graustein, W.C., Embree, G.F., and Ahlborn, F.C., 1974, Mica granites of the Kern Mountains pluton, eastern White Pine County, Nevada: Remobilized basement of the Cordilleran miogeosyncline: Geological Society of America Bulletin, v. 85, p. 1277–1286, doi:10.1130/0016-7606(1974)85<1277:MGOTKM>2.0.CO;2.

Best, M.G., Barr, D.L., Christiansen, E.H., Gromme, C.S., Deino, A.L., and Tingey, D.G., 2009, The Great Basin altiplano during the middle Cenozoic ignimbrite flareup: Insights from volcanic rocks: International Geology Review, v. 51, no. 6, p. 1–45.

Best, M.G., Christiansen, E.H., and Gromme, S., 2013a, Introduction: The 36–18 Ma southern Great Basin, USA, ignimbrite province and flareup: Swarms of subduction-related supervolcanoes: Geosphere, v. 9, no. 2, p. 260–274, doi:10.1130/GES00870.1.

Best, M.G., Christiansen, E.H., Deino, A.L., Gromme, S., and Tingey, D.G., 2013b, The 36–18 Ma Indian Peak–Caliente ignimbrite field and calderas, southeastern Great Basin, USA: Multicyclic super-eruptions: Geosphere, v. 9, no. 4, p. 864–950, doi:10.1130/GES00902.1.

Best, M.G., Gromme, S., Deino, A.L., Christiansen, E.H., Hart, G.L., and Tingey, D.G., 2013c, The 36–18 Ma Central Nevada ignimbrite field and calderas, Great Basin, USA: Multicyclic super-eruptions: Geosphere, v. 9, no. 6, p. 1562–1636, doi:10.1130/GES00945.1.

Blackwell, D.D., 1971, The thermal structure of the continental crust, *in* Heacock, J.G., ed., The Structure and Physical Properties of the Earth's Crust: American Geophysical Union Geophysical Monograph 14, p. 169–184, doi:10.1029/GM014p0169.

Blaylock, G.W., 1998, Probable Correlation of the Oligocene Whitney Ash Beds of Western Nebraska to Ash-Flow Tuffs in Nevada and Utah [M.S. thesis]: Provo, Utah, Brigham Young University, 45 p.

Bonner, J.L., and Herrin, E.T., 1999, Surface wave studies of the Sierra Madre Occidental of northern Mexico: Bulletin of the Seismological Society of America, v. 89, p. 1323–1337.

Bornhorst, T.J., 1980, Major- and Trace-Element Geochemistry and Mineralogy of Upper Eocene to Quaternary Volcanic Rocks of the Mogollon-Datil Volcanic Field, Southwestern New Mexico [Ph.D. thesis]: Albuquerque, New Mexico, University of New Mexico, 1108 p.

Boroughs, S., Wolff, J., Bonnichsen, B., Godchaux, M., and Larson, P., 2005, Large-volume, low-^{18}O rhyolites of the Central Snake River Plain, Idaho, USA: Geology, v. 33, no. 10, p. 821–824, doi:10.1130/G21723.1.

Brandmeier, M., and Wörner, G., 2014, Andes Ignimbrite Database (AIDA): http://www.arcgis.com/home/item.html?id=47038ddc0628473f9f0ce67aa2eff8be (accessed 15 August 2015).

Brown, S.J.A., and Fletcher, I.R., 1999, SHRIMP U-Pb dating of the preeruption growth history of zircons from the 340 ka Whakamaru ignimbrite, New Zealand: Evidence for >250 k.y. magma residence times: Geology, v. 27, no. 11, p. 1035–1038, doi:10.1130/0091-7613(1999)027<1035:SUPDOT>2.3.CO;2.

Bryan, S.E., and Ferrari, L., 2013, Large igneous provinces and silicic large igneous provinces: Progress in our understanding over the last 25 years: Geological Society of America Bulletin, v. 125, p. 1053–1078, doi:10.1130/B30820.1.

Bryan, S.E., Ferrari, L., Reiners, P.W., Allen, C.M., Petrone, C.M., Ramos Rosique, A., and Campbell, I.H., 2008, New insights into crustal contributions to large volume rhyolite generation at the mid-Tertiary Sierra Madre Occidental province, Mexico, revealed by U-Pb geochronology: Journal of Petrology, v. 49, p. 47–77, doi:10.1093/petrology/egm070.

Bryan, S.E., Peate, I.U., Peate, D.W., Self, S., Jerram, D.A., Mawby, M.R., Marsh, J.S., and Miller, J.A., 2010, The largest volcanic eruptions on Earth: Earth-Science Reviews, v. 102, p. 207–229, doi:10.1016/j.earscirev.2010.07.001.

Burchfiel, B.C., Lipman, P.W., and Zoback, M.L., eds., 1992, The Cordilleran Orogen: Conterminous U.S.: Boulder, Colorado, Geological Society of America, The Geology of North America, v. G-3, 724 p.

Burns, D.H., de Silva, S.L., Tepley, F., III, Schmitt, A.K., and Loewen, M.W., 2015, Recording the transition from flare-up to steady-state arc magmatism at the Purico-Chascon volcanic complex, northern Chile: Earth and Planetary Science Letters, v. 422, p. 75–86, doi:10.1016/j.epsl.2015.04.002.

Caffe, P.J., Trumbull, R.B., and Siefel, W., 2012, Petrology of the Coyaguayma ignimbrite, northern Puna of Argentina: Origin and evolution of a peraluminous high-SiO_2 rhyolite magma: Lithos, v. 134–135, p. 179–200, doi:10.1016/j.lithos.2011.12.013.

Cameron, K.L., and Hanson, G.N., 1982, Rare earth element evidence concerning the origin of voluminous mid-Tertiary rhyolitic ignimbrites and related volcanic rocks, Sierra Madre Occidental, Chihuahua, Mexico: Geochimica et Cosmochimica Acta, v. 46, p. 1489–1503, doi:10.1016/0016-7037(82)90309-X.

Cameron, K.L., Nimz, G.J., Kuentz, D., Niemeyer, S., and Gunn, S., 1989, Southern Cordilleran basaltic andesite suite, southern Chihuahua, Mexico: A link between Tertiary continental arc and flood basalt magmatism in North America: Journal of Geophysical Research, v. 94, p. 7817–7840, doi:10.1029/JB094iB06p07817.

Campbell, S.K., 1994, A Geochemical and Strontium Isotopic Investigation of Laramide and Younger Igneous Rocks in Central Colorado, with Emphasis on the Petrogenesis of the Thirty-nine Mile Volcanic Field [Ph.D. thesis]: Tallahassee, Florida, Florida State University, 614 p.

Capitanio, F.A., Faccenna, C., Zlotnik, S., and Stegman, D.R., 2011, Subduction dynamics and the origin of Andean orogeny and the Bolivian orocline: Nature, v. 480, no. 7375, p. 83–86, doi:10.1038/nature10596.

Cashman, K.V., and Sparks, R.S.J., 2013, How volcanoes work: A 25 year perspective: Geological Society of America Bulletin, v. 125, p. 664–690, doi:10.1130/B30720.1.

Cassel, E.J., Breecker, D.O., Henry, C.D., Larson, T.E., and Stockli, D.F., 2014, Profile of a paleo-orogen: High topography across the present-day Basin and Range from 40 to 23 Ma: Geology, v. 42, p. 1007–1010, doi:10.1130/G35924.1.

Cather, S.M., Dunbar, N.W., McDowell, F.W., McIntosh, W.C., and Scholle, P.A., 2009, Climate forcing by iron fertilization from repeated ignimbrite eruptions: The icehouse-silicic large igneous province (SLIP) hypothesis: Geosphere, v. 5, no. 3, p. 315–324, doi:10.1130/GES00188.1.

Chapman, J.G., Ducea, M.N., DeCelles, P.G., and Profeta, L., 2015, Tracking changes in crustal thickness during orogenic evolution with Sr/Y: An example from the North American Cordillera: Geology, v. 43, p. 919–922, doi:10.1130/G36996.1.

Christiansen, E.H., 2005, Contrasting processes in silicic magma chambers: Evidence from very large volume ignimbrites: Geological Magazine, v. 142, p. 669–681, doi:10.1017/S0016756805001445.

Christiansen, E.H., and Best, M.G., 2014, Constraints on the origin of subduction-related ignimbrite flareups from source volume calculations: The southern Great Basin ignimbrite province: Geological Society of America Abstracts with Programs, v. 46, no. 6, p. 374.

Christiansen, E.H., and McCurry, M., 2008, Contrasting origins of Cenozoic silicic volcanic rocks from the western Cordillera of the United States: Bulletin of Volcanology, v. 70, p. 251–267, doi:10.1007/s00445-007-0138-1.

Christiansen, E.H., Sheridan, M.F., and Burt, D.M., 1986, The Geology and Geochemistry of Cenozoic Topaz Rhyolites from the Western United States: Geological Society of America Special Paper 205, 82 p, doi:10.1130/SPE205-p1.

Christiansen, E.H., Baxter, N., Ward, T.P., Zobell, E., Chandler, M.R., Dorais, M.J., Kowallis, B.J., and Clark, D.L., 2007a, Cenozoic Soldiers Pass volcanic field, central Utah—Implications for the transition to extension-related magmatism in the Basin and Range Province, *in* Willis, G.C., Hylland, M.D., Clark, D.L., and Chidsey, T.C., Jr., eds., Central Utah—Diverse Geology of a Dynamic Landscape: Utah Geological Association Guidebook 36, p. 123–142.

Christiansen, E.H., Haapala, I., and Hart, G., 2007b, Are Cenozoic topaz rhyolites the erupted equivalents of Proterozoic rapakivi granites?: Lithos, v. 97, p. 219–246, doi:10.1016/j.lithos.2007.01.010.

Christiansen, E.H., Kowallis, B.J., Dorais, M.J., Hart, G.L., Mills, C.N., Pickard, M., and Parks, E., 2015, The record of volcanism in the Brushy Basin Member of the Morrison Formation:

Implications for the Late Jurassic of western North America, *in* Anderson, T., Didenko, A., Johnson, C., Khanchuk, and MacDonald, J., eds., Late Jurassic Margin of the Laurasia: A Record of Faulting Accommodating Plate Rotation: Geological Society of America Special Paper 513, doi:10.1130/2015.2513(11).

Christiansen, R.L., 2001, The Quaternary and Pliocene Yellowstone Plateau Volcanic Field of Wyoming, Idaho, and Montana: U.S. Geological Survey Professional Paper 729-G, 145 p., map scale 1:500,000.

Christiansen, R.L., and Lipman, P.W., 1972, Cenozoic volcanism and plate tectonic evolution of the western United States—II. Late Cenozoic: Royal Society of London Philosophical Transactions, ser. A, v. 271, p. 249–284, doi:10.1098/rsta.1972.0009.

Coira, B., Davidson, J., Mpodozis, C., and Ramos, V., 1982, Tectonic and magmatic evolution of the Andes of northern Argentina and Chile: Earth-Science Reviews, v. 18, p. 302–332, doi:10.1016/0012-8252(82)90042-3.

Coira, B., Kay, S.M., and Viramonte, J., 1993, Upper Cenozoic magmatic evolution of the Argentine Puna—A model for changing subduction geometry: International Geology Review, v. 35, p. 677–720, doi:10.1080/00206819309465552.

Colgan, J.P., and Henry, C.D., 2009, Rapid middle Miocene collapse of the Mesozoic orogenic plateau in north-central Nevada: International Geology Review, v. 51, p. 920–961, doi:10.1080/00206810903056731.

Colgan, J.P., Egger, A.E., John, D.A., Cousens, B., Fleck, R.J., and Henry, C.D., 2011, Oligocene and Miocene arc volcanism in northeastern California: Evidence for post-Eocene segmentation of the subducting Farallon plate: Geosphere, v. 7, p. 733–755, doi:10.1130/GES00650.1.

Colgan, J.P., Watts, K.W., Henry, C., and John, D., 2013, Characterizing geographic variability in magma composition and eruptive style during voluminous mid-Tertiary magmatism in the northern Great Basin using zircon U-Pb geochronology and phenocryst O isotopic data: Washington, D.C., American Geophysical Union, Fall Meeting, abstract V33E-2831.

Colucci, M.T., Dungan, M.T., Ferguson, K.M., Lipman, P.W., and Moorbath, S., 1991, Precaldera lavas of the southeast San Juan volcanic field—Parent magmas and crustal interactions: Journal of Geophysical Research, v. 96, p. 13,412–13,434, doi:10.1029/91JB00282.

Comeau, M.J., Unsworth, M.J., Ticona, F., and Sunagua, M., 2015, Magnetotelluric images of magma distribution beneath Volcán Uturuncu, Bolivia: Implications for magma dynamics: Geology, v. 43, p. 243–246, doi:10.1130/G36258.1.

Coney, P.J., 1978, Mesozoic–Cenozoic Cordilleran plate tectonics, *in* Smith, R.B., and Eaton, G.P., eds., Cenozoic Tectonics and Regional Geophysics of the Western Cordillera: Geological Society of America Memoir 152, p. 33–50, doi:10.1130/MEM152-p33.

Coney, P.J., and Harms, T.A., 1984, Cordilleran metamorphic core complexes: Cenozoic extensional relicts of Mesozoic compression: Geology, v. 12, p. 550–554, doi:10.1130/0091-7613(1984)12<550:CMCCCE>2.0.CO;2.

Coney, P.J., and Reynolds, S.J., 1977, Cordilleran Benioff zones: Nature, v. 270, p. 403–406, doi:10.1038/270403a0.

Constenius, K.N., 1996, Late Paleogene extensional collapse of the Cordilleran foreland fold and thrust belt: Geological Society of America Bulletin, v. 108, p. 20–39, doi:10.1130/0016-7606(1996)108<0020:LPECOT>2.3.CO;2.

Costa, F., 2008, Residence times of silicic magmas associated with calderas, *in* Gottsmann, J., and Martí, J., eds., Caldera Volcanism: Analysis, Modelling and Response: Developments in Volcanology, Volume 10: Amsterdam, Elsevier, p. 1–55, doi:10.1016/S1871-644X(07)00001-0.

Couch, R.W., Ness, G.E., Sanchez-Zamora, O., Calderon-Riveroll, G., Doguin, P., Plowman, T., Ceperude, S., Huehn, B., and Gumma, W., 1991, Gravity anomalies and crustal structure of the Gulf and Peninsular Province of the Californias, *in* Dauphin, J.P., and Simonteil, B.R.T., eds., The Gulf and Peninsular Province of the Californias: American Association of Petroleum Geologists Memoir 47, p. 47–70.

Cousens, B., Prytulak, J., Henry, C., Alcazar, A., and Brownrigg, T., 2008, Geology, geochronology, and geochemistry of the Miocene–Pliocene Ancestral Cascades arc, northern Sierra Nevada, California and Nevada: The roles of the upper mantle, subducting slab, and the Sierra Nevada lithosphere: Geosphere, v. 4, no. 5, p. 829–853, doi:10.1130/GES00166.1.

Cunningham, C.G., Unruh, D.M., Steven, T.A., Rowley, P.D., Naeser, C.W., Mehnert, H.H., Hedge, C.E., and Ludwig, K.R., 1997, Geochemistry of Volcanic Rocks in the Marysvale Volcanic Field, West-Central Utah: U.S. Geological Survey Bulletin, v. 2158, p. 223–231.

Cunningham, C.G., Rowley, P.D., Steven, T.A., and Rye, R.O., 2007, Geologic evolution and mineral resources of the Marysvale volcanic field, west-central Utah, *in* Willis, G.C., Hylland, M.D., Clark, D.L., and Chidsey, T.C., Jr., eds., Central Utah—Diverse Geology of a Dynamic Landscape: Utah Geological Association Guidebook 36, p. 143–161.

Davis, G.H., 1999, Structural Geology of the Colorado Plateau Region of Southern Utah, with Special Emphasis on Deformation Bands: Geological Society of America Special Paper 342, 157 p, doi:10.1130/0-8137-2342-6.1.

Davis, J.M., and Hawkesworth, J.D., 1994, Early calc-alkaline magmatism in the Mogollon-Datil volcanic field, New Mexico, USA: Journal of the Geological Society, v. 151, p. 825–843, doi:10.1144/gsjgs.151.5.0825.

Davis, J.M., Elston, W.E., and Hawkesworth, C.J., 1993, Basic and intermediate volcanism of the Mogollon-Datil volcanic field: Implications for mid-Tertiary tectonic transitions in southwestern New Mexico, USA, *in* Prichard, H.M., Alabaster, T., Harris, N.B.W., and Neary, C.R., eds., Magmatic Processes and Plate Tectonics: Geological Society of London Special Publication 76, p. 469–488, doi:10.1144/GSL.SP.1993.076.01.25.

DeCelles, P.G., 2004, Late Jurassic to Eocene evolution of the Cordilleran thrust belt and foreland system, western USA: American Journal of Science, v. 304, p. 105–168, doi:10.2475/ajs.304.2.105.

DeCelles, P.G., Ducea, M.N., Kapp, P., and Zandt, G., 2009, Cyclicity in Cordilleran orogenic systems: Nature Geoscience, v. 2, p. 251–257, doi:10.1038/ngeo469.

del Potro, R., Diez, M., Blundy, J., Camacho, A.G., and Gottsmann, J., 2013, Diapiric ascent of silicic magma beneath the Bolivian Altiplano: Geophysical Research Letters, v. 40, p. 2044–2048, doi:10.1002/grl.50493.

de Silva, S.L., 1989, Altiplano-Puna volcanic complex of the Central Andes: Geology, v. 17, p. 1102–1106, doi:10.1130/0091-7613(1989)017<1102:APVCOT>2.3.CO;2.

de Silva, S.L., 1991, Styles of zoning in Central Andean ignimbrites. Insights into magma chamber processes, *in* Harmon, R.S., and Rapela, C.W., eds., Andean Magmatism and its Tectonic Setting: Geological Society of America Special Paper 265, p. 217–232, doi:10.1130/SPE265-p217.

de Silva, S.L., 2008, Arc magmatism, calderas, and supervolcanoes: Geology, v. 36, p. 671–672, doi:10.1130/focus082008.1.

de Silva, S.L., and Francis, P.W., 1991, Volcanoes of the Central Andes: Berlin, Springer-Verlag, 216 p.

de Silva, S.L., and Gosnold, W.D., 2007, Episodic construction of batholiths: Insights from the spatiotemporal development of an ignimbrite flareup: Journal of Volcanology and Geothermal Research, v. 167, p. 320–335, doi:10.1016/j.jvolgeores.2007.07.015.

de Silva, S.L., and Gregg, P.M., 2014, Thermomechanical feedbacks in magmatic systems: Implications for growth, longevity, and evolution of large caldera-forming magma reservoirs and their supereruptions: Journal of Volcanology and Geothermal Research, v. 282C, p. 77–91, doi:10.1016/j.jvolgeores.2014.06.001.

de Silva, S.L., Zandt, G., Trumbull, R., Viramonte, J.G., Salas, G., and Jimenez, N., 2006, Large ignimbrite eruptions and volcano-tectonic depressions in the Central Andes: A thermomechanical perspective, *in* Troise, C., de Natale, G., and Kilburn, C.R.J., eds., Mechanisms of Activity and Unrest at Large Calderas: Geological Society of London Special Publication 269, p. 47–63, doi:10.1144/GSL.SP.2006.269.01.04.

de Silva, S.L., Riggs, N.R., and Barth, A.P., 2015, Quickening the pulse: Fractal tempos in continental arc magmatism: Elements (Quebec), v. 11, p. 113–118, doi:10.2113/gselements.11.2.113.

Dickinson, W.R., 2002, The Basin and Range Province as a composite extensional domain: International Geology Review, v. 44, p. 1–38, doi:10.2747/0020-6814.44.1.1.

Dickinson, W.R., 2006, Geotectonic evolution of the Great Basin: Geosphere, v. 2, no. 7, p. 353–368, doi:10.1130/GES00054.1.

Dickinson, W.R., Klute, M.A., Hayes, M.J., Janeke, S.U., Lundin, E.R., McKittrick, M.A., and Olivares, M.D., 1988, Paleogeographic and paleotectonic setting of Laramide sedimentary basins in the central Rocky Mountain region: Geological Society of America Bulletin, v. 100, p. 1023–1039, doi:10.1130/0016-7606(1988)100<1023:PAPSOL>2.3.CO;2.

Dougherty, S.L., and Clayton, R.W., 2014, Seismicity and structure in central Mexico: Evidence for a possible slab tear in the South Cocos plate: Journal of Geophysical Research, v. 119, p. 3424–3447, doi:10.1002/2013JB010883.

Druitt, T.H., and Sparks, R.S.J., 1984, On the formation of calderas during ignimbrite eruptions: Nature, v. 310, p. 679–681, doi:10.1038/310679a0.

du Bray, E.A., 2007, Time, space, and composition relations among northern Nevada intrusive rocks and their metallogenic implications: Geosphere, v. 3, p. 381–405, doi:10.1130/GES00109.1.

Ellis, B.S., Wolff, J.A., Boroughs, S., Mark, D.F., Starkel, W.A., and Bonnichsen, B., 2013, Rhyolitic volcanism of the central Snake River Plain: A review: Bulletin of Volcanology, v. 75, p. 745, doi:10.1007/s00445-013-0745-y.

England, P.C., and Thompson, A.B., 1984, Pressure-temperature-time paths of regional metamorphism: I. Heat transfer during the evolution of regions of thickened continental crust: Journal of Petrology, v. 25, p. 894–928, doi:10.1093/petrology/25.4.894.

English, J.M., Johnston, S.T., and Wang, K., 2003, Thermal modeling of the Laramide orogeny: Testing the flat-slab subduction hypothesis: Earth and Planetary Science Letters, v. 214, p. 619–632, doi:10.1016/S0012-821X(03)00399-6.

Erslev, E.A., 1993, Thrusts, back-thrusts, and detachment of Rocky Mountain foreland arches, *in* Schmidt, C.J., Chase, R.B., and Erslev, E.A., eds., Laramide Basement Deformation in the Rocky Mountain Foreland of the Western United States: Geological Society of America Special Paper 280, p. 339–358, doi:10.1130/SPE280-p339.

Ewart, E., 1982, The mineralogy and petrology of Tertiary–Recent orogenic volcanic rocks with special reference to the andesite-basaltic composition range, *in* Thorpe, R.S., ed., Andesites: New York, John Wiley and Sons, p. 25–87.

Faccenna, C., Molin, P., Orecchio, B., Olivetti, V., Bellier, O., Funiciello, F., Minelli, L., Piromallo, C., and Billi, A., 2011, Topography of the Calabria subduction zone (southern Italy): Clues for the origin of Mt: Etna: Tectonics, v. 30, TC1003, doi:10.1029/2010TC002694.

Farmer, G.L., and DePaolo, D.J., 1983, Origin of Mesozoic and Tertiary granite in the western United States and implications for pre-Mesozoic crustal structure: 1. Nd and Sr isotopic studies in the geocline of the northern Great Basin: Journal of Geophysical Research, v. 88, no. B4, p. 3379–3401, doi:10.1029/JB088iB04p03379.

Farmer, G.L., Broxton, D.E., Warren, R.G., and Pickthorn, W., 1991, Nd, Sr, and O isotopic variations in metaluminous ash-flow tuffs and related volcanic rocks at the Timber Mountain/Oasis Valley caldera complex, SW Nevada: Implications for the origin and evolution of large-volume silicic magma bodies: Contributions to Mineralogy and Petrology, v. 109, p. 53–68, doi:10.1007/BF00687200.

Farmer, G.L., Bailley, T., and Elkins-Taunton, L.T., 2008, Mantle source volumes and the origin of the mid-Tertiary ignimbrite flare-up in the southern Rocky Mountains, western U.S: Lithos, v. 102, p. 279–294, doi:10.1016/j.lithos.2007.08.014.

Ferrari, L., Valencia-Moreno, M., and Bryan, S., 2007, Magmatism and tectonics of the Sierra Madre Occidental and its relation with the evolution of the western margin of North America, *in* Alaniz-Alvarez, S.A., and Nieto-Samaniego, A.F., eds., Geology of Mexico: Celebrating the Centenary of the Geological Society of Mexico: Geological Society of America Special Paper 422, p. 1–39, doi:10.1130/2007.2422(01).

Ferrari, L., Orozco-Esquivel, T., Manea, V., and Manea, M., 2012, The dynamic history of the Trans-Mexican volcanic belt and the Mexico subduction zone: Tectonophysics, v. 522–523, p. 122–149, doi:10.1016/j.tecto.2011.09.018.

Fialko, Y., and Pearse, J., 2012, Sombrero uplift above the Altiplano-Puna magma body: Evidence of a ballooning mid-crustal diapir: Science, v. 338, p. 250–252, doi:10.1126/science.1226358.

Folkes, C.B., Wright, H.M., Cas, R.A.F., de Silva, S.L., Lesti, C., and Viramonte, J.G., 2011, A re-appraisal of the stratigraphy and volcanology of the Cerro Galan volcanic system, NW Argentina: Bulletin of Volcanology, v. 73, p. 1427–1454, doi:10.1007/s00445-011-0459-y.

Folkes, C.B., de Silva, S.L., Bindeman, I.N., and Cas, R.A.F., 2013, Tectonic and climate history influence the geochemistry of large-volume silicic magmas: New $\delta^{18}O$ data from the Central Andes with comparison to N America and Kamchatka: Journal of Volcanology and Geothermal Research, v. 262, p. 90–103, doi:10.1016/j.jvolgeores.2013.05.014.

Freymuth, H., Brandmeier, M., and Wörner, G., 2015, The origin and crust/mantle mass balance of Central Andean ignimbrite magmatism constrained by oxygen and strontium isotopes and erupted volumes: Contributions to Mineralogy and Petrology, v. 169, p. 58, doi:10.1007/s00410-015-1152-5.

Frost, B.R., Barnes, C.G., Collins, W.J., Arculus, W.J., Ellis, D.J., and Frost, C.D., 2001, A geochemical classification for granitic rocks: Journal of Petrology, v. 42, p. 2033–2048, doi:10.1093/petrology/42.11.2033.

Gans, P.B., Mahood, G.A., and Schermer, E., 1989, Synextensional Magmatism in the Basin and Range Province: A Case Study from the Eastern Great Basin: Geological Society of America Special Paper 233, 53 p.

Garrity, C.P., and Soller, D.R., 2009, Database of the Geologic Map of North America: Adapted from the map by J.C. Reed, Jr., and others (2005): U.S. Geological Survey Data Series 424, http://pubs.usgs.gov/ds/424.

Gelman, S.E., Gutierrez, F.J., and Bachmann, O., 2013, On the longevity of large upper crustal silicic magma reservoirs: Geology, v. 41, p. 759–762, doi:10.1130/G34241.1.

Gilbert, H.J., 2012, Crustal structure and signatures of recent tectonism as influenced by ancient terranes in the western United States: Geosphere, v. 8, no. 1, p. 141–157, doi:10.1130/GES00720.1.

Gomberg, J.S., Priesley, K.F., Masters, G., and Brune, J., 1988, The structure of the crust and upper mantle in northern Mexico: Geophysical Journal, v. 94, p. 1–20.

Gregg, P.M., de Silva, S.L., Grosfils, E.B., and Parmigiani, J.P., 2012, Catastrophic caldera-forming eruptions: Thermomechanics and implications for triggering and maximum caldera dimensions on Earth: Journal of Volcanology and Geothermal Research, v. 241–242, p. 1–12, doi:10.1016/j.jvolgeores.2012.06.009.

Gregg, P.M., de Silva, S.L., and Grosfils, E.B., 2013, Thermomechanics of shallow magma chamber pressurization: Implications for the assessment of ground deformation data at active volcanoes: Earth and Planetary Science Letters, v. 384C, p. 100–108, doi:10.1016/j.epsl.2013.09.040.

Gregg, P.M., Grosfils, E.B., and de Silva, S.L., 2015, Catastrophic caldera-forming eruptions II: The subordinate role of magma buoyancy as an eruption trigger: Journal of Volcanology and Geothermal Research, v. 305, p. 100–113, doi:10.1016/j.jvolgeores.2015.09.022.

Grommé, C.S., McKee, E.H., and Blake, M.C., 1972, Paleomagnetic correlations and potassium-argon dating of middle Tertiary ash-flow sheets in the eastern Great Basin: Geological Society of America Bulletin, v. 83, p. 1619–1638, doi:10.1130/0016-7606(1972)83[1619:PCAPDO]2.0.CO;2.

Hamilton, W., 1969, The Volcanic Central Andes—A Modern Model for the Cretaceous Batholiths and Tectonics of Western North America: Oregon Department of Geology and Mineral Industries Bulletin, v. 65, p. 175–184.

Hansen, S.M., Dueker, K.G., Stachnik, J.C., Aster, R.C., and Karlstrom, K.E., 2013, A rootless Rockies—Support and lithospheric structure of the Colorado Rocky Mountains inferred from CREST and TA seismic data: Geochemistry Geophysics Geosystems, v. 14, p. 2670–2695, doi:10.1002/ggge.20143.

Hart, G.L., 1997, An Oxygen Isotope Investigation of the Indian Peak Volcanic Field, Southern Utah-Nevada: Magma Source Constraints for a Late Oligocene Caldera System [M.S. thesis]: Provo, Utah, Brigham Young University, 57 p.

Henry, C.D., and John, D.A., 2013, Magmatism, ash-flow tuffs, and calderas of the ignimbrite flareup in the western Nevada volcanic field, Great Basin, USA: Geosphere, v. 9, no. 4, p. 951–1008, doi:10.1130/GES00867.1.

Henry, C.D., McGrew, A.J., Colgan, J.P., Snoke, A.W., and Brueseke, M.E., 2011, Timing, distribution, amount, and style of Cenozoic extension in the northern Great Basin, *in* Lee, J., and Evans, J.P., eds., Geologic Field Trips to the Basin and Range, Rocky Mountains, Snake River Plain, and Terranes of the U.S. Cordillera: Geological Society of America Field Guide 21, p. 27–66.

Hildreth, W., 1981, Gradients in silicic magma chambers: Implications for lithospheric magmatism: Journal of Geophysical Research, v. 86, p. 10,153–10,192, doi:10.1029/JB086iB11p10153.

Hildreth, W., and Moorbath, S., 1988, Crustal contributions to arc magmatism in the Andes of central Chile: Contributions to Mineralogy and Petrology, v. 98, p. 455–489, doi:10.1007/BF00372365.

Hintze, L.F., and Kowallis, B.J., 2009, Geologic History of Utah: Brigham Young University Geology Studies Special Publication 9, 225 p.

Holtz, F., and Johannes, W., 1991, Genesis of peraluminous granites I. Experimental investigation of melt compositions at 3 and 5 kb and various H_2O activities: Journal of Petrology, v. 32, p. 935–958, doi:10.1093/petrology/32.5.935.

Hughes, G.R., and Mahood, G.A., 2008, Tectonic controls on the nature of large silicic calderas in volcanic arcs: Geology, v. 36, p. 627–630, doi:10.1130/G24796A.1.

Humphreys, E., 1995, Post-Laramide removal of the Farallon slab, western United States: Geology, v. 23, p. 987–990, doi:10.1130/0091-7613(1995)023<0987:PLROTF>2.3.CO;2.

Humphreys, E., 2009, Relation of flat subduction to magmatism and deformation in the western United States, *in* Kay, S.M., Ramos, V.A., and Dickinson, W.R., eds., Backbone of the Americas: Shallow Subduction, Plateau Uplift, and Ridge and Terrane Collision: Geological Society of America Memoir 204, p. 85–98, doi:10.1130/2009.1204(04).

Isacks, B.L., 1988, Uplift of the Central Andean plateau and bending of the Bolivian orocline: Journal of Geophysical Research, v. 93, p. 3211–3231, doi:10.1029/JB093iB04p03211.

Jay, J.A., Pritchard, M.E., West, M.W., Christensen, D., Haney, M., Minaya, E., Sunagua, M., McNutt, S.R., and Zabala, M., 2012, Shallow seismicity, triggered seismicity, and ambient noise tomography at the long-dormant Uturuncu Volcano, Bolivia: Bulletin of Volcanology, v. 74, p. 817–837, doi:10.1007/s00445-011-0568-7.

Jellinek, A.M., and DePaolo, D.J., 2003, A model for the origin of large silicic magma chambers: Precursors of caldera-forming eruptions: Bulletin of Volcanology, v. 65, p. 363–381, doi:10.1007/s00445-003-0277-y.

John, D.A., 1992, Stratigraphy, Regional Distribution, and Reconnaissance Geochemistry of Oligocene and Miocene Volcanic Rocks in the Paradise Range and Northern Pactolus Hills, Nye County, Nevada: U.S. Geological Survey Bulletin 1974, 67 p.

John, D.A., 1995, Tilted middle Tertiary ash-flow calderas and subjacent granitic plutons, southern Stillwater Range, Nevada: Cross-sections of an Oligocene igneous center: Geological Society of America Bulletin, v. 107, p. 180–200, doi:10.1130/0016-7606(1995)107<0180:TMTAFC>2.3.CO;2.

Johnson, C.M., 1991, Large-scale crust formation and lithosphere modification beneath middle to late Cenozoic calderas and volcanic fields, western North America: Journal of Geophysical Research, v. 96, p. 13,485–13,507, doi:10.1029/91JB00304.

Johnson, C.M., and Fridrich, C.J., 1990, Non-monotonic chemical and O, Sr, Nd, and Pb isotope zonations and heterogeneity in the mafic-to-silicic-composition magma chamber of the Grizzly Peak Tuff, Colorado: Contributions to Mineralogy and Petrology, v. 105, p. 677–690, doi:10.1007/BF00306533.

Johnson, C.M., Lipman, P.W., and Czamanske, G.K., 1990, H, O, Sr, Nd, and Pb isotope geochemistry of the Latir volcanic field and cogenetic intrusion, New Mexico, and relations between evolution of a continental magmatic center and modifications of the lithosphere: Contributions to Mineralogy and Petrology, v. 104, p. 99–124, doi:10.1007/BF00310649.

Johnson, M.C., and Rutherford, M.J., 1989, Experimentally determined conditions in the Fish Canyon Tuff, Colorado, magma chamber: Journal of Petrology, v. 30, p. 711–737, doi:10.1093/petrology/30.3.711.

Jones, C.H., Farmer, G.L., Sageman, B., and Zhong, S., 2011, Hydrodynamic mechanism for the Laramide orogeny: Geosphere, v. 7, p. 183–201, doi:10.1130/GES00575.1.

Jones, C.H., Mahan, K.H., Butcher, L.A., Levandowski, W.B., and Farmer, G.L., 2015, Continental uplift through crustal hydration: Geology, v. 43, p. 355–358, doi:10.1130/G36509.1.

Kay, R.W., and Kay, S.M., 1993, Delamination and delamination magmatism: Tectonophysics, v. 219, p. 177–189, doi:10.1016/0040-1951(93)90295-U.

Kay, S.M., 2014, 125th anniversary of the Geological Society of America: Looking at the past and into the future of science at GSA: GSA Today, v. 24, no. 3, p. 4–11, doi:10.1130/GSAT-13PresAdrs.1.

Kay, S.M., and Coira, B.L., 2009, Shallowing and steepening subduction zones, continental lithospheric loss, magmatism, and crustal flow under the Central Andean Altiplano-Puna plateau, *in* Kay, S.M., Ramos, V.A., and Dickinson, W.R., eds., Backbone of the Americas: Shallow Subduction, Plateau Uplift, and Ridge and Terrane Collision: Geological Society of America Memoir 204, p. 229–259, doi:10.1130/2009.1204(11).

Kay, S.M., Coira, B.L., Caffe, P.J., and Chen, C.-H., 2010, Regional chemical diversity, crustal and mantle sources and evolution of Central Andean Puna plateau ignimbrites: Journal of Volcanology and Geothermal Research, v. 198, p. 81–111, doi:10.1016/j.jvolgeores.2010.08.013.

Kay, S.M., Coira, B.L., Worner, G., Kay, R.W., and Singer, B.S., 2011, Geochemical, isotopic and single crystal $^{40}Ar/^{39}Ar$ age constraints on the evolution of the Cerro Galan ignimbrites: Bulletin of Volcanology, v. 73, p. 1487–1511, doi:10.1007/s00445-010-0410-7.

Kay, S.M., Mpodozis, C., and Gardeweg, M., 2014, Magma sources and tectonic setting of Central Andean andesites (25.5–28°S) related to crustal thickening, forearc subduction erosion and delamination, *in* Gómez-Tuena, A., Straub, S.M., and Zellmer, G.F., eds., Orogenic Andesites and Crustal Growth: Geological Society of London Special Publication 385, p. 303–334, doi:10.1144/SP385.11.

Keith, S.B., 1978, Paleosubduction geometries inferred from Cretaceous and Tertiary magmatic patterns in southwestern North America: Geology, v. 6, no. 9, p. 516–521, doi:10.1130/0091-7613(1978)6<516:PGIFCA>2.0.CO;2.

Kowallis, B.J., Christiansen, E.H., Batter, T.K., and Keith, J.D., 1995, Tertiary paleostress variation in time and space near the eastern margin of the Basin and Range Province, Utah, *in* Rossmanith, H.P., ed., Mechanics of Jointed and Faulted Rock: Springer-Verlag, p. 297–302.

Lake, E.T., and Farmer, G.L., 2015, Oligo-Miocene mafic intrusions of the San Juan volcanic field, southwestern Colorado, and their relationship to voluminous, caldera-forming magmas: Geochimica et Cosmochimica Acta, v. 157, p. 86–108, doi:10.1016/j.gca.2015.02.020.

Larson, P.B., and Taylor, H.P., Jr., 1986, $^{18}O/^{16}O$ ratios in ash-flow tuffs and lavas erupted from the central Nevada caldera complex and the central San Juan caldera complex, Colorado: Contributions to Mineralogy and Petrology, v. 92, p. 146–156, doi:10.1007/BF00375290.

Lee, D.E., and Christiansen, E.H., 1983, The granite problem as exposed in the southern Snake Range, Nevada: Contributions to Mineralogy and Petrology, v. 83, p. 99–116, doi:10.1007/BF00373083.

Le Maitre, R.W., 1989, A Classification of Igneous Rocks and Glossary of Terms: Boston, Massachusetts, Blackwell Scientific, 193 p.

Lindsay, J., Schmitt, A., Trumbull, R., de Silva, S., Siebel, W., and Emmermann, R., 2001, Magmatic evolution of the La Pacana caldera system, Central Andes, Chile: Compositional variation of two cogenetic, large volume felsic ignimbrites: Journal of Petrology, v. 42, p. 459–486, doi:10.1093/petrology/42.3.459.

Lipman, P.W., 1980, Cenozoic volcanism in the western United States—Implications for continental tectonics, *in* Burchfiel, B.C., Oliver, J.E., and Silver, L.T., eds., Continental Tectonics: Washington, D.C., National Research Council, p. 161–174.

Lipman, P.W., 1982, Tectonic setting of the mid- to late-Tertiary in the Rocky Mountain region—A review, *in* Denver Region Exploration Geologists Symposium on the Genesis of Rocky Mountain Ore Deposits; Changes with Time and Tectonics: Denver, Colorado, Denver Region Exploration Geologists, p. 125–131.

Lipman, P.W., 1988, Evolution of silicic magma in the upper crust: Relations between the middle Tertiary Latir volcanic field and its cogenetic upper-crustal granitic batholith, New Mexico, USA: Royal Society Edinburgh Transactions, v. 79, p. 265–288, doi:10.1017/S0263593300014279.

Lipman, P.W., 1992, Magmatism in the Cordilleran United States; progress and problems, *in* Burchfiel, B.C., Lipman, P.W., and Zoback, M.L., eds., The Cordilleran Orogen: Conterminous U.S.: Boulder, Colorado, Geological Society of America, Geology of North America, v. G-3, p. 481–514.

Lipman, P.W., 2004, Chemical Analyses of Tertiary Volcanic Rocks, Central San Juan Caldera Complex, Southwestern Colorado: U.S. Geological Survey Open-File Report 2004-1194, 7 p.

Lipman, P.W., 2006, Geologic Map of the Central San Juan Caldera Cluster, Southwestern Colorado: U.S. Geological Survey Geologic Investigations Series I-2799, scale 1:50,000.

Lipman, P.W., 2007, Incremental assembly and prolonged consolidation of Cordilleran magma chambers: Evidence from the Southern Rocky Mountain volcanic field: Geosphere, v. 3, p. 42–70, doi:10.1130/GES00061.1.

Lipman, P.W., and Bachmann, O., 2015, Ignimbrites to batholiths: Integrating perspectives from geological, geophysical, and geochronological data: Geosphere, v. 11, no. 3, p. 1–39, doi:10.1130/GES01091.1.

Lipman, P.W., and McIntosh, W.C., 2008, Eruptive and noneruptive calderas, northeastern San Juan Mountains, Colorado: Where did the ignimbrites come from?: Geological Society of America Bulletin, v. 120, p. 771–795, doi:10.1130/B26330.1.

Lipman, P.W., Prostka, H.J., and Christiansen, R.L., 1972, Cenozoic volcanism and plate tectonic evolution of western United States: Part 1. Early and middle Cenozoic: Philosophical Transactions of the Royal Society of London, ser. A, v. 271, p. 217–248, doi:10.1098/rsta.1972.0008.

Lipman, P.W., Doe, B.R., Hedge, C.E., and Steven, T.A., 1978, Petrologic evolution of the San Juan volcanic field, southwestern Colorado: Pb and Sr isotope evidence: Geological Society of America Bulletin, v. 89, p. 59–82, doi:10.1130/0016-7606(1978)89<59:PEOTSJ>2.0.CO;2.

Lipman, P.W., Dungan, M.A., Brown, L.L., and Deino, A., 1996, Recurrent eruption and subsidence at the Platoro caldera complex, southeastern San Juan volcanic field, Colorado: New tales from old tuffs: Geological Society of America Bulletin, v. 108, p. 1039–1055, doi:10.1130/0016-7606(1996)108<1039:REASAT>2.3.CO;2.

Lipman, P.W., Zimmerer, M.J., and McIntosh, W.C., 2015, An ignimbrite caldera from the bottom up: Erosionally exhumed floor and fill of the resurgent Bonanza caldera, Southern Rocky Mountain volcanic field, Colorado: Geosphere, v. 11, no. 6, 46 p., doi:10.1130/GES01184.1.

Liu, L., Gurnis, M., Seton, M., Saleeby, J., Muller, R.D., and Jackson, J.M., 2010, The role of oceanic plateau subduction in the Laramide orogeny: Nature Geoscience, v. 3, p. 353–357, doi:10.1038/ngeo829.

Liu, S., and Currie, C.A., 2016, Farallon plate dynamics prior to the Laramide orogeny: Numerical models of flat subduction: Tectonophysics, v. 666, p. 33–47, doi:10.1016/j.tecto.2015.10.010.

Long, S.P., 2012, Magnitude and spatial patterns of erosional exhumation in the Sevier hinterland, eastern Nevada and western Utah: Insights from a Paleogene paleogeologic map: Geosphere, v. 8, p. 881–901, doi:10.1130/GES00783.1.

Long, S.P., Henry, C.D., Muntean, J.L., Edmondo, G.P., and Cassel, E.J., 2014, Early Cretaceous construction of a structural culmination, Eureka, Nevada, U.S.A.: Implications for out-of-sequence deformation in the Sevier hinterland: Geosphere, v. 10, p. 564–584, doi:10.1130/GES00997.1.

Mamani, M., Wörner, G., and Sempere, T., 2009, Geochemical variations in igneous rocks of the Central Andean orocline (13°S to 18°S): Tracing crustal thickening and magma generation through time and space: Geological Society of America Bulletin, v. 122, no. 1–2, p. 162–182, doi:10.1130/B26538.1.

Maughan, L.L., Christiansen, E.H., Best, M.G., Grommé, C.S., Deino, A.L., and Tingey, D.G., 2002, The Oligocene Lund Tuff, Great Basin, USA: A very large volume monotonous intermediate: Journal of Volcanology and Geothermal Research, v. 113, p. 129–157, doi:10.1016/S0377-0273(01)00256-6.

McDowell, F.W., and McIntosh, W., 2012, Timing of intense magmatic episodes in the northern and central Sierra Madre Occidental, western Mexico: Geosphere, v. 8, no. 6, p. 1505–1526, doi:10.1130/GES00792.1.

McGlashan, N., Brown, L.D., and Kay, S.M., 2008, Crustal thicknesses in the Central Andes from teleseismically recorded depth phase precursors: Geophysical Journal International, v. 175, p. 1013–1022, doi:10.1111/j.1365-246X.2008.03897.x.

McIntosh, W.C., Chapin, C.E., Ratte, J.C., and Sutter, J.F., 1992, Time-stratigraphic framework for the Eocene–Oligocene Mogollon-Datil volcanic field, southwest New Mexico: Geological Society of America Bulletin, v. 104, p. 851–871, doi:10.1130/0016-7606(1992)104<0851:TSFFTE>2.3.CO;2.

McQuarrie, N., and Chase, C.G., 2000, Raising the Colorado Plateau: Geology, v. 28, p. 91–94, doi:10.1130/0091-7613(2000)028<0091:RTCP>2.0.CO;2.

McQuarrie, N., and Oskin, M., 2010, Palinspastic restoration of NavDAT and implications for the origin of magmatism in southwestern North America: Journal of Geophysical Research, v. 115, no. B10, B10401, doi:10.1029/2009JB006435.

McQuarrie, N., and Wernicke, B.P., 2005, An animated tectonic reconstruction of southwestern North America since 36 Ma: Geosphere, v. 1, p. 147–172, doi:10.1130/GES00016.1.

Memeti, V., and Lipman, P.W., 2014, Exploring volcanic-plutonic connections in the Bonanza caldera, Colorado: Geological Society of America Abstracts with Programs, v. 46, no. 6, p. 374.

Miller, C.F., and Wark, D.A., 2008, Supervolcanoes: Elements (Quebec), v. 4, no. 1, p. 11–16, doi:10.2113/GSELEMENTS.4.1.11.

Miller, E.L., Dumitru, T.A., Brown, R.W., and Gans, P.B., 1999, Rapid Miocene slip on the Snake Range–Deep Creek Range fault system, east-central Nevada: Geological Society of America Bulletin, v. 111, p. 886–905, doi:10.1130/0016-7606(1999)111<0886:RMSOTS>2.3.CO;2.

Mix, H.T., Mulch, A., Kent-Corson, M.L., and Chamberlain, C.P., 2011, Cenozoic migration of topography in the North American Cordillera: Geology, v. 39, p. 87–90, doi:10.1130/G31450.1.

Morgan, G.B., VI, London, D., and Luedke, R.G., 1998, Petrochemistry of late Miocene peraluminous silicic volcanic rocks from the Morococala field, Bolivia: Journal of Petrology, v. 39, p. 601–632, doi:10.1093/petroj/39.4.601.

Muir, D.D., Blundy, J.D., Rust, A.C., and Hickey, J., 2014, Experimental constraints on dacite pre-eruptive magma storage conditions beneath Uturuncu volcano: Journal of Petrology, v. 55, p. 749–767, doi:10.1093/petrology/egu005.

Murray, B.P., Busby, C.J., Ferrari, L., and Solari, L.A., 2013, Synvolcanic crustal extension during the mid-Cenozoic ignimbrite flare-up in the northern Sierra Madre Occidental, Mexico: Evidence from the Guazapares Mining District region, western Chihuahua: Geosphere, v. 9, no. 5, p. 1201–1235, doi:10.1130/GES00862.1.

Nabelek, P.I., Hofmeister, A.M., and Whittington, A.G., 2012, The influence of temperature-dependent thermal diffusivity on the conductive cooling rates of plutons and temperature-time paths in contact aureoles: Earth and Planetary Science Letters, v. 317–318, p. 157–164, doi:10.1016/j.epsl.2011.11.009.

Nelson, S.T., and Davidson, J.P., 1993, Interactions between mantle-derived magmas and mafic crust, Henry Mountains, Utah: Journal of Geophysical Research, v. 98, p. 1837–1852, doi:10.1029/92JB02689.

Nelson, S.T., and Davidson, J.P., 1998, The petrogenesis of the Colorado Plateau laccoliths and their relationship to regional magmatism, *in* Friedman, J.D., and Huffman, A.C., eds., Laccolithic Complexes of Southeastern Utah: Time of Emplacement and Tectonic Setting—Workshop Proceedings: U.S. Geological Survey Professional Paper 2158, p. 85–100.

Nelson, S.T., Davidson, J.P., and Sullivan, K.R., 1992, New age determinations of central Colorado Plateau laccoliths, Utah: Recognizing disturbed K-Ar systematics and re-evaluating tectonomagmatic relationships: Geological Society of America Bulletin, v. 104, p. 1547–1560, doi:10.1130/0016-7606(1992)104<1547:NADOCC>2.3.CO;2.

New Mexico Bureau of Geology and Mineral Resources, 2003, Geologic map of New Mexico: Socorro, New Mexico, scale 1:500,000.

Noble, D.C., 1972, Some observations on the Cenozoic volcano-tectonic evolution of the Great Basin, western United States: Earth and Planetary Science Letters, v. 17, p. 142–150, doi:10.1016/0012-821X(72)90269-5.

Oldow, J.S., Bally, A.W., Avé Lallemant, H.G., and Leeman, W.P., 1989, Phanerozoic evolution of the North American Cordillera; United States and Canada, *in* Bally, A.W., and Palmer, A.R., eds., The Geology of North America—An Overview: Boulder, Colorado, Geological Society of America, Geology of North America, v. A, p. 139–232.

Ort, M.H., Coira, B.L., and Mazzoni, M., 1996, Generation of crust-mantle mixture: Magma sources and contamination at Cerro Panizos, Central Andes: Contributions to Mineralogy and Petrology, v. 123, p. 308–322, doi:10.1007/s004100050158.

Oskin, M., Stock, J., and Martín-Barajas, A., 2001, Rapid localization of Pacific–North American plate motion in the Gulf of California: Geology, v. 29, p. 459–462, doi:10.1130/0091-7613(2001)029<0459:RLOPNA>2.0.CO;2.

Page, B.G.N., Bennett, J.D., Cameron, N.R., Bridge, D.M., Jeffrey, D.H., Keats, W., and Thaib, J., 1979, A review of the main structural and magmatic features of northern Sumatra: Journal of the Geological Society, v. 136, p. 569–579, doi:10.1144/gsjgs.136.5.0569.

Parat, F., Dungan, M.A., and Lipman, P.W., 2005, Contemporaneous trachydacitic and calc-alkaline volcanism of the Huerto Andesite, San Juan volcanic field, Colorado, USA: Journal of Petrology, v. 46, p. 859–891, doi:10.1093/petrology/egi003.

Patiño-Douce, A.E., and Harris, N., 1998, Experimental constraints on Himalayan anatexis: Journal of Petrology, v. 39, p. 689–710, doi:10.1093/petroj/39.4.689.

Patiño-Douce, A.E., Humphreys, E.D., and Johnson, A.D., 1990, Anatexis and metamorphism in tectonically thickened continental crust exemplified by the Sevier hinterland, western North America: Earth and Planetary Science Letters, v. 97, p. 290–315, doi:10.1016/0012-821X(90)90048-3.

Pesicek, J.D., Thurber, C.H., Widiyantoro, S., Engdahl, E.R., and DeShon, H.R., 2008, Complex slab subduction beneath northern Sumatra: Geophysical Research Letters, v. 35, L20303, doi:10.1029/2008GL035262.

Phillips, L.V., 1989, The Petrology and Magmatic Evolution of the Large-Volume Ash-Flow Tuffs of the Central Nevada Caldera Complex, Nye County, Nevada [Ph.D. thesis]: Athens, Georgia, University of Georgia, 300 p.

Prezzi, C.B., Gotze, H.J., and Schmidt, S., 2009, 3D density model of the Central Andes: Physics of the Earth and Planetary Interiors, v. 177, no. 3–4, p. 217–234, doi:10.1016/j.pepi.2009.09.004.

Prodehl, C., and Lipman, P.W., 1989, Crustal structure of the Rocky Mountain region, *in* Pakiser, L.C., and Mooney, W.D., eds., Geophysical Framework of the Continental United States: Geological Society of America Memoir 172, p. 249–284, doi:10.1130/MEM172-p249.

Radke, L.E., 1992, Petrology and Temporal Evolution of the Rhyolite Ash-Flow Tuffs of the 35.3 Ma Stone Cabin Formation, Central Nevada [M.S. thesis]: Provo, Utah, Brigham Young University, 102 p.

Rampino, M.R., and Self, S., 1992, Volcanic winter and accelerated glaciation following the Toba super-eruption: Nature, v. 359, p. 50–52, doi:10.1038/359050a0.

Ren, X., Kowallis, B.J., and Best, M.G., 1989, Paleostress history of the Basin and Range Province in western Utah and eastern Nevada from healed microfracture orientations in granites: Geology, v. 17, p. 487–490, doi:10.1130/0091-7613(1989)017<0487:PHOTBA>2.3.CO;2.

Riciputi, L.R., Johnson, C.M., Sawyer, D.A., and Lipman, P.W., 1995, Crustal and magmatic evolution in a large multicyclic caldera complex: Isotopic evidence from the central San Juan volcanic field: Journal of Volcanology and Geothermal Research, v. 67, p. 1–28, doi:10.1016/0377-0273(94)00097-Z.

Riller, U., Petrinovic, I., Ramelow, J., Strecker, M., and Oncken, O., 2001, Late Cenozoic tectonism, collapse caldera and plateau formation in the Central Andes: Earth and Planetary Science Letters, v. 188, p. 299–311, doi:10.1016/S0012-821X(01)00333-8.

Rivera, J., and Ponce, L., 1986, Estructura de la corteza al oriente de la Sierra Madre occidental, Mexico, basada en la velocidad del grupo de las ondas Rayleigh: Geofísica Internacional, v. 25, p. 383–402.

Roche, O., Druitt, T.H., and Merle, O., 2000, Experimental study of caldera formation: Journal of Geophysical Research, v. 105, p. 395–416, doi:10.1029/1999JB900298.

Rowley, P.D., Cunningham, C.G., Steven, T.A., Workman, J.B., Anderson, J.J., and Theissen, K.M., 2002, Geologic Map of the Central Marysvale Volcanic Field, Southwestern Utah: U.S. Geological Survey Geologic Investigations Series I-2645-A, scale 1:100,000.

Rupke, L.H., Morgan, J.P., Hort, M., and Connolly, J.A.D., 2004, Serpentine and the subduction zone water cycle: Earth and Planetary Science Letters, v. 223, p. 17–34, doi:10.1016/j.epsl.2004.04.018.

Saleeby, J., 2003, Segmentation of the Laramide slab—Evidence from the southern Sierra Nevada region: Geological Society of America Bulletin, v. 115, no. 6, p. 655–668, doi:10.1130/0016-7606(2003)115<0655:SOTLSF>2.0.CO;2.

Salisbury, M.J., Jicha, B.R., de Silva, S.L., Singer, B.S., Jimenez, N.C., and Ort, M.H., 2011, $^{40}Ar/^{39}Ar$ chronostratigraphy of Altiplano-Puna volcanic complex ignimbrites reveals the development of a major magmatic province: Geological Society of America Bulletin, v. 123, p. 821–840, doi:10.1130/B30280.1.

Schmitt, A., de Silva, S., Trumbull, R., and Emmermann, R., 2001, Magma evolution in the Purico ignimbrite complex, northern Chile: Evidence for zoning of a dacitic magma by injection of rhyolitic melts following mafic recharge: Contributions to Mineralogy and Petrology, v. 140, p. 680–700, doi:10.1007/s004100000214.

Schmitt, A.K., Lindsay, J.M., de Silva, S., and Trumbull, R.B., 2003, U-Pb zircon chronostratigraphy of early-Pliocene ignimbrites from La Pacana, north Chile: Implications for the formation of stratified magma chambers: Journal of Volcanology and Geothermal Research, v. 120, no. 1, p. 43–53, doi:10.1016/S0377-0273(02)00359-1.

Schneider, R.V., and Keller, G.R., 1994, Crustal structure of the western margin of the Rio Grande rift and Mogollon-Datil volcanic field, southwestern New Mexico and southeastern Arizona: Geological Society of America. Special Paper, v. 291, p. 207–226, doi:10.1130/SPE291-p207.

Severinghaus, J., and Atwater, T., 1990, Cenozoic geometry and thermal state of the subducting slabs beneath western North America, *in* Wernicke, B.P., ed., Basin and Range Extensional Tectonics near the Latitude of Las Vegas, Nevada: Geological Society of America Memoir 176, p. 1–22, doi:10.1130/MEM176-p1.

Sigloch, K., McQuarrie, N., and Nolet, G., 2008, Two-stage subduction history under North America inferred from multiple-frequency tomography: Nature Geoscience, v. 1, p. 458–462, doi:10.1038/ngeo231.

Sisson, T.W., Ratajeski, K., and Hankins, W.B., 2005, Voluminous granitic magmas from common basaltic sources: Contributions to Mineralogy and Petrology, v. 148, p. 635–661, doi:10.1007/s00410-004-0632-9.

Smith, D.L., Gans, P.B., and Miller, E.A., 1991, Palinspastic restoration of Cenozoic extension in the central and eastern Basin and Range Province at latitude 39–40°N, *in* Raines, G.L., Lisle, R.E., Schafer, R.W., and Wilkinson, W.J., eds., Geology and Ore Deposits of the Great Basin: Symposium Proceedings, sponsored by the Geological Society of Nevada and the U.S. Geological Survey, April 1–5, 1990: Reno, Nevada, Geological Society of Nevada, p. 75–86.

Sparks, R.S.J., Self, S., Grattan, J.P., Oppenheimer, C., Pyle, D.M., and Rymer, H., 2005, Super-Eruptions: Global Effects and Future Threats: Report of the Geological Society Working Group: London, Geological Society, 24 p.

Spera, F., 1980, Thermal evolution of plutons: A parameterized approach: Science, v. 207, no. 4428, p. 299–301, doi:10.1126/science.207.4428.299.

Stein, H.J., and Crock, J.G., 1990, Late Cretaceous–Tertiary magmatism in the Colorado Mineral Belt: Rare earth element and samarium-neodymium isotopic studies, *in* Anderson, J.L., ed., The Nature and Origin of Cordilleran Magmatism: Geological Society of America Memoir 174, p. 195–224, doi:10.1130/MEM174-p195.

Steven, T.A., Rowley, P.D., and Cunningham, C.G., 1984, Calderas of the Marysvale volcanic field, west-central Utah: Journal of Geophysical Research, v. 89, p. 8751–8764, doi:10.1029/JB089iB10p08751.

Stewart, J.H., 1980, Geology of Nevada: Nevada Bureau of Mines and Geology Special Publication 4, 136 p.

Stewart, J.H., and Carlson, J.E., 1976, Cenozoic Rocks of Nevada: Nevada Bureau of Mines and Geology Map 52, scale 1:1,000,000.

Stockli, D.F., Linn, J.K., Walker, J.D., and Dumitru, T.A., 2001, Miocene unroofing of the Canyon Range during extension along the Sevier Desert detachment, west central Utah: Tectonics, v. 20, no. 3, p. 289–307, doi:10.1029/2000TC001237.

Stockli, D.F., Surpless, B.E., and Dumitru, T.A., 2002, Thermochronological constraints on the timing and magnitude of Miocene and Pliocene extension in the central Wassuk Range, western Nevada: Tectonics, v. 21, no. 4, 19 p., doi:10.1029/2001TC001295.

Swanson, E.R., Kempter, K.A., McDowell, F.W., and McIntosh, W.C., 2006, Major ignimbrites and volcanic centers of the Copper Canyon area: A view into the core of Mexico's Sierra Madre Occidental: Geosphere, v. 2, p. 125–141, doi:10.1130/GES00042.1.

Tingey, D.G., Christiansen, E.H., Best, M.G., Ruiz, J., and Lux, D.R., 1991, Tertiary minette and melanephelinite dikes, Wasatch Plateau, Utah: Records of mantle heterogeneities and changing tectonics: Journal of Geophysical Research, v. 96, p. 13,529–13,544, doi:10.1029/91JB00327.

Ukstins-Peate, I., Baker, J.A., Al-Kadasi, M., Al-Subbary, A., Knight, K.B., Riisager, P., Thirlwall, M.F., Peate, D.W., Renne, P.R., and Menzies, M.A., 2005, Volcanic stratigraphy of large-volume silicic pyroclastic eruptions during Oligocene Afro-Arabian flood volcanism in Yemen: Bulletin of Volcanology, v. 68, p. 135–156, doi:10.1007/s00445-005-0428-4.

Usui, T., Nakamura, E., Kobayashi, K., Maruyama, S., and Helmstaedt, H., 2003, Fate of the subducted Farallon plate inferred from eclogitic xenoliths in the Colorado Plateau: Geology, v. 31, p. 589–592, doi:10.1130/0091-7613(2003)031<0589:FOTSFP>2.0.CO;2.

Vanderhaeghe, O., Medvedev, S., Fullsack, P., Beaumont, C., and Jamieson, R.A., 2003, Evolution of orogenic wedges and continental plateaux: Insights from crustal thermal-mechanical models overlying subducting mantle lithosphere: Geophysical Journal International, v. 153, p. 27–51, doi:10.1046/j.1365-246X.2003.01861.x.

Vigneresse, J.L., 1995, Crustal regime of deformation and ascent of granitic magmas: Tectonophysics, v. 249, p. 187–202, doi:10.1016/0040-1951(95)00005-8.

Vigneresse, J.L., and Clemens, J.C., 2000, Granitic magma ascent and emplacement: Neither diapirism nor neutral buoyancy, *in* Vendeville, B., Mart, Y., and Vigneresse, J.-L., eds., Salt, Shale and Igneous Diapirs In and Around Europe: Geological Society of London Special Publication 174, p. 1–19, doi:10.1144/GSL.SP.1999.174.01.01.

Viramonte, J.G., Galliski, M.A., Arana Saavedra, V., Aparicio, A., Garcia Cacho, L., and Martin Escorza, C., 1984, El finivulcanismo basico de la Depression de Arizaro, Provincia de Salta, Republica Argentina, *in* IX Congreso Geologico Argentino, Actas III: San Carlos De Bailoche, Argentina, Asociacion Geologica Argentina, p. 234–254.

Wannamaker, P.E., Hasterok, D.P., Johnston, J.M., Stodt, J.A., Hall, D.B., Sodergren, T.L., Pellerin, L., Maris, V., Doerner, W.M., Groenewold, K.A., and Unsworth, M.J., 2008, Lithospheric dismemberment and magmatic processes of the Great Basin–Colorado Plateau transition, Utah, implied from magnetotellurics: Geochemistry, Geophysics, Geosystems, v. 9, no. 5, 38 p.

Ward, K.M., Zandt, G., Beck, S.L., Christensen, D.H., and McFarlin, H., 2014, Seismic imaging of the magmatic underpinnings beneath the Altiplano-Puna volcanic complex from the joint inversion of surface wave dispersion and receiver functions: Earth and Planetary Science Letters, v. 404, p. 43–53, doi:10.1016/j.epsl.2014.07.022.

Ward, P.L., 1995, Subduction cycles under western North America during the Mesozoic and Cenozoic eras, *in* Miller, D.M., and Busby, C., eds., Jurassic Magmatism and Tectonics of the North American Cordillera: Geological Society of America Special Paper 299, p. 1–45, doi:10.1130/SPE299-p1.

Weinberg, R.F., and Podladchikov, Y., 1994, Diapiric ascent of magmas through power-law crust and mantle: Journal of Geophysical Research, v. 99, p. 9543–9559, doi:10.1029/93JB03461.

Whitaker, M.L., Nekvasil, H., Lindsley, D.H., and Difrancesco, N.J., 2007, The role of pressure in producing compositional diversity in intraplate basaltic magmas: Journal of Petrology, v. 48, p. 365–393, doi:10.1093/petrology/egl063.

Whitmeyer, S.J., and Karlstrom, K.E., 2007, Tectonic model for the Proterozoic growth of North America: Geosphere, v. 3, p. 220–259, doi:10.1130/GES00055.1.

Whittington, A.G., Hofmeister, A.M., and Nabelek, P.I., 2009, Temperature-dependent thermal diffusivity of the Earth's crust and implications for magmatism: Nature, v. 458, p. 319–321, doi:10.1038/nature07818.

Willis, G.C., 1999, The Utah thrust system—An overview, *in* Spangler, L.W., and Allen, C.J., eds., Geology of Northern Utah and Vicinity: Utah Geological Association Publication 27, p. 1–9.

Wilson, C.J.N., 2008, Supereruptions and supervolcanoes: Processes and products: Elements (Quebec), v. 4, no. 1, p. 29–34, doi:10.2113/GSELEMENTS.4.1.29.

Wooden, J.L., Kistler, R.W., and Tosdal, R.M., 1999, Strontium, Lead, and Oxygen Isotopic Data for Granitoid and Volcanic Rocks from the Northern Great Basin and Sierra Nevada, California, Nevada, and Utah: U.S. Geological Survey Open-File Report 99-569, 20 p.

Wotzlaw, J.F., Schaltegger, U., Frick, D.A., Dungan, M.A., Gerdes, A., and Gunther, D., 2013, Tracking the evolution of large-volume silicic magma reservoirs from assembly to supereruption: Geology, v. 41, no. 8, p. 867–870, doi:10.1130/G34366.1.

Yonkee, W.A., Dehler, C.D., Link, P.K., Balgord, E.A., Keeley, J.A., Hayes, D.S., Wells, M.L., Fanning, C.M., and Johnston, S.M., 2014, Tectono-stratigraphic framework of Neoproterozoic to Cambrian strata, west-central U.S.: Protracted rifting, glaciation, and evolution of the North American Cordilleran margin: Earth-Science Reviews, v. 136, p. 59–95, doi:10.1016/j.earscirev.2014.05.004.

Yuan, X., Sobolev, S.V., and Kind, R., 2002, Moho topography in the Central Andes and its geodynamic implications: Earth and Planetary Science Letters, v. 199, p. 389–402, doi:10.1016/S0012-821X(02)00589-7.

Zandt, G., Leidig, M., Chmielowski, J., Baumont, D., and Yuan, X.H., 2003, Seismic detection and characterization of the Altiplano-Puna magma body, Central Andes: Pure and Applied Geophysics, v. 160, p. 789–807, doi:10.1007/PL00012557.